2021

Constraining models of inflation with galaxy clustering

Ankit Shrestha
University of Wollongong

Constraining models of inflation with galaxy clustering

Ankit Shrestha

This thesis is presented as part of the requirements for the conferral of the degree:

Master of Philosophy

Supervisors:
Dr. George Takacs & Prof. Michael Lerch

The University of Wollongong
School of Physics

September, 2021

This research has been conducted with the support of an Australian Government Research Training Program Scholarship.

Declaration of Authorship

I, *Ankit Shrestha*, declare that this thesis, submitted in partial fulfilment of the requirements for the award of *Master of Philosophy*, of the School of Physics, University of Wollongong, is wholly my own work unless otherwise referenced or acknowledged. The document has not been submitted for qualifications at any other academic institution.

Ankit Shrestha
3 September 2021

Acknowledgement

First and foremost, I would like to thank the University of Wollongong for providing me with this amazing opportunity to pursue my passion and for supporting me financially whilst I do so. And of course, none of this would be possible without the support of my supervisors, Dr. George Takacs and Prof. Michael Lerch, so I would like to thank them both as well. They have both been very approachable throughout this journey, and their guidance and encouragement during these trying times has made an enormous difference in my life. Furthermore, I really appreciate that they have given me the freedom to follow my interests.

I would also like to express my gratitude towards the institutions Ludwig-Maximilians-Universität München, Technische Universität München and Max Planck Institut für Astrophysik in Germany, where I had the pleasure to collaborate with two of the leading researchers in the field: Dr. Fabian Schmidt and Prof. Eiichiro Komatsu. They have been extremely generous with their time and have provided me with extensive feedback throughout the project, and I have genuinely learnt a lot from them in this process. A majority of the work that I have done is based around their (novel) research, so in a literal sense none of what follows would be possible without them - so I owe my deepest gratitude to both of them.

Finally, I want to thank my family and friends for always believing in me and loving me unconditionally. This hasn't been an easy journey, but they have supported me through all my decisions, both academically and personally, both good and bad, and I highly doubt I would have been able to make it to the other side without their support.

Abstract

In the currently accepted theory of inflation, the early universe is permeated by a quantum scalar field, which has small inhomogeneities, referred to as primordial perturbations, and these perturbations grow over time to form lumps of matter such as stars, galaxies, and clusters. Numerous predictions of this theory including the near scale invariance of the power spectrum, the Gaussianity, and the adiabatic nature of these perturbations have been supported by observations. Nonetheless, the uncertainties in the observations still leave some room for other theories with similar predictions. One such theory is a theory with multiple scalar fields, which naturally leads to slight deviations from the Gaussianity and adiabaticity of the perturbations that can still be within the uncertainty range of the observations. The aim of my master project is to use the clustering of galaxies as a tool to test these predictions thereby constraining models of inflation, since galaxy clustering across the sky can be mapped out via observations.

We first developed expressions for the non-Gaussianity and the non-adiabaticity in the primordial perturbations generated in a theory of inflation with two scalar fields (the predictions are essentially the same in a theory with more fields). Non-adiabatic perturbations, known as isocurvature perturbations, are relative perturbations in energy densities of different energy components, such as baryonic matter and radiation. This is unlike the case of single field inflation, where only the total energy density is perturbed. These features were then incorporated into our galaxy bias expansion, which is a technique developed to relate galaxy density/distribution (an observable) to the primordial perturbations. The possibility of non-Gaussian initial conditions had already been considered in the existing theory of galaxy bias expansion while that for the isocurvature perturbations had not. In particular, we incorporated compensated isocurvature perturbations, which are perturbations between baryonic matter and dark matter, as these would directly affect the distribution of galaxies and hence their densities. Subsequently, theoretical expressions for the galaxy statistics (power spectrum and bispectrum) were determined and plotted, which along with observational data, can be used to constrain the initial conditions and hence the models of inflation in the future.

Contents

List of Figures

Acronyms

CIPs Compensated Isocurvature Perturbations. 13, 15, 20, 39, 49, 50, 66, 68–70

CMB Cosmic Microwave Background. 1, 2, 5, 7, 12, 13, 15, 20

LSS Large-scale Structure Surveys. 15, 39

PBS Peak Background Split. 43, 48

PNG Primordial non-Gaussianity. 15, 55, 58, 68, 70

1. Introduction

1.1. The horizon problem

The cosmological principle tells us that the universe is isotropic and homogeneous on very large scales. But one only needs to check his or her surroundings to see that this is not exactly true on small scales – the universe, as we know it, is very lumpy and inhomogeneous on small scales. This can be seen in figure 1.1, where we have a survey of galaxies in the sky mapped out via the measurements of their redshifts. We can see that large segments of the survey are nearly identical, while if we zoom into the figure, the story becomes quite different, as there are regions of over-densities and under-densities.

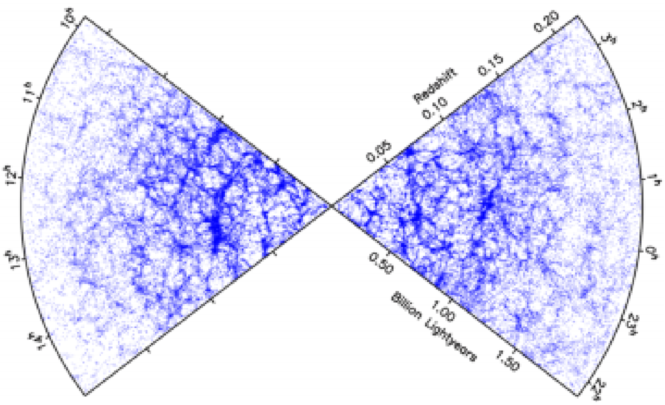

Figure 1.1.: An example of a redshift survey [1]

We can look even further back in time, at around 380,000 years after the big bang, when the universe had cooled off enough to allow the decoupling of photons from primordial plasma. These photons form what we call the Cosmic Microwave Background (CMB) and has been shown in figure 1.2. The figure corroborates the cosmological principle, as on large scales the figure shows a very homogeneous universe, even more so than in the late time universe as seen in figure 1.1. However, there are still fluctuations on small scales of order one in ten thousand [2]. One can explain the existence of these inhomogeneities by imagining a universe that begins in an extremely homogeneous state, but with minute fluctuations, and these fluctuations seed the inhomogeneities that we see in the CMB, which grow further over time under gravity to form lumps of matter like stars, galaxies and voids.

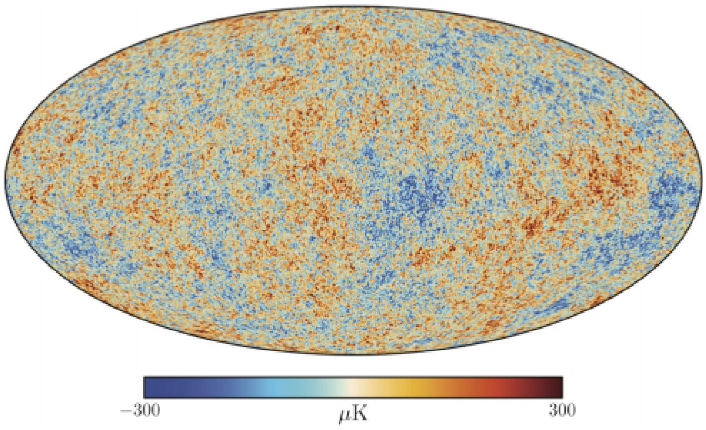

Figure 1.2.: Cosmic Microwave Background captured by the Planck satellite [2]

This all seems to be make sense, but there is one very big problem, a problem so big that we even have a name for it - THE HORIZON PROBLEM. The problem is that the temperature distribution in the CMB is remarkably homogeneous - the homogeneity of the CMB spans scales that are much larger than the scales that could have been in causal contact when the CMB was formed. This is an apparent paradox - how could photons from two opposite directions “know” that they should be at nearly the same temperature, if they were never in causal contact? This is illustrated in figure 1.3. We see that points p and q in opposite directions in the night sky have past light cones that never overlap, meaning that they could have never been in causal contact. This is because in standard cosmology, the horizon of causal contact is given by the comoving Hubble radius, $(aH)^{-1}$, and it increases with time, meaning that in the early universe its value was significantly smaller than it is today [2].

1.2. Inflationary paradigm

How do we get around a problem that is very fundamental to the well established standard cosmology? A possible solution would be to assume that in the very early universe, the standard cosmology doesn’t apply and we have a phase of decreasing comoving Hubble radius [4].

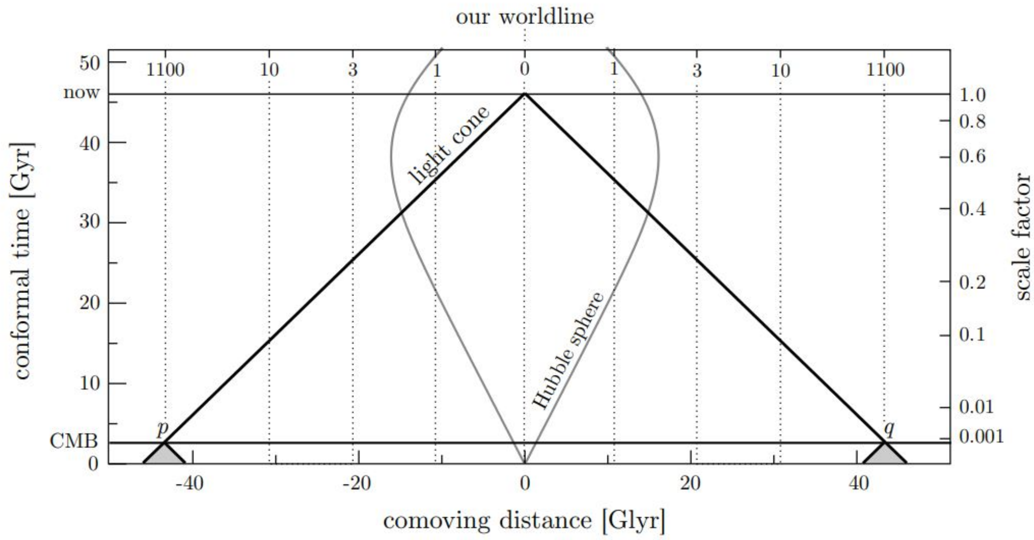

Figure 1.3.: The horizon problem in the Big Bang model [3]

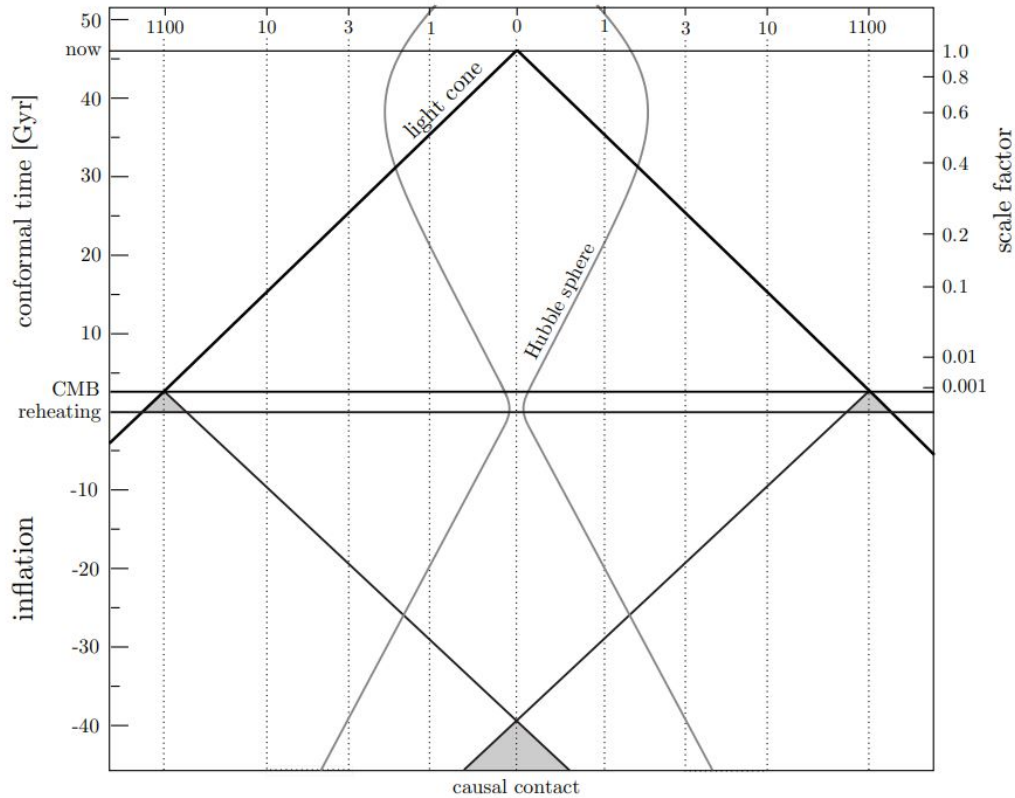

Figure 1.4.: Solution to the horizon problem [3]

Mathematically this can be expressed as

$$\frac{d}{dt}(aH)^{-1} < 0 \tag{1.1}$$

This would mean that the comoving Hubble radius at the very beginning of the universe was extremely large - on the scale that allows the homogeneity we see in the early universe. The comoving Hubble radius then decreases exponentially to a very small value at the end of this phase and then starts increasing again once the universe transitions into one where the standard cosmology applies. This is what we now call inflation. The inflationary solution to the horizon problem has been illustrated visually in figure 1.4. Please note that from the figure it might seem like inflation lasted a very long time, but that is not the case since the vertical axis is in conformal time, and in the inflationary phase conformal time passes much faster.

The shrinking Hubble sphere can be taken as the fundamental requirement of inflation since it directly addresses the horizon problem. Before we discuss the physical model of the early universe that can achieve a shrinking comoving Hubble radius, we want to show some equivalent definitions of inflation.

- **Accelerated expansion**

  $$\frac{d}{dt}(aH)^{-1} = \frac{d}{dt}(\dot{a})^{-1} = -\frac{\ddot{a}}{(\dot{a})^2} < 0 \iff \ddot{a} > 0, \tag{1.2}$$

  meaning that the universe underwent a period of accelerated expansion during the inflationary phase.

- **Negative Pressure**

  Inflation requires negative pressure, meaning a violation of the strong energy condition, satisfied by ordinary energy components. This can be shown by combining the Friedmann equation, $H^2 = \rho/(3M_{pl}^2)$, and the continuity equation, $\dot{\rho} = -3H(\rho + P)$, which yields

  $$\frac{d}{dt}(aH)^{-1} = \frac{1}{2a}\left(1 + 3\frac{P}{\rho}\right) < 0 \iff P < -\frac{\rho}{3}. \tag{1.3}$$

  Therefore, any viable physical model of inflation should imply the existence of negative pressure.

- **Slowly decreasing Hubble parameter H**

  We can express the condition of shrinking comoving Hubble radius

  $$\frac{d}{dt}(aH)^{-1} = -\frac{\dot{a}H + a\dot{H}}{(aH)^2} = -\frac{1}{a}(1-\varepsilon) < 0 \text{ as } \varepsilon = -\frac{\dot{H}}{H^2} < 1, \tag{1.4}$$

which implies that the Hubble parameter H decreases slowly over time. We call ε a slow roll parameter, the reason for which will be clear very shortly.

Therefore, we have defined the various equivalent ways we can use to establish the inflationary paradigm. The last definition can be re-expressed as follows

$$\varepsilon = -\frac{\dot{H}}{H^2} = -\frac{d\ln H}{dN} < 1, \tag{1.5}$$

where we have defined N through $\mathrm{d}N = \mathrm{d}\ln \mathrm{a}$, which measures the number of e-folds of inflationary growth. In order to obtain the kind of homogeneity that we see in the CMB, it can be shown that inflation would have to last a long time ($N \sim 60$), meaning that ε has to remain small for a sufficiently long time [5]. Defining a new parameter

$$\eta = \frac{d\ln\varepsilon}{dN}, \tag{1.6}$$

we require $|\eta| < 1$. We also call η a slow roll parameter and along with ε, it forms the set of defining conditions for inflation to occur.

1.3. The Physics of inflation

In the currently accepted theory of inflation, the early universe is permeated by a scalar field, called the inflaton $\phi(t, \boldsymbol{x})$ [5]. Its dynamics coupled to gravity is governed by the action:

$$S = \int \mathrm{d}^4x\, \mathcal{L} = \int \mathrm{d}^4x \sqrt{-g}\left(R + \frac{1}{2}\partial_\mu\phi\partial^\mu\phi - V(\phi)\right) \tag{1.7}$$

The corresponding stress-energy tensor for the scalar field is given by

$$T_{\mu\nu} = \partial_\mu\phi\partial_\nu\phi - g_{\mu\nu}\left(\frac{1}{2}g^{\alpha\beta}\partial_\alpha\phi\partial_\beta\phi - V(\phi)\right) \tag{1.8}$$

The metric consistent with the conditions of homogeneity, isotropy and flatness of the background is the FRW spacetime, which is given by

$$\mathrm{d}s^2 = \mathrm{d}t^2 - a^2(t)\delta_{ij}\mathrm{d}x^i\mathrm{d}x^j. \tag{1.9}$$

In addition, the homogeneity of the background implies that the background value $\phi(t, \boldsymbol{x}) = \phi(t)$, and therefore the field ϕ plays the role of a local “clock” for the duration of inflationary expansion.

Then, using the relations $T^0_0 = \rho$ and $T^i_j = -P\delta^i_j$, we find that

$$\rho = \frac{1}{2}\dot{\phi}^2 + V(\phi), \qquad P = \frac{1}{2}\dot{\phi}^2 - V(\phi) \tag{1.10}$$

Recall that for inflation to occur, we require the pressure to be sufficiently negative, and this occurs if the kinetic energy density, $\frac{1}{2}\dot{\phi}^2$ is sufficiently smaller than the potential energy density V and hence the total energy density ρ. This is why we call this scenario slow roll inflation. The precise condition can be established through the slow roll parameter ε, which can be shown to be

$$\varepsilon = \frac{3}{2}\frac{\dot{\phi}^2}{\rho} < 1. \tag{1.11}$$

One can show that this is equivalent to $\dot{\phi}^2 < V$. Therefore, as long as the value of the background field $\phi(t)$ increases very slowly over time, inflation can occur [2]. This is the first slow roll condition. Since we want inflation to occur for a sufficiently long enough time, we find another restricting condition for $\phi(t)$, through the second slow roll parameter η, which is found to be

$$\eta = 2\frac{\ddot{\phi}}{H\dot{\phi}} + 2\varepsilon. \tag{1.12}$$

The second slow roll condition $|\eta| < 1$ is equivalent to $\ddot{\phi} < H\dot{\phi}$. This establishes the slow roll inflation even further, since this shows that the derivative of inflaton field also changes slowly allowing for the inflation to last long enough, which makes sense since once the derivative becomes large enough, the pressure in equation (1.10) becomes positive and inflation stops [2]. The equations of motion governing the scalar field can be determined through the action and are given by:

$$H^2 = \frac{1}{3M_{\rm pl}^2}\left[\frac{1}{2}\dot{\phi}^2 + V\right] \tag{1.13}$$

and

$$\ddot{\phi} + 3H\dot{\phi} + V_{,\phi} = 0. \tag{1.14}$$

Using these equations, one can write the slow roll parameters in terms of the potential $V(\phi)$ as follows

$$\varepsilon = \frac{M_{\rm pl}^2}{2}\left(\frac{V_{,\phi}}{V}\right)^2 \quad , \quad \eta = -2M_{\rm pl}^2\frac{V_{,\phi\phi}}{V} + 4\varepsilon \tag{1.15}$$

Therefore, only potential functions that satisfy the condition that $\varepsilon < 1$ and $|\eta| < 1$ can successfully produce the inflationary scenario [2]. An example of a slow roll potential is provided in figure 1.5.

In the figure, $\phi_{\rm CMB}$ is the minimum value of ϕ required to explain the scale of causality in the

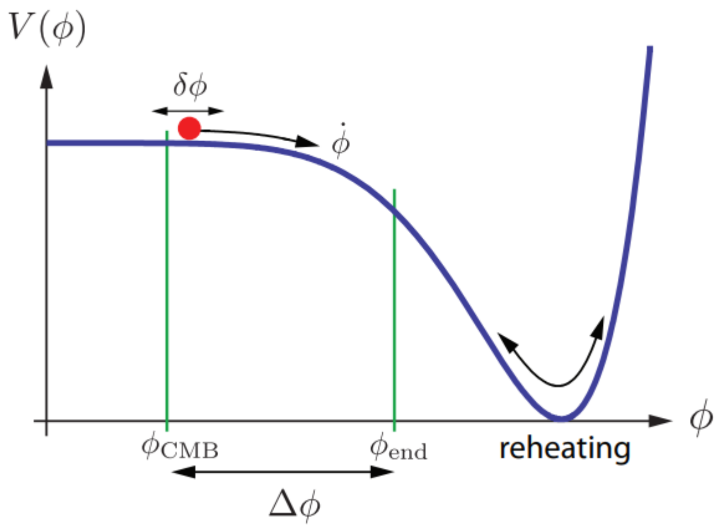

Figure 1.5.: An example of a slow roll potential [4]

CMB and ϕ_{end} is the essentially a measure of the end of inflation. During this time the potential function changes very gradually, i.e. the gradient of the potential function (V_ϕ) and its gradient ($V_{\phi\phi}$) are very small compared to V. Then, at the end of inflation, the gradient becomes steep and the field moves faster. As a result, the condition for inflation is no longer met, and the inflaton field has to decay into the particles of the Standard Model [4]. This phase is called reheating, as shown in figure 1.5.

1.4. Quantum theory of inflation

In the previous section, we established the physics of inflation for the homogeneous isotropic background. However, recall that our observation of the CMB tells us that there must be small fluctuations in the energy density in the primordial universe, which seed the large scale structures that we see around us. It turns out the theory of inflation also provides a mechanism to achieve these fluctuations. This is because the inflaton field $\phi(t, \boldsymbol{x})$ acts as a local "clock" during inflation and using the uncertainty principle, we know that it is impossible to precisely tell time [4]. This leads to quantum mechanical fluctuations in the inflaton field, $\delta\phi(t, \boldsymbol{x}) = \phi(t, \boldsymbol{x}) - \overline{\phi}(t)$, where we now use $\overline{\phi}(t)$ to represent the background field value. Since the inflaton field $\phi(t, \boldsymbol{x})$ completely determines the energy density of the primordial universe, the fluctuations in the inflaton field lead to fluctuations in the local densities after inflation, $\delta\rho(t, \boldsymbol{x})$. In this section, we briefly go over the quantisation procedure for the fluctuations and the results of the quantisation.

We begin by considering the inflaton action

$$S = \int \mathrm{d}^4x\,\mathcal{L} = \int \mathrm{d}^4x\sqrt{-g}\left(\frac{1}{2}\partial_\mu\phi\partial^\mu\phi - V(\phi)\right)$$

Since we consider a perturbed inflaton field $\phi(t,\boldsymbol{x}) = \phi(t) + \delta\phi(t,\boldsymbol{x})$, we also add scalar perturbations to the FRW metric, which then reads

$$ds^2 = a^2(\tau)\{(1+2A)\mathrm{d}\tau^2 - 2B_{,i}\mathrm{d}x^i\mathrm{d}\tau - [(1-2\Phi)\delta_{ij} + 2E_{,ij}]\mathrm{d}x^i\mathrm{d}x^j\}, \tag{1.16}$$

where we now use the conformal time τ instead of the coordinate time t. We perform the quantization in spatially flat gauge, a choice that will become clear very shortly. In order to obtain a linear equation of motion for the field perturbations $\delta\phi(\tau,\boldsymbol{x})$, we need to expand S in second order in the perturbations. Before we do so, hindsight tells us that it is easier to perform quantization on $f(\tau,\boldsymbol{x})$, defined as $f(\tau,\boldsymbol{x}) = a(\tau)\,\delta\phi(\tau,\boldsymbol{x})$ [5]. Keeping only terms quadratic in f, the perturbed action becomes

$$S^{(2)} = \frac{1}{2}\int \mathrm{d}\tau\mathrm{d}^3x\left[(f')^2 - (\nabla f)^2 + \left(\frac{a''}{a} - a^2V_{,\phi\phi}\right)f^2\right], \tag{1.17}$$

where $'$ represents derivative with respect to conformal time τ [5]. Since $a' = a^2H$ and $H \approx const.$ during inflation, we have that

$$\frac{a''}{a} \approx 2a'H = 2a^2H^2 \gg a^2V_{,\phi\phi}, \tag{1.18}$$

where the last inequality follows from the condition of slow roll inflation that $|\eta| \ll 1$. Then the equation (1.17) becomes

$$S^{(2)} = \frac{1}{2}\int \mathrm{d}\tau\mathrm{d}^3x\left[(f')^2 - (\nabla f)^2 + \frac{a''}{a}f^2\right], \tag{1.19}$$

which yields the Mukhanov-Sasaki equation

$$f'' - \nabla^2 f - \frac{a''}{a}f = 0. \tag{1.20}$$

In Fourier space, this becomes

$$f_k'' + \left(k^2 - \frac{a''}{a}\right)f_k = 0. \tag{1.21}$$

At sufficiently early times, all modes of cosmological interest were deep inside the horizon (shown in figure 1.6), i.e. $k^{-1} \ll (aH)^{-1}$, since the comoving Hubble radius was very large at the beginning. This implies that $k^2 \gg (aH)^2 \approx \frac{a''}{a}$ and therefore the Mukhanov-Sasaki equation becomes

$$f_k'' + k^2 f_k = 0. \tag{1.22}$$

Therefore, each Fourier mode satisfies the equation of motion of a simple harmonic oscillator, which can be quantized fairly easily. Upon quantization, we promote the field perturbations f_k to an operator $\hat{f}_k$ and one can show that the operator can be expressed in terms of ladder operators $\hat{a}_k$ [4]. We find that

$$\hat{f}_k(\tau, \boldsymbol{k}) = \frac{e^{-ik\tau}}{\sqrt{2k}}(\hat{a}_{\boldsymbol{k}} + \hat{a}^\dagger_{-\boldsymbol{k}}), \tag{1.23}$$

where the ladder operators satisfy

$$[\hat{a}_{\boldsymbol{k}}, \hat{a}^\dagger_{\boldsymbol{k'}}] = (2\pi)^3 \delta^3_D(\boldsymbol{k} + \boldsymbol{k'}). \tag{1.24}$$

The vacuum state $|0\rangle$ is defined via the condition

$$\hat{a}_{\boldsymbol{k}}|0\rangle = 0, \quad \text{for all } \boldsymbol{k} \tag{1.25}$$

and all the quantum states in the Hilbert space are constructed by applying creation operators on the vacuum state, as shown below:

$$|\boldsymbol{k_1}, \boldsymbol{k_2}, \boldsymbol{\ldots}\rangle = \left[a^\dagger_{\boldsymbol{k_1}} a^\dagger_{\boldsymbol{k_2}} \ldots\right]|0\rangle \tag{1.26}$$

In position space, $\hat{f}(\tau, \boldsymbol{x})$ can be expressed as

$$\hat{f}(\tau, \boldsymbol{x}) = \int \frac{\mathrm{d}^3 k}{(2\pi)^3} \hat{f}_{\boldsymbol{k}}(\tau, \boldsymbol{k}) e^{i\boldsymbol{k}.\boldsymbol{x}} \tag{1.27}$$

The expected value of the operator $\hat{f}$ in the ground state vanishes since

$$\langle \hat{f} \rangle = \langle 0|\hat{f}|0\rangle = \int \frac{\mathrm{d}^3 k}{(2\pi)^3} \langle 0|\hat{f}_{\boldsymbol{k}}(\tau, \boldsymbol{k})|0\rangle e^{i\boldsymbol{k}.\boldsymbol{x}} = \int \frac{\mathrm{d}^3 k}{(2\pi)^3} \frac{e^{i(\boldsymbol{k}.\boldsymbol{x} - k\tau)}}{\sqrt{2k}} \langle 0|\hat{a}_{\boldsymbol{k}} + \hat{a}^\dagger_{-\boldsymbol{k}}|0\rangle = 0, \tag{1.28}$$

where in the last step $\hat{a}$ annihilates $|0\rangle$ from the left and $\hat{a}^\dagger$ annihilates $|0\rangle$ from the right. However, the variance of the inflaton perturbations receives finite zero-point fluctuations as shown below

$$\begin{aligned}
\langle |\hat{f}|^2 \rangle &= \langle 0|\hat{f}^\dagger(\tau, \boldsymbol{x})\hat{f}(\tau, \boldsymbol{x})|0\rangle \\
&= \int \frac{\mathrm{d}^3 k}{(2\pi)^3} \int \frac{\mathrm{d}^3 k'}{(2\pi)^3} \frac{1}{\sqrt{4kk'}} \langle 0|(\hat{a}^\dagger_{\boldsymbol{k}} + \hat{a}_{-\boldsymbol{k}})(\hat{a}_{\boldsymbol{k'}} + \hat{a}^\dagger_{-\boldsymbol{k'}})|0\rangle \; e^{i(k-k')\tau} \\
&= \int \frac{\mathrm{d}^3 k}{(2\pi)^3} \frac{1}{2k}.
\end{aligned} \tag{1.29}$$

We define the power spectrum of $\hat{f}(\boldsymbol{k})$, $\mathcal{P}_f(k)$ as

$$\langle \hat{f}^\dagger(\boldsymbol{k})\hat{f}(\boldsymbol{k}')\rangle = (2\pi)^3\delta_D^3(\boldsymbol{k}+\boldsymbol{k}')\mathcal{P}_f(k), \tag{1.30}$$

which yields

$$P_f(k) = \frac{1}{2k}. \tag{1.31}$$

One can then find the power spectrum of the fluctuations $\delta\phi$ as

$$P_{\delta\phi}(k) = a^{-2}P_f(k) = \frac{2\pi^2}{k^3}\left(\frac{k}{2\pi a}\right)^2 \tag{1.32}$$

Although all modes of interest were deep inside the Hubble sphere at very early times, they exit the horizon at some point during inflation, since the Hubble sphere $(aH)^{-1}$ shrinks exponentially during inflation. This can be seen in figure 1.6. Note that the shrinking of Hubble sphere is taken to be linear because the figure considers comoving scales. Once outside the horizon, the Fourier modes renounce their quantum nature and the quantum expectation value becomes the ensemble average of the now classical field [4]. At horizon exit, we have $k \sim aH$ and the power spectrum becomes

$$P_{\delta\phi}(k) = \frac{2\pi^2}{k^3}\left(\frac{H}{2\pi}\right)\Bigg|^2_{k=aH} \tag{1.33}$$

Once outside the horizon, we switch from inflaton fluctuations $\delta\phi$ to fluctuations in a quantity called the comoving curvature perturbations $\mathcal{R}$, a gauge invariant quantity defined as

$$\mathcal{R} = \Phi - \frac{H}{\bar{\rho}+\bar{P}}\delta q = \Phi - \frac{1}{\sqrt{2\varepsilon}M_{\mathrm{pl}}}\delta\phi, \tag{1.34}$$

where δq is the perturbation in momentum density, defined later in section 2. In spatially flat gauge, we obtain a simpler relationship between $\mathcal{R}$ and $\delta\phi$, given by

$$\mathcal{R} = -\frac{1}{\sqrt{2\varepsilon}M_{\mathrm{pl}}}\delta\phi. \tag{1.35}$$

The reason behind the switch is the fact that $\mathcal{R}$ is conserved on superhorizon scales, meaning that it stays constant from the time of horizon exit to the time of horizon re-entry which occurs because the causal horizon starts increasing again in the standard Lambda-CDM universe (see figure 1.6) [3]. Therefore the power spectrum of $\mathcal{R}$ is frozen for this entire duration, and is given by

$$P_{\mathcal{R}}(k) = \frac{2\pi^2}{k^3}\frac{1}{2\varepsilon}\left(\frac{H}{2\pi M_{\mathrm{pl}}}\right)\Bigg|^2_{k=aH} \tag{1.36}$$

In addition, at horizon re-entry, $\mathcal{R}$ can be related to observables such as the energy density

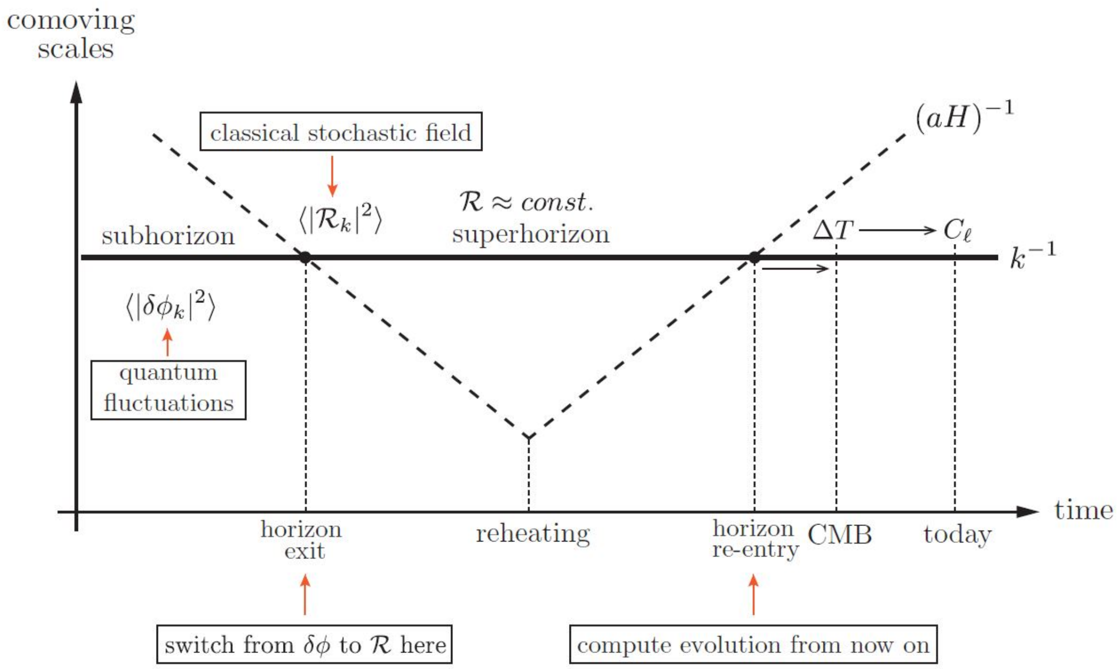

Figure 1.6.: Comparison of the size of a particular scale k^{-1} to the horizon scale $(aH)^{-1}$ at various times [3]

perturbation, δ, defined as

$$\delta(\boldsymbol{x}) = \frac{\rho(\boldsymbol{x}) - \overline{\rho}}{\overline{\rho}} \tag{1.37}$$

One then finds that in comoving gauge,

$$\delta(\boldsymbol{k}, z) = \mathcal{M}(k)\mathcal{R}(\boldsymbol{k}), \text{ where } \mathcal{M}(k) = \frac{2}{5}\frac{k^2c^2T(k)g(z)}{\Omega_m H_0^2(1+z)}, \tag{1.38}$$

$T(k)$ is the matter transfer function and $g(z)$ is the linear growth rate of the gravitational potential during the matter dominated epoch. This shows us exactly how a non-zero curvature perturbation after horizon exit translates to non zero fluctuations in total energy density, which then seeds the large scale structure formation [9].

In equation (1.36), we see that the power spectrum depends on k^{-3} explicitly. We know that H is a slowly varying function of time, meaning that H will slightly depend on the time of horizon exit. But we also know that the time of horizon exit depends on the scale k^{-1}, meaning that there will a slight dependence on k through H. Therefore, we can postulate that

$$P_{\mathcal{R}}(k) = \frac{2\pi^2 A_s}{k^3}\left(\frac{k}{k_*}\right)^{n_s-1}, \tag{1.39}$$

where A_s is the amplitude of scalar spectrum and k_* is some pivot scale. We call n_s the spectral index and expect it to be nearly one. One can precisely show that

$$n_s - 1 = -2\varepsilon - \eta, \tag{1.40}$$

where $\varepsilon \ll 1$ and $\eta \ll 1$ [2]. With the help of the temperature power spectrum and polarisation power spectrum, the Planck satellite has been able to confirm this prediction to be fairly accurate, finding that

$$n_s = 0.965 \pm 0.004 \tag{1.41}$$

This is one of the biggest predictions of scalar field inflation, which has been confirmed [10]. In addition, the theory of single scalar field inflation also predicts that the fluctuations to be nearly Gaussian. The fluctuations that we obtained in our analysis above are obviously Gaussian since we only consider the action up to second order in perturbations and there were no higher order interaction terms. However, even if we were to consider higher order interaction terms by expanding the action up to third order in perturbations, we would find that the interaction terms are quite well suppressed, meaning that the non-Gaussianity is very low. This has been observed to be true in the CMB, where the fluctuations were constrained to be Gaussian with a very high accuracy [11].

Another main prediction of single scalar field inflation is that the fluctuations are adiabatic, meaning that only the total energy density is perturbed, while the distribution of energy density across different energy components such as ordinary matter and radiation is uniform. Fluctuations orthogonal to adiabatic perturbations are called isocurvature perturbations, and component wise isocurvature perturbations are defined as follows

$$\mathcal{S}_{ij} = \left(\frac{\delta n_i}{\overline{n_i}} - \frac{\delta n_j}{\overline{n_j}}\right), \tag{1.42}$$

where n is the number density, and i and j are different energy components [12]. A non-zero isocurvature perturbation would mean that there is a relative perturbation between different energy components as well. As we will see in chapter 2, in the case of single field inflation, $\mathcal{S}_{ij} = 0$, meaning that only the total energy density is perturbed through a non-zero $\mathcal{R}$, and that all the energy components scale in a way that ensures that the relative perturbation is zero. The reason behind a zero isocurvature perturbation in single field inflation is due to the fact that the field perturbation $\delta\phi$ also follows the classical trajectory since the field space is one-dimensional, while in theories with multiple fields, there is a trajectory in field space that is always orthogonal to the classical trajectory and field perturbations along these trajectories can produce a non-zero isocurvature perturbation. This idea will be delved into in detail in chapter 2. Isocurvature perturbations between matter and radiation have been constrained by the Planck CMB data, and their power spectrum has been shown to contribute less than 2% to the CMB power spectrum, in line with the prediction of single field inflation that isocurvature perturbations are negligible [13].

In this chapter, we have briefly discussed the history and the physics of single field inflation. We have also established that a lot of the predictions of single field inflation have been supported by observations. However, the uncertainties in the observations still leave some room for other theories with similar predictions. One such theory would be a theory of multiple scalar fields, which predicts slight deviations from the Gaussianity and adiabaticity of the perturbations, and hence it would be interesting to see if these deviations lie within the uncertainty range of the current observations. In addition, only the matter-radiation isocurvature perturbations have been tightly constrained using the CMB, and constraints on other forms of isocurvature perturbations such as Compensated Isocurvature Perturbations (CIPs), which are perturbations between baryonic and dark matter, is still very loose [14]. In fact, recent constraint studies [13] allow for amplitudes of the primordial CIP power spectrum to be over 5 orders of magnitude larger than the amplitude of the matter power spectrum. This loose constraint indicates that there is a lot of room for improvement in early-universe physics, and hence is a driving force for looking beyond single field inflation [14]. Another reason to investigate the theory of multiple field inflation comes from the fact that many grand unified models have several light fields. We delve deeper into an inflationary model with multiple fields in chapter 2.

1.5. Galaxy bias expansion

The obvious question now is: how do we test the predictions of multi field inflation? The answer is large-scale structure surveys. These surveys map out the positions of millions of galaxies by measuring their redshifts. An example of redshift survey has been provided in figure 1.1. Having information about the positions of galaxies can provide a great deal of information about the origin and evolution of primordial cosmological perturbations, since the large scale structures that we see around us result from the growth of these primordial perturbations. The way we retrieve this information is via the correlation of the number density of these tracers (such as galaxies and clusters). The reason we use statistical quantities is because we cannot precisely predict the initial conditions, since the initial conditions were generated from quantum mechanical fluctuations. We assume that ensemble averages can be replaced with spatial averages, as long as the volume of our survey is large enough, since samples extracted from distant regions can be considered independent, and therefore all statistical quantities pertaining to tracers are calculated as spatial averages. Since it is very difficult to extract information from one-point correlation functions, the lowest order statistic that we use to extract information is the two-point correlation function of the tracer density and its Fourier transform, the power spectrum.

We want to connect the observed statistics of galaxies to theoretical predictions, which are based on the statistics of the initial density fluctuations as well as their evolution under gravity. On sufficiently large scales, correlations are weak and one would hope that a perturbative approach could be implemented to create a theoretical framework to relate galaxy distribution to the initial conditions. Unfortunately, the process of galaxy formation involves highly non-linear, small scale mechanisms, and therefore cannot be described perturbatively. Nonetheless, there exists a general framework for an effective perturbative description of galaxy clustering which does not make any specific assumptions about the process of galaxy formation. It does however involve unknown "bias parameters", which in general need to be determined observationally. The simplest and most well-known bias expansion is the local (galaxy or tracer) bias expansion in terms of matter density perturbation, defined as

$$\delta(\boldsymbol{x}) = \frac{\delta\rho(\boldsymbol{x})}{\overline{\rho}} = \frac{\rho(\boldsymbol{x}) - \overline{\rho}}{\overline{\rho}}. \tag{1.43}$$

In a local bias expansion, we express the tracer density, $n_{h,L}(\boldsymbol{x})$ coarse grained ("averaged") over a scale R_L, in terms of the matter density perturbation coarse grained over a scale R_L, $\delta_L(\boldsymbol{x})$, as shown below

$$n_{h,L}(\boldsymbol{x}) = c_0 + c_1\delta_L(\boldsymbol{x}) + \frac{c_2}{2}\delta_L^2(\boldsymbol{x}) + \ldots, \tag{1.44}$$

where c_n are the bias parameters [17]. If the tracer is a galaxy, then $n_{h,L}(\boldsymbol{x})$ measures the average abundance of galaxies in a region of characteristic size R_L centred at position $\boldsymbol{x}$. The above bias expansion essentially links the abundance of tracers at a point to the matter density at that point, which seems like a valid assumption, since tracers such as galaxies and clusters form as lumps of matter come together under gravity. However, given the complex formation processes of tracers such as galaxies and clusters, it is very unlikely that the abundance of tracers is truly a local function of the matter density perturbation. In fact, it would be perfectly reasonable to assume that the abundance of tracers at position $\boldsymbol{x}$ depends on the matter density in some finite region around $\boldsymbol{x}$, say of size R_*, which we can refer to as the "non-locality scale". Then, one can show that the statistics of the tracer on very large scales (our scales of interest), $r \gg R_*$, can be accurately described by the local biasing, with corrections suppressed by $(R_*/r)^2$. Therefore, the local bias expansion provides the correct effective description on large scales [18].

We want to go beyond this simple model of galaxy bias, and include bias terms for Primordial non-Gaussianity (PNG) in the curvature perturbation, and Compensated Isocurvature Perturbations (CIPs), which are both predictions of multi-field inflationary models, which will be shown in chapter 2. The inclusion of these bias terms is physically motivated. The existence of PNG in curvature perturbations would have a direct effect on the three-point tracer correlation function and its Fourier transform - the bispectrum. In addition, clusters, which are rare objects and form from the tails of the probability distribution of density perturbations, are highly sensitive to changes in the distribution function, and therefore any deviation of the distribution from being perfectly Gaussian would have a measurable effect on the formation of clusters [18]. Currently, the value of non-Gaussianity parameter $f_{\rm NL}$ has been constrained by the Planck Collaboration using CMB temperature and polarization maps to be -0.9 ± 5.1, which is a very loose constraint [11]. This provides us with further impetus to find evidence for PNG using galaxy clustering, and this can be achieved with the help of Large-scale Structure Surveys (LSS), which are surveys of sections of the sky to measure the positions and redshifts of astronomical objects such as galaxies [20]. CIPs are perturbations in the ratio of energy densities of baryonic matter and dark matter, and would naturally influence the abundance of galaxies and clusters in the universe, and hence should also appear in the bias expansion. In addition, as in the case of PNG in the curvature perturbation, CIPs are very loosely constrained by current observations of the CMB, and therefore it makes sense to look for their signatures elsewhere (such as in the LSS) [14]. We go a step further and also include non-Gaussianity in the CIPs in the bias expansion, as this non-Gaussianity would appear in the galaxy bispectrum. All of this will be done in chapter 3.

2. Multi-field inflation

In this chapter, we develop a theory of inflation with two scalar fields (the predictions are essentially the same in a theory with more fields), and develop expressions for the (small) non-Gaussianity and non-adiabaticity of the primordial perturbations. To achieve our goal, we will have to employ cosmological perturbation theory. We assume that the background universe is flat, homogeneous and isotropic, and there are small metric perturbations in addition to the background metric. We know that the background metric for a flat universe satisfying the cosmological principle is given by

$$\mathrm{d}s^2 = \mathrm{d}t^2 - a^2(t)\delta_{ij}\mathrm{d}x^i\mathrm{d}x^j \tag{2.1}$$

We then add perturbations to the metric, which reads

$$ds^2 = (1+2A)\mathrm{d}t^2 - 2a(t)B_{,i}\mathrm{d}x^i\mathrm{d}t - a^2(t)[(1-2\Phi)\delta_{ij} + 2E_{,ij}]\mathrm{d}x^i\mathrm{d}x^j, \tag{2.2}$$

where the perturbations are considered small enough to be first order. In addition, we have to include perturbations in the matter sector. We know that the matter in a homogeneous and isotropic universe takes the form of a perfect fluid, with stress-energy tensor

$$\overline{T}^{\mu}_{\nu} = \begin{pmatrix} \overline{\rho} & 0 & 0 & 0 \\ 0 & -\overline{P} & 0 & 0 \\ 0 & 0 & -\overline{P} & 0 \\ 0 & 0 & 0 & -\overline{P} \end{pmatrix}, \tag{2.3}$$

where the overline represents background value, a convention that we will use throughout the thesis. Next, we consider small perturbations in the stress energy tensor

$$T^{\mu}_{\nu} = \overline{T}^{\mu}_{\nu} + \delta T^{\mu}_{\nu} \tag{2.4}$$

Then, one finds that the perturbations in the stress energy tensor can be expressed as

$$
\begin{aligned}
\delta T^0_0 &= \delta\rho \ , \\
\delta T^i_0 &= (\overline{\rho} + \overline{P})v^i \ , \\
\delta T^0_j &= -(\overline{\rho} + \overline{P})(v_j + B_{,j}) \ , \\
\delta T^i_j &= \delta p \ \delta^i_j \ ,
\end{aligned}
\tag{2.5}
$$

where v^i is the coordinate velocity, i.e.

$$
v^i = a(t)\frac{\mathrm{d}x^i}{\mathrm{d}t} \tag{2.6}
$$

We will use δq^i as the momentum density perturbation $(\overline{\rho} + \overline{P})v^i$; δq^i can be decomposed into scalar and vector parts, i.e. $\delta q_i = \delta q_{,i} + \widehat{\delta q}_i$, where $\nabla^i \widehat{\delta q}_i = 0$. Since we are only interested in the scalar perturbations, we can ignore the vector part, and as a result we have $\delta q_i = \delta q_{,i}$ [4]. In the next section, we will consider a universe permeated by scalar fields, and the perturbations in these scalar fields give rise to the perturbations in the stress energy tensor. We then combine these scalar field perturbations with the perturbations in the metric to obtain their equations of motion.

2.1. Equations of motion

We first work with a theory with N scalar fields, and later specialise it to the case of $N = 1$ and $N = 2$. Recall that the Lagrangian for N scalar fields reads:

$$
S = \int \mathrm{d}^4x\,\mathcal{L} = \int \mathrm{d}^4x\sqrt{-g}\left(\frac{1}{2}\sum_{I=1}^{N}\partial_\mu\varphi_I\partial^\mu\varphi_I - V(\varphi_I)\right) \tag{2.7}
$$

As with the metric, we will have perturbations in the scalar field, such that the perturbed scalar field φ_I can be expressed as $\varphi_I = \overline{\varphi}_I + \delta\varphi_I$. We can use this definition to separate the action into first and second order in perturbations. The first order action gives us the equation of motion for the background, which reads:

$$
\ddot{\overline{\varphi}}_I + 3H\dot{\overline{\varphi}}_I + V_{\varphi_I} = 0, \tag{2.8}
$$

where $V_{\varphi_I} = \frac{\partial V}{\partial \overline{\varphi}_I}$. All the derivatives of V taken with respect to the field throughout this paper are evaluated at the background field value, despite the lack of overline on the field value in the subscript. The second order action gives us the following equations of motion for the first order perturbations:

$$\delta\ddot{\varphi}_I + 3H\delta\dot{\varphi}_I + \frac{k^2}{a^2}\delta\varphi_I + \sum_{J=1}^{N} V_{\varphi_I\varphi_J}\delta\varphi_J = -2V_{\varphi_I}A + \dot{\bar{\varphi}}_I\left[\dot{A} + 3\dot{\Phi} + \frac{k^2}{a^2}(a^2\dot{E} - aB)\right] \tag{2.9}$$

We get additional equations from the variation of the Einstein-Hilbert action, as shown below:

$$3H(\dot{\Phi} + HA) + \frac{k^2}{a^2}\left[\Phi + H(a^2\dot{E} - aB)\right] = -4\pi G\delta\rho \tag{2.10}$$

$$\dot{\Phi} + HA = -4\pi G\delta q, \tag{2.11}$$

We have the following expressions for the energy density ρ and pressure P:

$$\rho = \frac{1}{2}\sum_{I=1}^{N}\partial_\mu\varphi_I\partial^\mu\varphi_I + V(\varphi_I), \qquad P = \frac{1}{2}\sum_{I=1}^{N}\partial_\mu\varphi_I\partial^\mu\varphi_I - V(\varphi_I) \tag{2.12}$$

The perturbations in the energy density, pressure and momentum density are given as follows:

$$\delta\rho = \sum_I \left[\dot{\bar{\varphi}}_I(\dot{\delta\varphi}_I - \dot{\bar{\varphi}}_I A) + V_{\varphi_I}\delta\varphi_I\right] \tag{2.13}$$

$$\delta P = \sum_I \left[\dot{\bar{\varphi}}_I(\dot{\delta\varphi}_I - \dot{\bar{\varphi}}_I A) - V_{\varphi_I}\delta\varphi_I\right] \tag{2.14}$$

$$\delta q = -\sum_I \dot{\bar{\varphi}}_I\delta\varphi_I \tag{2.15}$$

We can now define a gauge invariant quantity called the comoving density perturbation as follows:

$$\delta\rho_m = \delta\rho - 3H\delta q = \sum_I \left[\dot{\bar{\varphi}}_I(\dot{\delta\varphi}_I - \dot{\bar{\varphi}}_I A) - \ddot{\bar{\varphi}}_I\delta\varphi_I\right] \tag{2.16}$$

One can then combine equations (2.10) and (2.11) together in Newtonian gauge ($E = B = 0$) to obtain

$$\frac{k^2}{a^2}\Phi_n = -4\pi G\delta\rho_m, \tag{2.17}$$

where Φ_n is the value of Φ in Newtonian gauge. Equation (2.17) will be referred to quite often in the calculations that follow, as it can be used to discard terms on large scales ($k \ll aH$) [21].

2.2. Curvature and Isocurvature perturbations: An Introduction

The perturbation Φ defined in equation (2.2) is also called the curvature perturbation since the spatial Ricci scalar, which is otherwise zero for the unperturbed universe, is proportional to $\nabla^2\Phi$. This quantity is not gauge invariant, but we can define two gauge invariant quantities related to the curvature perturbation. One is the curvature perturbation on uniform density hypersurfaces, ζ, and the other is the comoving curvature perturbation, $\mathcal{R}$, defined below:

$$-\zeta = \Phi + H\frac{\delta\rho}{\dot{\overline{\rho}}} \tag{2.18}$$

$$\mathcal{R} = \Phi - \frac{H}{\overline{\rho}+\overline{P}}\delta q \tag{2.19}$$

The reason these quantities are important is because we can relate them to the Bardeen potential after the end of inflation, which is further related to the density contrast, an observable quantity, as illustrated in equation (1.38) [4]. In addition, these two quantities can be related to each other which we show below:

$$\begin{aligned}
-\zeta &= \mathcal{R} + \frac{H}{\overline{\rho}+\overline{P}}\delta q + H\frac{\delta\rho}{\dot{\overline{\rho}}} \\
&= \mathcal{R} + \frac{1}{3(\overline{\rho}+\overline{P})}(-\delta\rho_m) \\
&= \mathcal{R} + \frac{2\overline{\rho}}{9(\overline{\rho}+\overline{P})}\left(\frac{k}{aH}\right)^2\Phi_n,
\end{aligned} \tag{2.20}$$

where in the second line, we have used the fact that $\dot{\overline{\rho}} = -3H(\overline{\rho}+\overline{P})$ and in the third line, we have used equation (2.17). One then concludes that on large scales (which are our scales of interest), $-\zeta$ and $\mathcal{R}$ coincide with each other.

Next, we define the isocurvature (entropy) perturbations as

$$\mathcal{S} = H\left(\frac{\delta P}{\dot{\overline{P}}} - \frac{\delta\rho}{\dot{\overline{\rho}}}\right), \tag{2.21}$$

where $\mathcal{S}=0$ implies

$$\frac{\delta\rho_b+\delta\rho_c}{\overline{\rho}_b+\overline{\rho}_c} = \frac{3}{4}\frac{\delta\rho_\gamma+\delta\rho_\nu}{\overline{\rho}_\gamma+\overline{\rho}_\nu}, \tag{2.22}$$

which is further equivalent to

$$\frac{\delta n_b+\delta n_c}{\overline{n}_b+\overline{n}_c} = \frac{\delta n_\gamma+\delta n_\nu}{\overline{n}_\gamma+\overline{n}_\nu}, \tag{2.23}$$

where n is the number density, b stands for baryons, c for cold dark matter, γ for photons and ν for neutrinos [21]. The relation in equation (2.23) is a condition for the constancy of the entropy per matter (baryons + cold dark matter) in the universe, since the entropy per matter $S_{\text{ent}} \sim T^3/(n_b+n_c) \sim (n_\gamma+n_\nu)/(n_b+n_c)$, where T is the temperature of relativistic particles in the early universe (photons + neutrinos) [5]. Therefore, $\mathcal{S}=0$ implies a constant entropy per matter, making equation (2.21) a viable definition for entropy perturbation $\mathcal{S}$. Another great feature about the definition (2.21) is that $\mathcal{S}$ is a gauge invariant quantity. Now, the question is: how are the isocurvature perturbations defined in equation (2.21) related to those defined in equation (1.42)? After all we only care about component wise isocurvature perturbations, in particular the CIPs in our galaxy bias expansion, since these have a much more significant effect on galaxy formation.

First of all, recall that the total matter-radiation isocurvature perturbations defined as

$$\mathcal{S}_{m\gamma} = \left(\frac{\delta n_m}{\overline{n}_m} - \frac{\delta n_\gamma}{\overline{n}_\gamma} \right) \tag{2.24}$$

have been observed by the Planck to contribute less than 2% to the CMB power spectrum [13]. This means we can essentially set $\mathcal{S}_{m\gamma} = 0$. Then, since we can express $\mathcal{S}_{m\gamma} = \frac{\Omega_c}{\Omega_m}\mathcal{S}_{c\gamma} + \frac{\Omega_b}{\Omega_m}\mathcal{S}_{b\gamma} = 0$, we obtain the following condition:

$$\mathcal{S}_{b\gamma} = -\frac{\Omega_c}{\Omega_b}\mathcal{S}_{c\gamma} \tag{2.25}$$

Any isocurvature perturbations between baryonic matter and dark matter that satisfies the condition in equation 2.25 are called CIPs [14]. Now, we can determine the CIPs $\mathcal{S}_{cb}$ as

$$\mathcal{S}_{cb} = \mathcal{S}_{c\gamma} - \mathcal{S}_{b\gamma} = \left(1 + \frac{\Omega_c}{\Omega_b} \right) \mathcal{S}_{c\gamma} \tag{2.26}$$

Therefore $\mathcal{S}_{cb}$ can be completely expressed in terms of $\mathcal{S}_{c\gamma}$. The advantage of this is that there are numerous multi-field inflation models, such as ones with one heavy field and one light field, which predict that $\mathcal{S} = \mathcal{S}_{c\gamma}$ [22]. This would mean that $\mathcal{S}$ is a direct measure of $\mathcal{S}_{cb}$, and therefore incorporating $\mathcal{S}$ into the galaxy bias expansion is akin to incorporating CIPs into the expansion. Unfortunately, it is very difficult to find a direct relationship between $\mathcal{S}$ and $\mathcal{S}_{cb}$ in general, since it would depend on our assumptions of the reheating era. Nevertheless, using other multi-field inflation models as motivation, we will assume $\mathcal{S}$ to be a direct measure of $\mathcal{S}_{cb}$. We will therefore calculate $\mathcal{S}$ in this chapter, and then incorporate it as CIPs into the galaxy bias expansion in the next chapter.

After a long calculation, one can show that in multi-field inflationary setting, $\mathcal{S}$ can be expressed as

$$\mathcal{S} = \frac{2\big(\dot{V} + \sum_I 3H\dot{\varphi}_I^2\big)\delta V + 2\dot{V}\sum_I \dot{\varphi}_I\big(\delta\dot{\varphi}_I - \dot{\varphi}_I A\big)}{3\big(2\dot{V} + \sum_I 3H\dot{\varphi}_I^2\big)\sum_J \dot{\varphi}_J^2}, \tag{2.27}$$

where $\dot{V} = \frac{\partial V}{\partial t}$ and $\delta V = \sum_I V_{\varphi_I}\delta\varphi_I$ [12].

2.3. Single field inflation (revisited)

In this section, we calculate the evolution of the curvature perturbation after horizon exit in single field inflation – the point of this exercise is to show that it is conserved until horizon re-entry in single field inflation. This will contrasted with multi-field inflation later, where the curvature perturbation changes after horizon exit. We determine the curvature perturbation on uniform density surfaces, ζ, instead of the comoving curvature perturbation $\mathcal{R}$ as done in chapter 1, since they have been shown to be equivalent on large scales in section 2.2. First, we calculate the evolution of ζ for a model with any number of fields. After some algebra, one finds that

$$\dot{\zeta} = -H\frac{\dot{\bar{P}}}{\dot{\bar{\rho}}}\left(\frac{k}{aH}\right)^2\Phi_n + 3H\frac{\dot{\bar{P}}}{\dot{\bar{\rho}}}\mathcal{S} \tag{2.28}$$

We want to calculate the change of ζ after horizon exit, since ζ becomes classical on large scales. In the large scale limit, i.e. $k \ll aH$, we have

$$\dot{\zeta} = 3H\frac{\dot{\bar{P}}}{\dot{\bar{\rho}}}\mathcal{S} \tag{2.29}$$

Although equation (2.29) was calculated in Newtonian gauge, it is gauge covariant since ζ and $\mathcal{S}$ are both gauge invariant, and the other terms are background terms. We now specialise the expression to the case of single field inflation. The first step would be to calculate S in single field inflation. Equation (2.27) for one field becomes

$$\begin{aligned}
\mathcal{S} = \frac{2\big(\dot{V} + 3H\dot{\bar{\varphi}}^2\big)\,\delta V + 2\dot{V}\dot{\bar{\varphi}}\left(\dot{\delta\varphi} - \dot{\bar{\varphi}}A\right)}{3\big(2\dot{V} + 3H\dot{\bar{\varphi}}^2\big)\dot{\bar{\varphi}}^2} &= \frac{2V_{\bar{\varphi}}}{3\dot{\bar{\varphi}}^2\left(2V_{\bar{\varphi}} + 3H\dot{\bar{\varphi}}\right)}\left[\dot{\bar{\varphi}}(\dot{\delta\varphi} - \dot{\bar{\varphi}}A) - \ddot{\bar{\varphi}}\delta\varphi\right] \\
&= \frac{2V_{\bar{\varphi}}}{3\dot{\bar{\varphi}}^2\left(2V_{\bar{\varphi}} + 3H\dot{\bar{\varphi}}\right)}\delta\rho_m \\
&= \frac{2V_{\bar{\varphi}}}{3\dot{\bar{\varphi}}^2\left(2V_{\bar{\varphi}} + 3H\dot{\bar{\varphi}}\right))}\left(\frac{k^2}{a^2}\frac{-\Phi_n}{4\pi G}\right) \\
&= -\frac{V_{\bar{\varphi}}}{6\pi G\dot{\bar{\varphi}}^2\left(2V_{\bar{\varphi}} + 3H\dot{\bar{\varphi}}\right)}\left(\frac{k^2}{a^2}\Phi_n\right),
\end{aligned} \tag{2.30}$$

where we invoke equation (2.16) in the second line and equation (2.17) in the third line. Using equations (2.20) and (2.30), we find that in single field inflation,

$$\dot{\zeta} = -\frac{H}{\dot{H}}\frac{k^2}{a^2}\Phi_n \tag{2.31}$$

One then concludes that in single field inflation, on large scales, the isocurvature perturbation $\mathcal{S}$ vanishes and the uniform density curvature perturbation ζ (and $\mathcal{R}$) is conserved outside the horizon [21]. We will now show that this is not necessarily the case in two (or more) field inflation.

2.4. Two field inflation

We consider two fields $\phi = \varphi_1$ and $\chi = \varphi_2$. We make a local rotation in the field space as shown below:

$$\begin{pmatrix} \dot{\overline{\sigma}} \\ \dot{\overline{s}} \end{pmatrix} = \begin{pmatrix} \cos\theta & \sin\theta \\ -\sin\theta & \cos\theta \end{pmatrix} \begin{pmatrix} \dot{\overline{\phi}} \\ \dot{\overline{\chi}} \end{pmatrix}, \tag{2.32}$$

where $\cos\theta = \frac{\dot{\overline{\phi}}}{\sqrt{\dot{\overline{\phi}}^2 + \dot{\overline{\chi}}^2}}$ and $\sin\theta = \frac{\dot{\overline{\chi}}}{\sqrt{\dot{\overline{\phi}}^2 + \dot{\overline{\chi}}^2}}$ [12].

It is evident from equation (2.32) that $\overline{\sigma}$ gives the path length of the classical (background) trajectory. On the other hand, we also see that $\dot{\overline{s}} = 0$, which implies that $\overline{s}$ is constant along the classical trajectory. We call $\overline{\sigma}$ the adiabatic field, while we refer to $\overline{s}$ as the entropy field. The intuition behind this naming will be clear very shortly.

The perturbations $\delta\sigma$ and δs are defined likewise, as shown below:

$$\begin{pmatrix} \delta\sigma \\ \delta s \end{pmatrix} = \begin{pmatrix} \cos\theta & \sin\theta \\ -\sin\theta & \cos\theta \end{pmatrix} \begin{pmatrix} \delta\phi \\ \delta\chi \end{pmatrix} \tag{2.33}$$

The entropy field perturbation δs is zero along the classical trajectory, and perturbations with $\delta s = 0$ describe adiabatic field perturbations $\delta\sigma$ [12]. A sketch is provided in figure 2.1 to demonstrate the decomposition of a field perturbation into adiabatic component $\delta\sigma$ and entropy component δs.

The background fields $\overline{\phi}$ and $\overline{\chi}$ satisfy the following equations of motion.

$$\ddot{\overline{\phi}} + 3H\dot{\overline{\varphi}} + V_\phi = 0 \tag{2.34}$$

$$\ddot{\overline{\chi}} + 3H\dot{\overline{\chi}} + V_\chi = 0, \tag{2.35}$$

Combining these two equations, we see that the adiabatic field satisfies the following equation of motion:

$$\ddot{\overline{\sigma}} + 3H\dot{\overline{\sigma}} + V_\sigma = 0, \tag{2.36}$$

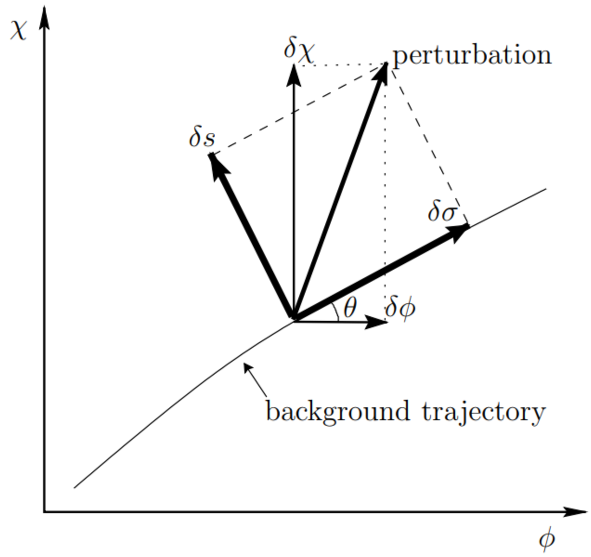

Figure 2.1.: Decomposition of field perturbation into adiabatic component ($\delta\sigma$) and entropy component (δs) [12]

where $V_\sigma = \cos\theta\, V_\phi + \sin\theta\, V_\chi$. On the other hand, the entropy field satisfies

$$\ddot{s} = 0 \tag{2.37}$$

Instead, θ plays the role of the other dynamical quantity for the background, and can be shown to evolve as

$$\dot{\theta} = -\frac{V_s}{\dot{\sigma}}, \tag{2.38}$$

where $V_s = \cos\theta\, V_\chi - \sin\theta\, V_\phi$.

We want to show that in an inflationary model with two or more fields, there is a non vanishing isocurvature perturbation and the uniform density curvature perturbation ζ evolves over time, unlike in the case of single field inflation. We will find that both of these phenomena are sourced by the entropy field perturbations. This result can be produced at first order of perturbations, which is the theory we have been working with so far. However, later on, we will work with second order perturbations, where the aforementioned phenomena still occur, but we get an additional feature of non-Gaussianity in both isocurvature and curvature perturbations. This is crucial since we intend to also incorporate non-Gaussianity into our galaxy bias expansion. Let's first calculate the first order curvature and isocurvature perturbations.

2.4.1. First order curvature and isocurvature perturbations

For two fields, the curvature perturbation on uniform density hypersurfaces is given by:

$$\begin{aligned}\zeta = -\mathcal{R} = -\Phi + \frac{H}{\overline{\rho}+\overline{P}}\delta q &= -\Phi - H\left(\frac{\dot{\overline{\phi}}\delta\phi + \dot{\overline{\chi}}\delta\chi}{\dot{\overline{\phi}}^2 + \dot{\overline{\chi}}^2}\right) \\ &= -\Phi - H\frac{\delta\sigma}{\dot{\overline{\sigma}}}\end{aligned} \tag{2.39}$$

We specialise the expression we obtained for $\mathcal{S}$ in equation (2.27) for multiple fields to the case of two fields. One then obtains the following expression

$$\mathcal{S} = -\frac{V_\sigma}{6\pi G\dot{\overline{\sigma}}^2\left(2V_\sigma + 3H\dot{\overline{\sigma}}\right)}\left(\frac{k^2}{a^2}\Phi\right) + \frac{2HV_s}{\left(2V_\sigma\dot{\overline{\sigma}} + 3H\dot{\overline{\sigma}}^2\right)}\delta s. \tag{2.40}$$

On large scales, the first term can be ignored, and we obtain

$$\mathcal{S} = \frac{2HV_s}{\left(2V_\sigma\dot{\overline{\sigma}} + 3H\dot{\overline{\sigma}}^2\right)}\delta s = -\frac{2HV_s}{\dot{\overline{P}}}\delta s. \tag{2.41}$$

We see that the isocurvature perturbation no longer vanishes, and is sourced by the entropy field perturbation δs. It is now evident that the name for δs is quite fitting. Substituting the above expression into equation (2.29) and using the fact that $\dot{\overline{\rho}} = -3H\dot{\overline{\sigma}}^2$ yields

$$\dot{\zeta} = 2H\frac{V_s}{\dot{\overline{\sigma}}^2}\delta s = -\frac{2H}{\dot{\overline{\sigma}}}\dot{\theta}\delta s \tag{2.42}$$

We can now see that even on large scales, ζ is no longer constant and its evolution is sourced by the entropy perturbation δs. We are mostly interested in auto and cross correlation functions of ζ and $\mathcal{S}$, since we want to incorporate ζ and $\mathcal{S}$ into our galaxy bias expansion. A convenient way to achieve this would be express both ζ and $\mathcal{S}$ in terms of $\delta\sigma$ and δs at the time of horizon crossing, since they can be expressed in terms of $\delta\phi$ and $\delta\chi$ whose correlation functions are known.

Let t_* be the time when relevant perturbation scales exit the Hubble horizon, evaluated on a spatially flat hypersurface. A spatially flat hypersurface is characterised by the gauge fixing $\Phi = E = 0$, where Φ and E are as defined in equation (2.2). Then, at the time of horizon crossing,

$$\zeta(t_*, \boldsymbol{x}) = -\frac{H}{\dot{\overline{\sigma}}}\delta\sigma\bigg|_*, \tag{2.43}$$

where the * represents the value at horizon crossing. Let t_c be some time at the end of inflation, evaluated on a uniform density hypersurface. A uniform density hypersurface is characterised by the gauge fixing $E = 0 = \delta\rho$. The reason we use these specific gauges for t_* and t_c is because later on in section 2.4.2, we will use a formalism called the δN formalism to express ζ, and in that formalism, we require the time at horizon and the time at the end of inflation to be in these specific gauges. The value of ζ at $t = t_c$ is given by

$$\zeta(t_c, \boldsymbol{x}) = -\left(\frac{H}{\dot{\sigma}}\delta\sigma\right)_* - \int_{t_*}^{t_c} \frac{2H}{\dot{\sigma}}\dot{\theta}\delta s \,\mathrm{d}t \tag{2.44}$$

We want to express the second term on the right hand side of the above expression in terms of δs_*. In order to do so, we need to know the evolution of the entropy perturbation δs after horizon crossing. Using equation (2.9), we can find the equation of motion for the entropy field perturbation δs, as presented below:

$$\begin{aligned} \ddot{\delta s} + 3H\dot{\delta s} + \left(\frac{k^2}{a^2} + V_{ss} + 3\dot{\theta}^2\right)\delta s &= -2\frac{\dot{\theta}}{\dot{\sigma}}\delta\rho_m \\ &= \frac{\dot{\theta}}{\dot{\sigma}}\frac{k^2}{2\pi G a^2}\Phi_n, \end{aligned} \tag{2.45}$$

where $V_{ss} = \sin^2\theta V_{\phi\phi} - 2\cos\theta\sin\theta V_{\phi\chi} + \cos^2\theta V_{\chi\chi}$ [12]. On the large scales, the right hand side vanishes and the equation becomes homogeneous. The equation of motion then simplifies to

$$\ddot{\delta s} + 3H\dot{\delta s} + \big(V_{ss} + 3\dot{\theta}^2\big)\delta s = 0 \tag{2.46}$$

To evaluate this further, we define the following slow roll parameters:

$$V_{\sigma s} = -\sin\theta cos\theta V_{\phi\phi} + (\cos^2\theta - \sin^2\theta)V_{\phi\chi} + \cos\theta\sin\theta V_{\chi\chi} \tag{2.47}$$

$$\eta_{\sigma s} = M_{\rm pl}^2\frac{V_{\sigma s}}{V} = -\sin\theta cos\theta\eta_{\phi\phi} + (\cos^2\theta - \sin^2\theta)\eta_{\phi\chi} + \cos\theta\sin\theta\eta_{\chi\chi} \tag{2.48}$$

$$\eta_{ss} = M_{\rm pl}^2\frac{V_{ss}}{V} = \sin^2\theta\eta_{\phi\phi} - 2\cos\theta\sin\theta\eta_{\phi\chi} + \cos^2\theta\eta_{\chi\chi}, \tag{2.49}$$

where $\eta_{\phi\phi} = M_{\rm pl}^2\frac{V_{\phi\phi}}{V}, \eta_{\phi\chi} = M_{\rm pl}^2\frac{V_{\phi\chi}}{V}$ and $\eta_{\chi\chi} = M_{\rm pl}^2\frac{V_{\chi\chi}}{V}$ [23]. Slow roll necessitates that $\eta_{\phi\phi}, \eta_{\phi\chi}$, $\eta_{\chi\chi} \ll 1$, which further implies that $\eta_{ss}, \eta_{\sigma s} \ll 1$. Using the fact that during slow roll, $H^2 = \frac{1}{3M_{\rm pl}}V$, the equation of motion can be further simplified to

$$\ddot{\delta s} + 3H\dot{\delta s} + 3H^2\big(\eta_{ss} + \eta_{\sigma s}^2\big)\delta s = 0 \tag{2.50}$$

Although we don't know precisely what happens at the end of inflation, we will still assume that the slow roll conditions don't completely breakdown. Therefore, we make the assumption that

$\eta_{ss} + \eta_{\sigma s}^2 \ll \frac{1}{2}$ [24]. In that case, one can show that among the two solutions that equation (2.50) yields, one is approximately constant (slowly decaying or growing depending on the sign of $\eta_{ss} + \eta_{\sigma s}^2$) and the other one decays rapidly and hence can be neglected. As a result, we can express δs as

$$\delta s(t_c) = T_{\delta s}(t_c, t_*)\,\delta s_*, \tag{2.51}$$

where $T_{\delta s}(t_c, t_*)$ is the transfer function that tracks the evolution of δs after horizon exit from time t_* to t_c.

As a consequence, equations (2.44) and (2.41) become

$$\zeta(t_c, \boldsymbol{x}) = \left(-\frac{H}{\dot{\sigma}}\right)_* \delta\sigma_* + \left(-\int_{t_*}^{t_c} \frac{2H}{\dot{\sigma}}\dot{\theta}T_{\delta s}(t, t_*)\,\mathrm{d}t\right)\delta s_* \tag{2.52}$$

$$\mathcal{S}(t_c, \boldsymbol{x}) = \left(\frac{2HV_s}{2V_\sigma\dot{\sigma} + 3H\dot{\sigma}^2}\right)_c T_{\delta s}(t_c, t_*)\delta s_* \tag{2.53}$$

We can express this more succinctly as follows

$$\begin{pmatrix} \zeta \\ \mathcal{S} \end{pmatrix} = \begin{pmatrix} T_{\zeta\sigma} & T_{\zeta s} \\ 0 & T_{\mathcal{S}s} \end{pmatrix} \begin{pmatrix} \delta\sigma_* \\ \delta s_* \end{pmatrix}, \tag{2.54}$$

where we have defined

$$T_{\zeta\sigma} = -\frac{H}{\dot{\sigma}}\Big|_*,\ T_{\zeta s} = \left(-\int_{t_*}^{t_c} \frac{2H}{\dot{\sigma}}\dot{\theta}T_{\delta s}(t, t_*)\,\mathrm{d}t\right), \text{ and } T_{\mathcal{S}s} = \left(\frac{2HV_s}{2V_\sigma\dot{\sigma} + 3H\dot{\sigma}^2}\right)_c T_{\delta s}(t_c, t_*) \tag{2.55}$$

Let's now define two quantities: the power spectrum $\mathcal{P}_{\delta\phi_*}(k)$ and two point cross correlation function $\mathcal{P}_{\delta\phi_*\delta\chi_*}(k)$. In the following the definitions are only given for fields $\delta\phi_*$ and $\delta\chi_*$, but these definitions apply in general for any fields, including curvature and isocurvature.

$$\langle\delta\phi_*(\boldsymbol{k})\delta\phi_*(\boldsymbol{k'})\rangle = (2\pi)^3\delta_D^3(\boldsymbol{k} + \boldsymbol{k'})\mathcal{P}_{\delta\phi_*}(k), \tag{2.56}$$

$$\langle\delta\phi_*(\boldsymbol{k})\delta\chi_*(\boldsymbol{k'})\rangle = (2\pi)^3\delta_D^3(\boldsymbol{k} + \boldsymbol{k'})\mathcal{P}_{\delta\phi_*\delta\chi_*}(k). \tag{2.57}$$

We now calculate the power spectrum of the curvature perturbation ζ and isocurvature perturbation $\mathcal{S}$ in terms of the power spectra of the field perturbations at horizon exit. The power spectra of the field perturbations $\delta\phi$ and $\delta\chi$ are given by

$$\mathcal{P}_{\delta\phi_*}(k) = \mathcal{P}_{\delta\chi_*}(k) = \frac{2\pi^2}{k^3}\left(\frac{H}{2\pi}\right)_*^2, \tag{2.58}$$

where the non-Gaussianity in field perturbations at horizon exit is ignored, since the non-

Gaussianity is highly suppressed due to the fact that the local non-Gaussianity parameter of the field perturbations contribute at second power. Using the definition in equation (2.33), we can show that the power spectra for the field perturbations $\delta\sigma$ and δs are given by

$$\mathcal{P}_{\delta\sigma_*}(k) = \mathcal{P}_{\delta s_*}(k) = \frac{2\pi^2}{k^3}\left(\frac{H}{2\pi}\right)^2_* \tag{2.59}$$

In addition, since the two field perturbations $\delta\phi$ and $\delta\chi$ follow a set of equations of motion coupled via the $V_{\phi\chi}$ term, as can be seen from equation (2.9), we obtain a two point cross-correlation function between the two field perturbations. This further translates to a two point cross-correlation function between $\delta\sigma$ and δs, which is presented below

$$\mathcal{P}_{\delta\sigma_*\delta s_*}(k) = -\frac{4C\pi^2}{k^3}\left(\frac{\eta_{\sigma s}H}{2\pi}\right)^2_*, \tag{2.60}$$

where $C = 2 - \ln 2 - \gamma \approx 0.729637$ [25]. The correlation between the field perturbations at horizon exit $C_{\delta\sigma_*\delta s_*}$ is suppressed by the slow roll parameter $\eta_{\sigma s}(t_*)$, which is much less than 1, and hence can be ignored. Using all this information, we can then find the power spectra pertaining to ζ and $\mathcal{S}$

$$\mathcal{P}_\zeta = (T^2_{\zeta\sigma} + T^2_{\zeta s})\mathcal{P}_{\delta\sigma_*} \tag{2.61}$$

$$\mathcal{P}_\mathcal{S} = T^2_{\mathcal{S}s}\mathcal{P}_{\delta\sigma_*} \tag{2.62}$$

$$\mathcal{P}_{\zeta\mathcal{S}} = T_{\zeta s}T_{\mathcal{S}s}\mathcal{P}_{\delta\sigma_*} \tag{2.63}$$

So far, all the analysis that we have done has been performed using first order perturbation theory. We want to go one step further and use second order perturbation theory, precisely with the goal of obtaining three point auto and cross-correlation functions (bispectrum in momentum space). In the next two sections, we derive second order expressions for curvature and isocurvature perturbations respectively, and in the section that follows, we will use these results to obtain the correlation functions.

2.4.2. Second order curvature perturbation and non-Gaussianity

In order to obtain the expression for ζ at second order in field perturbations, we will use the well established δN formalism. The curvature perturbation ζ is gauge invariant, and therefore can be evaluated in any gauge; if we evaluate it at the end of inflation in the uniform density gauge, whilst using a spatially flat gauge for the time at horizon exit, then it turns out that we can express ζ in terms of the number of e-folds as follows:

$$\zeta(t_c, \boldsymbol{x}) = \delta N(t_c, t_*, \boldsymbol{x}) = \mathcal{N}(t_c, t_*, \boldsymbol{x}) - N(t_c, t_*), \tag{2.64}$$

where $\mathcal{N}(t_c, t_*, \boldsymbol{x})$ is the perturbed number of e-folds and $N(t_c, t_*)$ is the unperturbed number of e-folds [27]. This explains why the choice of gauge for t_c and t_* as chosen before is necessary. The above way of expressing ζ in terms of the number of e-folds is referred to as the δN formalism. We can further simplify the above expression by writing $\mathcal{N}(t_c, t_*, x)$ as a function of $\delta\varphi_I(t_*)$, as shown below

$$\mathcal{N}(t_c, \delta\varphi_1(t_*, \boldsymbol{x}), \delta\varphi_2(t_*, \boldsymbol{x})) = N(t_c, t_*) + \sum_{I=1}^{2} N_I \delta\varphi_{I*} + \frac{1}{2}\sum_{I,J=1}^{2} N_{IJ}\delta\varphi_{I*}\delta\varphi_{J*}, \tag{2.65}$$

where $N_I = \frac{\partial N}{\partial \varphi_{I*}}$ and $N_{IJ} = \frac{\partial^2 N}{\partial \varphi_{I*}\partial \varphi_{J*}}$. We have also used the fact that $\mathcal{N}(t_c, \delta\varphi_1(t_*, \boldsymbol{x}) = \delta\varphi_2(t_*, \boldsymbol{x}) = 0) = N(t_c, t_*)$. This then yields

$$\zeta(t_c, \boldsymbol{x}) = \sum_{I=1}^{2} N_I \delta\varphi_{I*} + \frac{1}{2}\sum_{I,J=1}^{2} N_{IJ}\delta\varphi_{I*}\delta\varphi_{J*}. \tag{2.66}$$

Using the expression above, we can express the power spectrum of ζ in terms of that of $\delta\varphi_{I*}$. We know that

$$\langle \delta\varphi_{I*}(\boldsymbol{k})\delta\varphi_{J*}(\boldsymbol{k'})\rangle = \delta_{IJ}(2\pi)^3\delta_D^3(\boldsymbol{k}+\boldsymbol{k'})\mathcal{P}_{\delta\varphi_*}(k), \tag{2.67}$$

where $\mathcal{P}_{\delta\varphi_*}(k) = \frac{2\pi^2}{k^3}\left(\frac{H_*}{2\pi}\right)^2$ and as in the previous section, the correlation between different fields at horizon exit has been ignored as it is slow roll suppressed. Then, using equation (2.66), we deduce that

$$\mathcal{P}_\zeta(k) = \sum_I N_I^2 \mathcal{P}_{\delta\varphi_*}(k). \tag{2.68}$$

In equation (2.66), we see that ζ has been expressed up to second order in field perturbations $\delta\phi_{I*}$, which makes ζ non-Gaussian. There is another effect that could contribute to its non-Gaussianity, even without the second order term in equation (2.66), an effect that we have been ignoring so far – the non-Gaussianity in the field perturbations themselves. We have ignored this so far, primarily because we have been mostly interested in the power spectrum, and in the power spectrum this non-Gaussianity is highly suppressed. We will now show that both these effects will contribute to the non-Gaussianity as expected, but one of them will be negligible and hence ignored. We start by making an ansatz that

$$\zeta(t_c, \boldsymbol{x}) = \zeta_G(t_c, \boldsymbol{x}) - \frac{3}{5} f_{\mathrm{NL}} \zeta_G^2(t_c, \boldsymbol{x}), \tag{2.69}$$

where ζ_G is the Gaussian part of the expression $\sum_{I=1}^{2} N_I \delta\varphi_{I*}$. The bispectrum $\mathcal{B}_\zeta(k_1, k_2, k_3)$ is defined such that

$$\big\langle \zeta(\boldsymbol{k_1})\zeta(\boldsymbol{k_2})\zeta(\boldsymbol{k_3}) \big\rangle = (2\pi)^3 \delta_D^3(\boldsymbol{k_1} + \boldsymbol{k_2} + \boldsymbol{k_3}) \mathcal{B}_\zeta(k_1, k_2, k_3). \tag{2.70}$$

Using these definitions above, it follows that

$$\mathcal{B}_\zeta(k_1, k_2, k_3) = -\frac{6}{5} f_{\mathrm{NL}} \bigg(\mathcal{P}_\zeta(k_1)\mathcal{P}_\zeta(k_2) + 2 \text{ perms} \bigg), \tag{2.71}$$

We will assume that all k's are of the same order of magnitude, so that all relevant scales cross the horizon at similar times, meaning that the Hubble parameter and hence the power spectrum are nearly the same for all the relevant scales. This is a valid assumption since the distances between different points considered for the three point function in position space will be taken to be of the same order of magnitude.

Our goal is to determine an expression for f_{NL}, and we do so by determining the bispectrum using the definition (2.66) and then comparing it to the expression in equation (2.71). The three-point correlation function can be calculated as

$$\begin{aligned}
\big\langle \zeta(\boldsymbol{k_1})\zeta(\boldsymbol{k_2})\zeta(\boldsymbol{k_3}) \big\rangle &= \sum_{I,J,K=1}^{2} N_I N_J N_K \big\langle \delta\varphi_{I*}(\boldsymbol{k_1}) \delta\varphi_{J*}(\boldsymbol{k_2}) \delta\varphi_{K*}(\boldsymbol{k_3}) \big\rangle + \sum_{I,J,K,L=1}^{2} \frac{N_I N_J N_{KL}}{2} \\
&\quad \bigg(\big\langle \delta\varphi_{I*}(\boldsymbol{k_1}) \delta\varphi_{J*}(\boldsymbol{k_2}) (\delta\varphi_{K*} * \delta\varphi_{L*})(\boldsymbol{k_3}) \big\rangle + 2 \text{ perms} \bigg) \\
&= \sum_{I,J,K=1}^{2} N_I N_J N_K \big\langle \delta\varphi_{I*}(\boldsymbol{k_1}) \delta\varphi_{J*}(\boldsymbol{k_2}) \delta\varphi_{K*}(\boldsymbol{k_3}) \big\rangle + (2\pi)^3 \delta_D^3(\boldsymbol{k_1} + \boldsymbol{k_2} + \boldsymbol{k_3}) \\
&\quad \sum_{I,J,K,L=1}^{2} N_I N_J N_{KL} \bigg(\delta_{IK}\delta_{JL} \mathcal{P}_{\delta\varphi_*}(k_1) \mathcal{P}_{\delta\varphi_*}(k_2) + 2 \text{ perms} \bigg),
\end{aligned} \tag{2.72}$$

where

$$(\delta\varphi_{K*} * \delta\varphi_{L*})(\boldsymbol{k}) = \int \frac{\mathrm{d}^3\boldsymbol{k'}}{(2\pi)^3} \delta\varphi_{K*}(\boldsymbol{k'}) \delta\varphi_{L*}(\boldsymbol{k} - \boldsymbol{k'}) \tag{2.73}$$

Going from the first line to the second line in equation (2.72), in the second term, we have ignored the non-Gaussianity in the field perturbations, since the contribution will be at higher order in the non-Gaussianity parameter and thus is highly suppressed. The calculation for the three point correlation function of the field perturbations at horizon exit requires solving the equations of motion for the action up to third order in perturbations. This has already been performed, and the result is given below:

$$\left\langle \delta\varphi_{I*}(\boldsymbol{k_1})\delta\varphi_{J*}(\boldsymbol{k_2})\delta\varphi_{K*}(\boldsymbol{k_3})\right\rangle = (2\pi)^3\delta_D^3(\boldsymbol{k_1}+\boldsymbol{k_2}+\boldsymbol{k_3})\frac{1}{\sum_i k_i^3}\sum_{\text{perms}}\frac{\dot{\varphi}_{I*}\delta_{JK}}{4HM_{\text{pl}}^2}\mathcal{M}(k_1,k_2,k_3) \left(\mathcal{P}_{\delta\varphi_*}(k_1)\mathcal{P}_{\delta\varphi_*}(k_2)+2\text{ perms}\right), \tag{2.74}$$

where

$$\mathcal{M}(k_1,k_2,k_3) = -k_1k_2^2 - 4\frac{k_2^2k_3^2}{\sum_i k_i} + \frac{1}{2}k_1^3 + \frac{k_2^2k_3^2}{(\sum_i k_i)^2}(k_2-k_3), \tag{2.75}$$

and the permutation runs simultaneously over $\{I,J,K\}$ and $\{k_1,k_2,k_3\}$ [30]. When we combine the results from equations (2.72), (2.74) and (2.75), we obtain the following expression for the bispectrum $\mathcal{B}_\zeta(k_1,k_2,k_3)$:

$$\begin{aligned}\mathcal{B}_\zeta(k_1,k_2,k_3) =& \left(\sum_{I,J,K=1}^{2} N_IN_JN_K\frac{1}{\sum_i k_i^3}\sum_{\text{perms}}\frac{\dot{\varphi}_{I*}\delta_{JK}}{4HM_{\text{pl}}^2}\mathcal{M}(k_1,k_2,k_3) + \sum_{I,J=1}^{2}N_IN_JN_{IJ}\right) \\ &\left(\mathcal{P}_{\delta\varphi_*}(k_1)\mathcal{P}_{\delta\varphi_*}(k_2)+2\text{ perms}\right) \\ =& \left(\frac{\sum_{I,J,K}N_IN_JN_K}{(\sum_K N_K^2)^2}\frac{1}{\sum_i k_i^3}\sum_{\text{perms}}\frac{\dot{\varphi}_{I*}\delta_{JK}}{4HM_{\text{pl}}^2}\mathcal{M}(k_1,k_2,k_3) + \frac{\sum_{I,J}N_IN_JN_{IJ}}{(\sum_K N_K^2)^2}\right) \\ &\left(\mathcal{P}_\zeta(k_1)\mathcal{P}_\zeta(k_2)+2\text{ perms}\right)\end{aligned} \tag{2.76}$$

Comparing equations (2.71) and (2.76), we obtain the following expression for $f_{\rm NL}$:

$$\begin{aligned} f_{\rm NL} &= -\frac{5}{6}\left(\frac{\sum_{I,J,K} N_I N_J N_K}{(\sum_K N_K^2)^2}\frac{1}{\sum_i k_i^3}\sum_{\rm perms}\frac{\dot{\varphi}_{I*}\delta_{JK}}{4HM_{\rm pl}^2}\mathcal{M}(k_1,k_2,k_3) + \frac{\sum_{I,J} N_I N_J N_{IJ}}{(\sum_K N_K^2)^2}\right) \\ &= -\frac{5}{6}\left(\frac{\sum_{I,J} N_I \dot{\varphi}_{I*} N_J^2}{(\sum_K N_K^2)^2}\frac{1}{\sum_i k_i^3}\sum_{\rm perms}\frac{\mathcal{M}(k_1,k_2,k_3)}{4HM_{\rm pl}^2} + \frac{\sum_{I,J} N_I N_J N_{IJ}}{(\sum_K N_K^2)^2}\right) \\ &= -\frac{5}{6}\left(\frac{1}{4M_{\rm pl}^2\sum_K N_K^2}\frac{-\mathcal{F}(k_1,k_2,k_3)}{\sum_i k_i^3} + \frac{\sum_{I,J} N_I N_J N_{IJ}}{(\sum_K N_K^2)^2}\right) \\ &= -\frac{5}{6}\left(\frac{\mathcal{P}_{\delta\varphi_*}}{M_{\rm pl}^2\mathcal{P}_\zeta}\left(\frac{-\mathcal{F}(k_1,k_2,k_3)}{4\sum_i k_i^3}\right) + \frac{\sum_{I,J} N_I N_J N_{IJ}}{(\sum_K N_K^2)^2}\right) \\ &= -\frac{5}{6}\left(\frac{r}{8}\left(\frac{-\mathcal{F}(k_1,k_2,k_3)}{4\sum_i k_i^3}\right) + \frac{\sum_{I,J} N_I N_J N_{IJ}}{(\sum_K N_K^2)^2}\right) \end{aligned} \tag{2.77}$$

where in the second line, the permutation only runs over $\{k_1, k_2, k_3\}$ now and in the third line we have used that $\sum_I N_I \dot{\varphi}_{I*} = -H$ and defined $\mathcal{F}(k_1,k_2,k_3) = \sum_{\rm perms}\mathcal{M}(k_1,k_2,k_3)$. In the fourth line, we use that $\mathcal{P}_\zeta = \sum_I N_I^2 \mathcal{P}_{\delta\varphi_*}$, and in the fifth line, we use that the tensor-to-scalar ratio $r = \frac{P_g}{P_\zeta} = \frac{8P_{\delta\varphi_*}}{M_{\rm pl}^2 P_\zeta}$ [31].

A calculation made by Maldacena shows that $0 \leq \frac{-\mathcal{F}(k_1,k_2,k_3)}{\sum_i k_i^3} \leq \frac{11}{12}$ [32]. In addition, the upper bound on the value of r has been calculated to be 0.46 [33]. This means that value of the first term on the right hand side of equation (2.77) is significantly smaller than 1. However, an extensive analysis by Komatsu has shown that the non-Gaussianity can only be measured if the value of $f_{\rm NL}$ exceeds 5, and as a result the contribution due to the first term on the right hand side of equation (2.77) can be ignored [34]. From here on, we can safely approximate the field perturbations at horizon exit as Gaussian fields. On the other hand, we do not have a bound for the second term on the right hand side of equation (2.77) and hence do not know if it is significant enough to have an observational signature. We will assume that it is significant enough for now, so that the non-Gaussianity parameter $f_{\rm NL}$ becomes

$$f_{\rm NL} = -\frac{5}{6}\frac{\sum_{I,J} N_I N_J N_{IJ}}{(\sum_K N_K^2)^2}. \tag{2.78}$$

The curvature perturbation, ζ is given by

$$\zeta = \zeta_G - \frac{3}{5} f_{\rm NL}\zeta_G^2, \tag{2.79}$$

where ζ_G is the Gaussian part of the expression $\sum_{I=1}^2 N_I \delta\varphi_{I*}$. Since we have shown that the non-Gaussianity in the field perturbations at horizon exit can be ignored, this implies that $\zeta_G =$

$\sum_{I=1}^{2} N_I \delta\varphi_{I*}$, where $\delta\varphi_{I*}$ is assumed to be Gaussian. In two field inflation, we have the fields ϕ and χ and rotated fields σ and s. Therefore,

$$\zeta_G = N_\phi \delta\phi_* + N_\chi \delta\chi_* = N_\sigma \delta\sigma_* + N_s \delta s_*, \tag{2.80}$$

where $N_\phi = \frac{\partial N}{\partial \varphi_*}$, $N_\chi = \frac{\partial N}{\partial \chi_*}$, $N_\sigma = N_\phi \cos\theta_* + N_\chi \sin\theta_* = -\frac{H}{\dot{\sigma}}\big|_*$ and $N_s = N_\chi \cos\theta_* - N_\phi \sin\theta_*$.

2.4.3. Second order isocurvature perturbations and non-Gaussianity

So far we have provided a survey of results, most of which was already obtained by various authors. We want to now go a step further and calculate second order contributions to the isocurvature perturbations. Although this has been done for specific potential functions $V(\phi, \chi)$ and with assumptions regarding the reheating era [19], [26], we use a more general approach and obtain a general expression for isocurvature perturbations. We begin by defining field perturbations up to second order as follows

$$\begin{aligned}
&\delta\rho = \delta\rho^{(1)} + \frac{\delta\rho^{(2)}}{2}, \quad \delta P = \delta P^{(1)} + \frac{\delta P^{(2)}}{2}, \quad \delta\varphi_I = \delta\varphi_I^{(1)} + \frac{\delta\varphi_I^{(2)}}{2}, \\
&\delta\sigma = \delta\sigma^{(1)} + \frac{\delta\sigma^{(2)}}{2}, \quad \delta s = \delta s^{(1)} + \frac{\delta s^{(2)}}{2}, \quad \mathcal{S} = \mathcal{S}^{(1)} + \frac{\mathcal{S}^{(2)}}{2}
\end{aligned} \tag{2.81}$$

The expressions for isocurvature perturbations at first and second order have been determined [36]. We have that

$$\mathcal{S}^{(1)} = H\left(\frac{\delta P^{(1)}}{\dot{P}} - \frac{\delta\rho^{(1)}}{\dot{\rho}}\right) \tag{2.82}$$

$$\mathcal{S}^{(2)} = H\left(\frac{\delta P^{(2)}}{\dot{P}} - \frac{\delta\rho^{(2)}}{\dot{\rho}} - \left(\frac{\ddot{P}}{\dot{P}} - \frac{\ddot{\rho}}{\dot{\rho}}\right)\frac{(\delta\rho^{(1)})^2}{\dot{\rho}^2}\right) \tag{2.83}$$

The expression for first order isocurvature is familiar to us and has already been calculated before, and is given by

$$\mathcal{S}^{(1)}(t_c, \boldsymbol{x}) = -\frac{2H}{\dot{P}} V_s \delta s^{(1)} = \left(\frac{2HV_s}{2V_\sigma\dot{\sigma} + 3H\dot{\sigma}^2}\right)_c T_{\delta s^{(1)}} \delta s_*^{(1)} = T_{\mathcal{S}s} \delta s_*^{(1)} \tag{2.84}$$

Recall that all the results that we obtained in sections prior to the 2.4.2 were calculated at first order, and are quoted in this section with a superscript (1) on the perturbations. In order to derive an expression for the second order isocurvature perturbation $\mathcal{S}^{(2)}$, we first need to make a few simplifications. First note that the definitions of P and ρ only differ in the sign of V, as a consequence of which, we obtain the following relations

$$P = \rho - 2V, \quad \dot{P} = \dot{\rho} - 2V_\sigma \dot{\sigma}, \quad \delta P^{(2)} = \delta\rho^{(2)} - 2\left(\sum_{I=1}^{2} V_{\varphi_I}\delta\varphi_I^{(2)} + \frac{1}{2}\sum_{I,J=1}^{2} V_{\varphi_I\varphi_J}\delta\varphi_I^{(1)}\delta\varphi_J^{(1)}\right) \tag{2.85}$$

These relations simplify our expression in equation (2.83):

$$\begin{aligned}
\mathcal{S}^{(2)} =& H\left(\frac{\delta P^{(2)}\dot{\rho} - \delta\rho^{(2)}\dot{P}}{\dot{P}\,\dot{\rho}} - \left(\frac{\ddot{P}}{\dot{P}} - \frac{\ddot{\rho}}{\dot{\rho}}\right)\frac{(\delta\rho^{(1)})^2}{\dot{\rho}^2}\right) \\
=& H\left[\frac{\left(\delta\rho^{(2)} - 2\left(\sum_{I=1}^{2} V_{\varphi_I}\delta\varphi_I^{(2)} + \frac{1}{2}\sum_{I,J=1}^{2} V_{\varphi_I\varphi_J}\delta\varphi_I^{(1)}\delta\varphi_J^{(1)}\right)\right)\dot{\rho} - \delta\rho^{(2)}(\dot{\rho} - 2V_\sigma\dot{\sigma})}{\dot{P}\,\dot{\rho}}\right. \\
& \left. - \left(\frac{\ddot{P}}{\dot{P}} - \frac{\ddot{\rho}}{\dot{\rho}}\right)\frac{(\delta\rho^{(1)})^2}{\dot{\rho}^2}\right] \\
=& H\left[\frac{-2\left(\sum_{I=1}^{2} V_{\varphi_I}\delta\varphi_I^{(2)} + \frac{1}{2}\sum_{I,J=1}^{2} V_{\varphi_I\varphi_J}\delta\varphi_I^{(1)}\delta\varphi_J^{(1)}\right)}{\dot{P}} + \frac{2V_\sigma\dot{\sigma}}{\dot{P}\,\dot{\rho}}\delta\rho^{(2)} - \left(\frac{\ddot{P}}{\dot{P}} - \frac{\ddot{\rho}}{\dot{\rho}}\right)\frac{(\delta\rho^{(1)})^2}{\dot{\rho}^2}\right]
\end{aligned} \tag{2.86}$$

At the end of inflation, $t = t_c$, where t_c is evaluated in uniform density gauge i.e. $\delta\rho^{(1)} = \delta\rho^{(2)} = 0$, and the expression for $\mathcal{S}^{(2)}$ becomes

$$\mathcal{S}^{(2)}(t_c, \boldsymbol{x}) = -\frac{2H}{\dot{P}}\left(\sum_{I=1}^{2} V_{\varphi_I}\delta\varphi_I^{(2)} + \frac{1}{2}\sum_{I,J=1}^{2} V_{\varphi_I\varphi_J}\delta\varphi_I^{(1)}\delta\varphi_J^{(1)}\right) \tag{2.87}$$

The expression for $\mathcal{S}^{(1)}$ turns out to be gauge invariant while the expression for $\mathcal{S}^{(2)}$ turns out to be gauge dependent [36]. We find that a second order quantity that is gauge invariant is the second order isocurvature perturbation on uniform density hypersurfaces as shown below

$$\mathcal{S}^{(2)}_{\text{g.i.}} = \mathcal{S}^{(2)} - \frac{2H}{\dot{P}}\frac{\delta\rho^{(1)}}{\dot{\rho}}\left(\delta P^{(1)} - \frac{\dot{P}}{\dot{\rho}}\delta\rho^{(1)}\right)' \tag{2.88}$$

The quantities $\mathcal{S}^{(2)}_{\text{g.i.}}$ and $\mathcal{S}$ are equal to each other at $t = t_c$, since $\delta\rho^{(1)} = 0$, and therefore we find that

$$\mathcal{S}^{(2)}_{\text{g.i.}}(t_c,\boldsymbol{x}) = \mathcal{S}^{(2)}(t_c,\boldsymbol{x}) = -\frac{2H}{\dot{\overline{P}}}\left(\sum_{I=1}^{2} V_{\varphi_I}\delta\varphi_I^{(2)} + \frac{1}{2}\sum_{I,J=1}^{2} V_{\varphi_I\varphi_J}\delta\varphi_I^{(1)}\delta\varphi_J^{(1)}\right) \tag{2.89}$$

Since we are interested in a gauge invariant quantity, we want $\mathcal{S}_{\text{g.i.}} = \mathcal{S}^{(1)}_{\text{g.i.}} + \frac{\mathcal{S}^{(2)}_{\text{g.i.}}}{2}$, where $\mathcal{S}^{(1)}_{\text{g.i.}} = \mathcal{S}^{(1)}$ and $\mathcal{S}^{(2)}_{\text{g.i.}}$ is defined as above in equation (2.88). Therefore, $\mathcal{S}_{g.i.}$ is the isocurvature perturbation on uniform density hypersurfaces. From here on, we will drop the subscripts and assume that $\mathcal{S}$ denotes an isocurvature perturbation on a uniform density hypersurface. Now, the expression for $\mathcal{S}^{(2)}$ can be written out as

$$\mathcal{S}^{(2)}(t_c,\boldsymbol{x}) = -\frac{2H}{\dot{\overline{P}}}\left(V_\sigma\delta\sigma^{(2)} + V_s\delta s^{(2)} + \frac{1}{2}V_{\sigma\sigma}(\delta\sigma^{(1)})^2 + V_{\sigma s}\delta\sigma^{(1)}\delta s^{(1)} + \frac{1}{2}V_{ss}(\delta s^{(1)})^2\right) \tag{2.90}$$

We will further simplify this expression by showing that $\delta\sigma^{(1)}(t_c,\boldsymbol{x}) = 0$, proven below:

$$\begin{aligned}
\frac{\delta\sigma^1}{\dot{\sigma}} = \frac{\delta\rho^1}{\dot{\rho}} - \frac{\delta\rho^1}{\dot{\rho}} + \frac{\delta\sigma^1}{\dot{\sigma}} = \frac{\delta\rho^1}{\dot{\rho}} - \frac{\delta\rho^1}{\dot{\rho}} + \frac{\delta q^1}{\overline{\rho}+\overline{P}} &= \frac{\delta\rho^1}{\dot{\rho}} - \frac{\delta\rho^1 - 3H\delta q^{(1)}}{\dot{\rho}} \\
&= \frac{\delta\rho^{(1)}}{\dot{\rho}} - \frac{\delta\rho_m^{(1)}}{\dot{\rho}} \\
&= \frac{\delta\rho^{(1)}}{\dot{\rho}} - \left(\frac{k^2}{4\pi Ga^2}\frac{\Phi_n}{\dot{\rho}}\right)
\end{aligned} \tag{2.91}$$

On large scales, the second term of the last line vanishes, and we see that $\delta\sigma^{(1)}(t_c,\boldsymbol{x}) = 0$ since $\delta\rho^{(1)}(t_c,\boldsymbol{x}) = 0$. Equation (2.90) further simplifies to

$$\mathcal{S}^{(2)}(t_c,\boldsymbol{x}) = -\frac{2H}{\dot{\overline{P}}}\left(V_\sigma\delta\sigma^{(2)} + V_s\delta s^{(2)} + \frac{1}{2}V_{ss}(\delta s^{(1)})^2\right) \tag{2.92}$$

The value of $\delta\sigma^{(2)}$ at horizon exit vanishes as we have shown that there is negligible non-Gaussianity at horizon exit. This means that $\delta\sigma^{(2)}$ grows only after horizon exit, sourced by terms that are proportional to $(\delta\sigma^{(1)})^2, \delta\sigma^{(1)}\delta s^{(1)}$ and $(\delta s^{(1)})^2$. The former two quantities vanish at $t = t_c$, since $\delta\sigma^{(1)}(t_c,\boldsymbol{x}) = 0$. Therefore, we can express $\delta\sigma^{(2)}$ as $\delta\sigma^{(2)} = T_{\delta\sigma^{(2)}}(\delta s_*^{(1)})^2$. The same argumentation for $\delta s^{(2)}$ yields $\delta s^{(2)} = T_{\delta s^{(2)}}(\delta s_*^{(1)})^2$. The expression in equation (2.92) then becomes

$$\mathcal{S}^{(2)}(t_c,\boldsymbol{x}) = -\frac{2H}{\dot{\overline{P}}}\left(V_\sigma T_{\delta\sigma^{(2)}} + V_s T_{\delta s^{(2)}} + \frac{1}{2}V_{ss}T^2_{\delta s^{(1)}}\right)(\delta s_*^{(1)})^2 \tag{2.93}$$

Since we have established that at horizon exit, the non-Gaussianity is negligible, we know that $\delta s_*^{(2)} = 0$, meaning that $\delta s_* = \delta s_*^{(1)}$ and hence we can drop the (1) superscript on δs_*. Hence, we have that

$$\mathcal{S}^{(1)}(t_c, \boldsymbol{x}) = -\frac{2H}{\dot{P}} V_s T_{\delta s^{(1)}} \delta s_* = \mathcal{S}_G \tag{2.94}$$

$$\mathcal{S}^{(2)}(t_c, \boldsymbol{x}) = -\frac{\dot{P}}{2H(V_s T_{\delta s^{(1)}})^2} \left(V_\sigma T_{\delta\sigma^{(2)}} + V_s T_{\delta s^{(2)}} + \frac{1}{2} V_{ss} T^2_{\delta s^{(1)}} \right) \mathcal{S}_G^2, \tag{2.95}$$

where $\mathcal{S}_G$ denotes the Gaussian part of the isocurvature perturbation on uniform density hypersurfaces $\mathcal{S}$. We then find that

$$\mathcal{S}(t_c, \boldsymbol{x}) = \mathcal{S}^{(1)}(t_c, \boldsymbol{x}) + \frac{\mathcal{S}^{(2)}(t_c, \boldsymbol{x})}{2} = \mathcal{S}_G + h_{\mathrm{NL}} \mathcal{S}_G^2, \tag{2.96}$$

where

$$h_{\mathrm{NL}} = \frac{\dot{P}}{4H(V_s T_{\delta s^{(1)}})^2} \left(V_\sigma T_{\delta\sigma^{(2)}} + V_s T_{\delta s^{(2)}} + \frac{1}{2} V_{ss} T^2_{\delta s^{(1)}} \right) \Bigg|_c, \tag{2.97}$$

where the subscript c at the end is a reminder that the expression is evaluated at $t = t_c$. Now that we have second order expressions for both ζ and $\mathcal{S}$, we can find the statistics of these fields as we did at first order in section 2.4.1.

2.4.4. Statistics

In this chapter, we have shown that in multi-field inflation, there are two types of perturbations - curvature perturbations ζ and isocurvature perturbations $\mathcal{S}$, in contrast to single field inflation, where we only encounter curvature perturbations ζ. We have gone a step further and actually derived the expressions for ζ and $\mathcal{S}$ up to second order (thereby including non-Gaussianity), as shown below

$$\zeta = \zeta_G - \frac{3}{5} f_{\mathrm{NL}} \zeta_G^2, \quad \mathcal{S} = \mathcal{S}_G + h_{\mathrm{NL}} \mathcal{S}_G^2 \tag{2.98}$$

We know from section 2.4.1 that first order ζ and $\mathcal{S}$ can be expressed as functions of $\delta\sigma_*$ and δs_* (which are both Gaussian), meaning that we can express ζ_G and $\mathcal{S}_G$ as follows

$$\begin{pmatrix} \zeta_G \\ \mathcal{S}_G \end{pmatrix} = \begin{pmatrix} T_{\zeta\sigma} & T_{\zeta s} \\ 0 & T_{\mathcal{S}s} \end{pmatrix} \begin{pmatrix} \delta\sigma_* \\ \delta s_* \end{pmatrix}, \tag{2.99}$$

where $T_{\zeta\sigma}$, $T_{\zeta s}$ and $T_{\mathcal{S}s}$ are as defined in equation (2.55). Since we are interested in galaxy statistics, and their dependence on the statistics of primordial quantities such as ζ and $\mathcal{S}$, we want to find statistical quantities pertaining to ζ and $\mathcal{S}$. We already have the power spectra results from equations (2.61), (2.62), (2.63), which state

$$\mathcal{P}_\zeta = (T_{\zeta\sigma}^2 + T_{\zeta s}^2)\mathcal{P}_{\delta\sigma_*}, \quad \mathcal{P}_\mathcal{S} = T_{\mathcal{S}s}^2\mathcal{P}_{\delta\sigma_*}, \quad \mathcal{P}_{\zeta\mathcal{S}} = T_{\zeta s}T_{\mathcal{S}s}\mathcal{P}_{\delta\sigma_*}. \tag{2.100}$$

Note that the power spectrum doesn't get any contribution from the non-Gaussianity. The non-Gaussianity manifests at first order in bispectrum calculations, as will be evident shortly. In the next section, we will use the Bardeen potential Φ as a measure of the primordial curvature perturbation ζ, since in matter dominated universe, on superhorizon scales (our scales of interest), the two can be related to each other via $\zeta = -\frac{5}{3}\Phi$ and Φ can be directly related to the density perturbation $\delta\rho$ in comoving gauge, which is an observable quantity, via equation (2.10) [32]. Therefore, it makes sense to write the power spectra and bispectra in terms of Φ instead of ζ. The power spectra of ζ and Φ can be related in a straightforward manner as follows

$$\mathcal{P}_\Phi = \frac{9}{25}\mathcal{P}_\zeta, \quad \mathcal{P}_{\Phi\mathcal{S}} = \frac{3}{5}\mathcal{P}_{\zeta\mathcal{S}} \tag{2.101}$$

The next step is to calculate three point correlation functions since we have non-Gaussian contributions from both curvature and isocurvature perturbations. Similar to the relationship between power spectrum and two point correlation function, we can define the bispectrum corresponding to the three point correlation function. The bispectrum of Φ, $\mathcal{B}_\Phi(k_1, k_2, k_3)$, is defined as follows

$$\big\langle \Phi(\boldsymbol{k_1})\Phi(\boldsymbol{k_2})\Phi(\boldsymbol{k_3})\big\rangle = (2\pi)^3\delta_D^3(\boldsymbol{k_1}+\boldsymbol{k_2}+\boldsymbol{k_3})\mathcal{B}_\Phi(k_1,k_2,k_3). \tag{2.102}$$

We first provide a derivation for the bispectrum of like fields, and then use that outline to derive an expression for the bispectrum of different fields. To do so, first note that the relationship between Φ and ζ yields the following expression

$$\Phi(t_c, \boldsymbol{x}) = \Phi_G(t_c, \boldsymbol{x}) + f_{\rm NL}\Phi_G^2(t_c, \boldsymbol{x}) \tag{2.103}$$

We then find that

$$\begin{aligned}\big\langle \Phi(\boldsymbol{k_1})\Phi(\boldsymbol{k_2})\Phi(\boldsymbol{k_3})\big\rangle = f_{\rm NL}\Big(&\big\langle(\Phi_G * \Phi_G)(\boldsymbol{k_1})\Phi_G(\boldsymbol{k_2})\Phi_G(\boldsymbol{k_3})\big\rangle + \big\langle\Phi_G(\boldsymbol{k_1})(\Phi_G * \Phi_G)(\boldsymbol{k_2})\Phi_G(\boldsymbol{k_3})\big\rangle + \\ &\big\langle\Phi_G(\boldsymbol{k_1})\Phi_G(\boldsymbol{k_2})(\Phi_G * \Phi_G)(\boldsymbol{k_3})\big\rangle\Big),\end{aligned} \tag{2.104}$$

where '*' denotes a convolution defined as

$$(\Phi_G * \Phi_G)(\boldsymbol{k_1}) = \int \frac{\mathrm{d}^3 k}{(2\pi)^3} \Phi_G(\boldsymbol{k}) \Phi_G(\boldsymbol{k}_1 - \boldsymbol{k}) \tag{2.105}$$

On the right hand side of equation (2.104), we essentially have four point correlation functions and we know that for Gaussian fields they can be expressed as products of two point correlation functions, which simplifies equation (2.104) to

$$\big\langle \Phi(\boldsymbol{k_1})\Phi(\boldsymbol{k_2})\Phi(\boldsymbol{k_3}) \big\rangle = (2\pi)^3 \delta_D^3(\boldsymbol{k_1} + \boldsymbol{k_2} + \boldsymbol{k_3}) f_{\rm NL} \Big(2\, \mathcal{P}_\Phi(k_2)\mathcal{P}_\Phi(k_3) + 2 \text{ perms} \Big) \tag{2.106}$$

This yields the following expression a familiar expression for the bispectrum

$$\mathcal{B}_\Phi(k_1, k_2, k_3) = 2 f_{\rm NL} \Big(\mathcal{P}_\Phi(k_1)\mathcal{P}_\Phi(k_2) + 2 \text{ perms} \Big), \tag{2.107}$$

which we had previously claimed to be true in equation (2.71). In the exact same manner, one can also determine the bispectrum of $\mathcal{S}$ and finds

$$\mathcal{B}_\mathcal{S}(k_1, k_2, k_3) = 2\, h_{\rm NL} \Big(\mathcal{P}_\mathcal{S}(k_1)\mathcal{P}_\mathcal{S}(k_2) + 2 \text{ perms} \Big), \tag{2.108}$$

We can also define three point cross-correlation functions between Φ and $\mathcal{S}$, as shown below:

$$\big\langle \Phi(\boldsymbol{k_1})\mathcal{S}(\boldsymbol{k_2})\mathcal{S}(\boldsymbol{k_3}) \big\rangle = (2\pi)^3 \delta_D^3(\boldsymbol{k_1} + \boldsymbol{k_2} + \boldsymbol{k_3}) \mathcal{B}_{\Phi\mathcal{S}\mathcal{S}}(k_1, k_2, k_3) \tag{2.109}$$

$$\big\langle \Phi(\boldsymbol{k_1})\Phi(\boldsymbol{k_2})\mathcal{S}(\boldsymbol{k_3}) \big\rangle = (2\pi)^3 \delta_D^3(\boldsymbol{k_1} + \boldsymbol{k_2} + \boldsymbol{k_3}) \mathcal{B}_{\Phi\Phi\mathcal{S}}(k_1, k_2, k_3) \tag{2.110}$$

In order to determine $\mathcal{B}_{\Phi\mathcal{S}\mathcal{S}}(k_1, k_2, k_3)$, we first determine an expression for $\big\langle \Phi(\boldsymbol{k_1})\mathcal{S}(\boldsymbol{k_2})\mathcal{S}(\boldsymbol{k_3}) \big\rangle$, as presented below:

$$\begin{aligned} \big\langle \Phi(\boldsymbol{k_1})\mathcal{S}(\boldsymbol{k_2})\mathcal{S}(\boldsymbol{k_3}) \big\rangle =& f_{\rm NL} \big\langle (\Phi_G * \Phi_G)(\boldsymbol{k_1}) \mathcal{S}_G(\boldsymbol{k_2}) \mathcal{S}_G(\boldsymbol{k_3}) \big\rangle + h_{\rm NL} \big\langle \Phi_G(\boldsymbol{k_1}) (\mathcal{S}_G * \mathcal{S}_G)(\boldsymbol{k_2}) \mathcal{S}_G(\boldsymbol{k_3}) \big\rangle + \\ & h_{\rm NL} \big\langle \Phi_G(\boldsymbol{k_1}) \mathcal{S}_G(\boldsymbol{k_2}) (\mathcal{S}_G * \mathcal{S}_G)(\boldsymbol{k_3}) \big\rangle \Big) \\ =& (2\pi)^3 \delta_D^3(\boldsymbol{k_1} + \boldsymbol{k_2} + \boldsymbol{k_3}) \Big(2 f_{\rm NL} \mathcal{P}_{\Phi\mathcal{S}}(k_2) \mathcal{P}_{\Phi\mathcal{S}}(k_3) + 2 h_{\rm NL} \mathcal{P}_{\Phi\mathcal{S}}(k_1) \mathcal{P}_\mathcal{S}(k_3) + \\ & 2 h_{\rm NL} \mathcal{P}_{\Phi\mathcal{S}}(k_1) \mathcal{P}_\mathcal{S}(k_2) \Big) \end{aligned} \tag{2.111}$$

This yields the following expression for $\mathcal{B}_{\Phi\mathcal{S}\mathcal{S}}(k_1, k_2, k_3)$:

$$\mathcal{B}_{\Phi\mathcal{S}\mathcal{S}}(k_1, k_2, k_3) = \left(2f_{\rm NL}\mathcal{P}_{\Phi\mathcal{S}}(k_2)\mathcal{P}_{\Phi\mathcal{S}}(k_3) + 2h_{\rm NL}\left[\mathcal{P}_{\Phi\mathcal{S}}(k_1)\mathcal{P}_{\mathcal{S}}(k_3) + \mathcal{P}_{\Phi\mathcal{S}}(k_1)\mathcal{P}_{\mathcal{S}}(k_2)\right]\right) \quad (2.112)$$

Using the same procedure, we find the expression for $\mathcal{B}_{\Phi\Phi\mathcal{S}}(k_1, k_2, k_3)$, which reads

$$\mathcal{B}_{\Phi\Phi\mathcal{S}}(k_1, k_2, k_3) = \left(2f_{\rm NL}\left[\mathcal{P}_{\Phi}(k_2)\mathcal{P}_{\Phi\mathcal{S}}(k_3) + \mathcal{P}_{\Phi}(k_1)\mathcal{P}_{\Phi\mathcal{S}}(k_3)\right] + 2\,h_{\rm NL}\mathcal{P}_{\Phi\mathcal{S}}(k_1)\mathcal{P}_{\Phi\mathcal{S}}(k_2)\right) \quad (2.113)$$

These bispectrum terms will appear again in chapter 3, when we try to relate galaxy statistics to statistics of Φ and $\mathcal{S}$.

3. Galaxy bias expansion

Large-scale Structure Surveys (LSS), which map out the positions and redshifts of millions of galaxies, can provide a great deal of information about the primordial universe. This information can then be used to test the predictions of various models of inflation such as single field inflation and multi-field inflation, discussed in previous chapters. In this chapter, we develop the formalism of galaxy bias, which is a technique that allows us to relate the galaxy or tracer density to matter density fields and initial conditions, which has already been introduced in section 1.5. We first discuss the currently established theory of galaxy bias in sections 3.1, 3.2 and 3.3, where we introduce the dependence of galaxy bias on the matter density field and non-Gaussianity in the curvature perturbation. In section 3.4, we introduce CIPs into the bias expansion. We expect CIPs to have a sizeable effect on the bias expansion since these directly affect the abundance of baryonic and dark matter, which further affects the distribution of tracers. Once we incorporate CIPs into the bias expansion, we will investigate the contribution of these perturbations to the galaxy power spectrum and bispectrum, and look for interesting limits where these perturbations have a significant effect on the galaxy statistics.

3.1. Bare bias expansion

Consider a filter function $W_L(\boldsymbol{x})$ of characteristic size R_L, satisfying

$$\int \mathrm{d}^3\boldsymbol{x}\, W_L(\boldsymbol{x}) = 1. \tag{3.1}$$

Assume that W_L is isotropic i.e. $W_L(\boldsymbol{x}) = W_L(|\boldsymbol{x}|)$, as the universe is isotropic on large scales. Then, we can define the coarse grained density field $\delta_L(\boldsymbol{x})$ in terms of the full density field $\delta(\boldsymbol{x})$:

$$\delta_L(\boldsymbol{x}) = \int \mathrm{d}^3\boldsymbol{y}\, W_L(\boldsymbol{x}-\boldsymbol{y})\delta(\boldsymbol{y}), \tag{3.2}$$

and the small-scale density field as the difference between δ and δ_L:

$$\delta_s(\boldsymbol{x}) = \delta(\boldsymbol{x}) - \delta_L(\boldsymbol{x}) \tag{3.3}$$

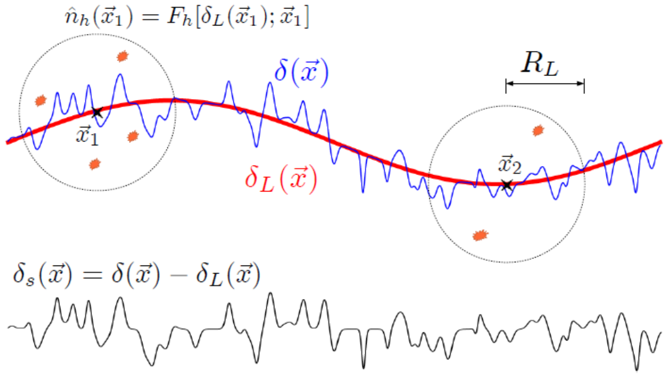

Figure 3.1.: Decomposition of matter density perturbation δ into large scale perturbations δ_L and small scale density field δ_s [20]

One can understand the coarse-graining as a way of averaging within a region $\mathcal{U}$ of size R_L centred at the position $\boldsymbol{x}$. The coarse grained density field $\delta_L(\boldsymbol{x})$ and the small scale density field $\delta_s(\boldsymbol{x})$ have been illustrated pictorially in figure 3.1. The number of tracers (orange dots in figure 3.1) within the region $\mathcal{U}$ is the weighted sum of the filter function at the discrete locations of the tracers:

$$n_{h,L}(\boldsymbol{x}) = \sum_i W_L(\boldsymbol{x}_i - \boldsymbol{x}), \tag{3.4}$$

where i runs over all the tracers in the region $\mathcal{U}$ and the expectation value of $n_{h,L}$ is calculated by averaging over N different regions $\mathcal{U}$ and taking the limit $N \to \infty$ [17]. Since we will always consider the tracer number density to be averaged over a region $\mathcal{U}$ of size R_L, we will drop the subscript L on $n_{h,L}(\boldsymbol{x})$. The task now is to relate the tracer density to the matter density perturbation.

We can write $n_h(\boldsymbol{x})$ as a general functional of the matter density field:

$$n_h(\boldsymbol{x}) = F_{h,L}(\delta_L(\boldsymbol{x}); \delta_s(\boldsymbol{y})), \tag{3.5}$$

where $|\boldsymbol{x} - \boldsymbol{y}| \lesssim R_*$, and $R_L \gg R_*$. The functional above depends on the value of the matter density field in the non-locality scale R_* (discussed earlier in section 1.5) through its dependence on $\delta_s(\boldsymbol{y})$ around $\boldsymbol{x}$; on the other hand, the functional depends on δ_L locally. This can be explained by the fact that the coarse graining scale R_L is taken to be much larger than the non-locality scale R_*, which means that the value of δ_L is more or less the same over a region of size R_*. This allows us to expand the tracer density in a Taylor series of $\delta_L(\boldsymbol{x})$:

$$n_h(\boldsymbol{x}) = \sum_{n=0}^{\infty} \frac{1}{n!} F_{h,L}^{(n)}(0;\delta_s)\,[\delta_L(\boldsymbol{x})]^n, \tag{3.6}$$

where

$$F_{h,L}^{(n)}(0;\delta_s) = \left.\frac{\partial^n F_{h,L}(\delta_L;\delta_s)}{\partial \delta_L^n}\right|_{\delta_L=0} \tag{3.7}$$

A key assumption that we will make is that the correlation of the small scale density fluctuations with large-scale perturbations is negligible. We now take the expectation value of equation (3.6) over realizations of the density field to obtain

$$\langle n_h \rangle = \sum_{n=0}^{\infty} \frac{1}{n!} \langle F_{h,L}^{(n)}(0;\delta_s)\rangle\,\langle \delta_L^n \rangle, \tag{3.8}$$

where we have used the negligible correlation between δ_L and δ_s to treat the factors involving δ_L and δ_s as independent random variables. We define bias parameters as

$$c_n = \frac{1}{\langle F_{h,L}(0;\delta_s)\rangle} \langle F_{h,L}^{(n)}(0;\delta_s)\rangle, \tag{3.9}$$

and the bias expansion becomes

$$\langle n_h \rangle = \langle F_{h,L}(0;\delta_s)\rangle \sum_{n=0}^{\infty} \frac{c_n}{n!}\,\langle \delta_L^n \rangle. \tag{3.10}$$

We now determine the correlation function ξ_h of tracers. In order to determine the correlation function at separation r, we need $R_L < r$ to hold in order to avoid large effects from the coarse graining. However, the final expression for the correlation function should be independent of the value of the coarse graining scale. The correlation function between tracers located at positions $\boldsymbol{x}_1$ and $\boldsymbol{x}_2$ separated by a distance $r = |\boldsymbol{x}_1 - \boldsymbol{x}_2|$ is given by

$$\xi_h(r) = \left\langle \left(\frac{n_h(1) - \langle n_h\rangle}{\langle n_h\rangle}\right)\left(\frac{(n_h(2) - \langle n_h\rangle)}{\langle n_h\rangle}\right)\right\rangle = \frac{\langle n_h(1) n_h(2)\rangle}{\langle n_h\rangle^2} - 1, \tag{3.11}$$

where '1' and '2' stand for positions $\boldsymbol{x}_1$ and $\boldsymbol{x}_2$ respectively [20]. Assuming that $F_{h,L}^{(n)}(0;\delta_s)$ at two locations separated by r can be treated as independent random variables, we use equation (3.6) to rewrite the above expression:

$$\xi_h(r) = \frac{1}{\mathcal{N}^2} \sum_{n,m=0}^{\infty} \frac{c_n}{n!}\frac{c_m}{m!} \langle \delta_L^n(1)\delta_L^m(2)\rangle - 1, \tag{3.12}$$

where

$$\mathcal{N} = \sum_{n=0}^{\infty} \frac{c_n}{n!} \langle \delta_L^n \rangle. \tag{3.13}$$

The correlation function $\xi_h(r)$ contains disconnected pieces such as $\langle \delta_L^2 \rangle$, $\langle \delta_L^3 \rangle$, and higher moments, multiplied by the bare bias parameters c_n. So, we essentially have terms in the sum in equation (3.12) which are products of R_L dependent coefficients and R_L dependent disconnected moments of the density field, and therefore convergence of the sum necessitates that the disconnected moments are much less than one. However, one would expect that a physically reasonable perturbative bias model for $\xi_h(r)$ would converge as long as the connected matter correlators are much less than one. One could get around this problem by reordering the sum into a sum of R_L independent coefficients multiplying only connected matter correlators. In effective field theory, this would be seen as renormalisation of bare parameters c_n into "renormalised" parameters b_N [17]. This is done in the section below.

3.2. PBS and renormalised bias parameters

Consider $\Pi_{n,m}$, the set of all partitions of

$$\{\underbrace{1, 1, \ldots, 1}_{\text{n times}}, \underbrace{2, 2, \ldots, 2}_{\text{m times}}\} \tag{3.14}$$

Then, we can express a two point correlation function of δ_L^n and δ_L^m separated by a distance r:

$$\langle \delta_L^n(1) \delta_L^m(2) \rangle = \sum_{\sigma \in \prod_{n,m}} \prod_{B \in \sigma} \left\langle \delta_L^{n_1(B)}(1)\, \delta_L^{n_2(B)}(2) \right\rangle_c, \tag{3.15}$$

where $n_1(B)$ and $n_2(B)$ represent the number of elements '1' and '2' in block B respectively. The above expression, although complicated, is a direct consequence of Wick's theorem, which essentially states that any correlation function is a sum of product of lower order correlators. This product of correlators clearly contains disconnected pieces such as $\langle \delta_L^2 \rangle$. We now define a correlation function that does not involve these disconnected pieces; we call it the no-zero lag (nzl) correlator, defined below

$$\langle \delta_L^n(1) \delta_L^m(2) \rangle_{\text{nzl}} = \sum_{\sigma \in \prod_{n,m}^{\text{nzl}}} \prod_{B \in \sigma} \left\langle \delta_L^{n_1(B)}(1)\, \delta_L^{n_2(B)}(2) \right\rangle_c, \tag{3.16}$$

where

$$\Pi_{n,m}^{\text{nzl}} = \{\sigma \in \Pi_{n,m} : \ \forall B \in \sigma,\ n_1(B) > 0 \ \&\ n_2(B) > 0\}. \tag{3.17}$$

It is clear that $\Pi^{\mathrm{nzl}}_{n,m}$ only contains partitions in which each block B has at least one '1' and one '2'. This means that the no-zero lag correlator consists of products of only connected correlators. This is exactly the kind of expression we would want in our two point tracer correlation function $\xi_h(r)$. One can then write the two point tracer correlation function in terms of the no-zero lag correlators [18] as

$$\xi_h(r) = \sum_{N,M=0}^{\infty} \frac{b_N}{N!}\frac{b_M}{M!}\langle \delta_L^N(1)\delta_L^M(2)\rangle_{\mathrm{nzl}}, \tag{3.18}$$

where

$$b_N = \frac{1}{\mathcal{N}}\sum_{n=N}^{\infty}\frac{c_n}{n!}\frac{n!}{(n-N)!}\langle\delta_L^{n-N}\rangle. \tag{3.19}$$

The b_N defined above are R_L independent, as required. This can be shown explicitly using the Peak Background Split (PBS) argument, which goes as follows: Since the tracer density can be described solely through its dependence on δ_L, the abundance of tracers in a region $\mathcal{U}$ with an overdensity $\delta_L = D$ can be approximated by the abundance of tracers in a fictitious FRW spacetime with modified background density given by

$$\overline{\rho}' = \overline{\rho}(1+D). \tag{3.20}$$

This idea is referred to as the "separate universe" approach [37]. Equation (3.20) is equivalent to perturbing the matter density by a fixed amount of uniform matter density $\Delta\overline{\rho} = D\overline{\rho}$ everywhere, where D is considered infinitesimal. Under such a perturbation, the matter density in a region with overdensity δ_L becomes

$$\overline{\rho}_L = \overline{\rho}(1+\delta_L) \to \overline{\rho}(1+\delta_L) + \Delta\overline{\rho} = \overline{\rho}(1+\delta_L+D) \tag{3.21}$$

Then the mean abundance of tracers in the region $\mathcal{U}$ becomes

$$\langle n_h\rangle|_D = \langle F_{h,L}(0;\delta_s)\rangle\sum_{n=0}^{\infty}\frac{c_n}{n!}\langle(\delta_L+D)^n\rangle, \tag{3.22}$$

where $F_{h,L}$ and c_n refer to a Universe with background density $\overline{\rho}$, i.e. $D = 0$. One can then show that the renormalised bias parameters defined in equation (3.19) can be expressed as

$$b_N = \frac{1}{\langle n_h\rangle|_{D=0}}\left.\frac{\partial^N\langle n_h\rangle|_D}{\partial D^N}\right|_{D=0}. \tag{3.23}$$

With the help of (3.20), this can be further expressed as

$$b_N = \frac{\overline{\rho}^N}{\langle n_h \rangle} \left. \frac{\partial^n \langle n_h \rangle}{\partial \overline{\rho}^N} \right|_{D=0}, \tag{3.24}$$

where the derivatives are calculated at the fiducial value of $\overline{\rho}$. We now see that b_N quantify the response of the cosmic mean abundance of tracers to a change in background matter density, and hence is independent of the fictitious coarse graining scale R_L. In addition, the expression above also illustrates that the exact expression for the function $F_{h,L}$ is not necessary for our analysis. This is in contrast to c_n, which measures the average response of the abundance of tracers within a region $\mathcal{U}$ to a change in the value of δ_L within that region, evaluated at $\delta_L = 0$ [17].

So, now that we have managed to express the two point tracer correlation function in terms of R_L independent bias parameters and products of connected matter correlators, it would seem like our worries have been put to rest. Unfortunately, that is only partially true. It turns out that if the matter density fields are Gaussian, then the expression in equation (3.18) is free of disconnected matter correlations; however, for non-Gaussian density fields, that is not the case. Let's first consider the Gaussian case. In this case, the no-zero lag condition requires $\delta_L(1)$ and $\delta_L(2)$ to appear in equal powers in the nzl correlators. As a result, the nzl correlators separate into products of $\langle \delta_L(1)\delta_L(2) \rangle$ as shown below

$$\langle \delta_L^N(1)\delta_L^M(2) \rangle_{\rm nzl} = N!\, [\langle \delta_L(1)\delta_L(2) \rangle]^N \delta_{NM} = N!\, [\xi_L(r)]^N \delta_{NM}, \tag{3.25}$$

where we have defined

$$\xi_L(r) = \langle \delta_L(1)\delta_L(2) \rangle. \tag{3.26}$$

Then, the two point tracer correlation function becomes

$$\xi_h(r) = \sum_N^\infty \frac{b_N^2}{N!} [\xi_L(r)]^N, \tag{3.27}$$

which is devoid of any disconnected matter correlators. Things become a lot more complicated when the initial conditions are non-Gaussian. We consider this scenario in the next section.

3.3. Non-Gaussian initial conditions

We consider non-Gaussianity of the local type in Bardeen potential, as defined in equation (2.103), and the non-Gaussianity in the density perturbation is derived from the Bardeen potential via the transfer function. In Fourier space, the density field and the Bardeen potential Φ are related via

$$\delta(\boldsymbol{k}, z) = \mathcal{M}(k)\Phi(\boldsymbol{k}), \tag{3.28}$$

where

$$\mathcal{M}(k) = \frac{2}{3}\frac{k^2 T(k) g(z)}{\Omega_m H_0^2 (1+z)}. \tag{3.29}$$

Here, $T(k)$ is the matter transfer function and $g(z)$ is the linear growth rate of the gravitational potential during the matter dominated epoch. At first order in $f_{\rm NL}$, the only relevant correlation function is the bispectrum:

$$\mathcal{B}_m(\boldsymbol{k}_1, \boldsymbol{k}_2, \boldsymbol{k}_3) = \mathcal{M}(k_1)\mathcal{M}(k_2)\mathcal{M}(k_3)\mathcal{B}_\Phi(\boldsymbol{k}_1, \boldsymbol{k}_2, \boldsymbol{k}_3), \tag{3.30}$$

where the subscript ‘m’ stands for matter and will be used for correlation functions of density fields only, and the expression for $\mathcal{B}_\Phi(\boldsymbol{k}_1, \boldsymbol{k}_2, \boldsymbol{k}_3)$ is as presented in equation (2.107). Let’s now turn our attention to the two point tracer correlation function. In order to see where the “problem” lies, it is sufficient to express the correlator at first order in $f_{\rm NL}$:

$$\xi_h(r) = b_1^2 \xi_L(r) + b_1 b_2 \langle \delta_L(1)\delta_L^2(2)\rangle + \mathcal{O}(\delta_L^4), \tag{3.31}$$

where the leading order non-Gaussianity appears in the second term. It can be expressed as

$$\langle \delta_L(1)\delta_L^2(2)\rangle = \int \frac{\mathrm{d}^3 k}{(2\pi)^3} e^{i\boldsymbol{k}.\boldsymbol{x}_1} \int \frac{\mathrm{d}^3 k_1}{(2\pi)^3} e^{i\boldsymbol{k}_1.\boldsymbol{x}_2} \int \frac{\mathrm{d}^3 k_2}{(2\pi)^3} e^{i\boldsymbol{k}_2.\boldsymbol{x}_2} \mathcal{M}_L(k)\mathcal{M}_L(k_1)\mathcal{M}_L(k_2)\langle \phi(\boldsymbol{k})\phi(\boldsymbol{k}_1)\phi(\boldsymbol{k}_2)\rangle, \tag{3.32}$$

where $\mathcal{M}_L(\boldsymbol{k}) = \mathcal{M}(\boldsymbol{k})\tilde{W}(\boldsymbol{k})$ and $\tilde{W}(\boldsymbol{k})$ is the Fourier transform of the filter function $W(\boldsymbol{x})$. Using equation (2.104), equation (3.32) simplifies to

$$\begin{aligned}\langle \delta_L(1)\delta_L^2(2)\rangle = \int \frac{\mathrm{d}^3 k}{(2\pi)^3} e^{i\boldsymbol{k}.\boldsymbol{r}} \int \frac{\mathrm{d}^3 k_1}{(2\pi)^3} \mathcal{M}_L(k)\mathcal{M}_L(k_1)\mathcal{M}_L(|\boldsymbol{k}+\boldsymbol{k}_1|)\, 2 f_{\rm NL} \big(\mathcal{P}_\Phi(k)\mathcal{P}_\Phi(k_1) \\ + \mathcal{P}_\Phi(k)\mathcal{P}_\Phi(|\boldsymbol{k}+\boldsymbol{k}_1|) + \mathcal{P}_\Phi(k_1)\mathcal{P}_\Phi(|\boldsymbol{k}+\boldsymbol{k}_1|)\big)\end{aligned} \tag{3.33}$$

The calculation further requires a bit of work and has been done in [17]. The reasoning can be summarised as follows: $\boldsymbol{k} \sim 1/r$, $\boldsymbol{k}_1 \sim 1/R_L$, and since $r \gg R_L$, we have $\boldsymbol{k} \ll \boldsymbol{k}_1$. We can therefore approximate $M_L(|\boldsymbol{k}+\boldsymbol{k}_1|) \sim M_L(k_1)$ and $\mathcal{P}_\Phi(|\boldsymbol{k}+\boldsymbol{k}_1|) = \mathcal{P}_\Phi(k_1)$. Then, the expression in (3.33) becomes

$$\begin{aligned}\langle \delta_L(1)\delta_L^2(2)\rangle = \int \frac{\mathrm{d}^3 k}{(2\pi)^3} e^{i\boldsymbol{k}.\boldsymbol{r}} \int \frac{\mathrm{d}^3 k_1}{(2\pi)^3} \mathcal{M}_L(k)\mathcal{M}_L^2(k_1)\, 2 f_{\rm NL} \big(\mathcal{P}_\Phi(k)\mathcal{P}_\Phi(k_1) + \mathcal{P}_\Phi(k)\mathcal{P}_\Phi(k_1) \\ + \mathcal{P}_\Phi(k_1)\mathcal{P}_\Phi(k_1)\big)\end{aligned} \tag{3.34}$$

Assuming $P_\Phi(k) \propto k^{-3}$, we obtain $P_\Phi(k_1)/P_\Phi(k) \sim (R_L/r)^3$, which allows us to neglect the last term in the expression above. So the expression becomes

$$\langle \delta_L(1)\delta_L^2(2)\rangle = 4f_{\rm NL}\int \frac{\mathrm{d}^3k}{(2\pi)^3}e^{i\boldsymbol{k}.\boldsymbol{r}}\mathcal{M}_L(k)\mathcal{P}_\Phi(k)\int \frac{\mathrm{d}^3k_1}{(2\pi)^3}\mathcal{M}_L^2(k_1)\mathcal{P}_\Phi(k_1) = 4f_{\rm NL}\sigma_L^2\xi_{\Phi\delta,L}(r), \tag{3.35}$$

where

$$\xi_{\Phi\delta,L}(r) = \int \frac{\mathrm{d}^3k}{(2\pi)^3}e^{i\boldsymbol{k}.\boldsymbol{r}}\mathcal{M}_L(k)\mathcal{P}_\Phi(k). \tag{3.36}$$

We can see the expression in equation (3.35) is strongly R_L dependent through σ_L^2. This shows us that in the case of non-Gaussian initial conditions, expressing $\xi_h(r)$ in terms of R_L independent bias parameters and connected matter correlators is not sufficient as the non-Gaussianity can still give rise to disconnected correlators such as σ_L^2 [20]. To get around this problem, we have to include the dependence of $n_h(r)$ through an additional variable, so that when the correlation function associated with this variable is included in the sum, we can redefine the renormalised bias parameters in such a way that they absorb the disconnected correlators coming from non-Gaussian terms like $\langle \delta_L(1)\delta_L^2(2)\rangle$. The amplitude of small scale fluctuations do just that. So far, we have ignored the correlation between small scale and large scale fluctuations, and although that is appropriate in the Gaussian case, things are more complicated when the initial conditions are non-Gaussian. In the non-Gaussian case, modes couple, and there are large scale modulations of small scale fluctuations, and therefore small scale fluctuations need to be included in the bias expansion. We shall do so now.

The small scale density field is defined as local fluctuations around the coarse grained density field δ_L, as shown below

$$\begin{aligned}\delta_s(\boldsymbol{x}) &:= \delta_*(\boldsymbol{x}) - \delta_L(\boldsymbol{x}) \\ &= \int \mathrm{d}^3\boldsymbol{y}[W_*(\boldsymbol{x}-\boldsymbol{y}) - W_L(\boldsymbol{x}-\boldsymbol{y})]\delta(\boldsymbol{y}) \\ &= \int \frac{\mathrm{d}^3\boldsymbol{k}}{(2\pi)^3}\, e^{i\boldsymbol{k}.\boldsymbol{x}}\, \tilde{W}_s(k)\delta(\boldsymbol{k})\,,\end{aligned} \tag{3.37}$$

where $\tilde{W}(k)$ is the Fourier transform of $W(|\boldsymbol{x}|)$ and

$$\tilde{W}_s(k) = \tilde{W}_*(k) - \tilde{W}_L(k). \tag{3.38}$$

Next, consider the correlation between the small scale density field δ_s and coarse grained field δ_L:

$$\langle \delta_s(\boldsymbol{x})\delta_L(\boldsymbol{y})\rangle = \int \frac{\mathrm{d}^3\boldsymbol{k}}{(2\pi)^3}\, e^{i\boldsymbol{k}.\boldsymbol{r}}\, \tilde{W}_L(k)\tilde{W}_s(k)\mathcal{P}(k) \xrightarrow{|\boldsymbol{x}-\boldsymbol{y}|\gg R_L} 0, \tag{3.39}$$

since in the large scale limit $|\boldsymbol{x}-\boldsymbol{y}| = r \gg R_L$, $k \sim 1/r$ and therefore $\tilde{W}_s(k) \approx 0$. Intuitively this happens since on the scale $k \sim 1/r$, there is very little overlap between $\tilde{W}_L(k)$ and $\tilde{W}_s(k)$. One can similarly show that on large scales, $\xi_s(r) = \langle \delta_s(\boldsymbol{x})\delta_s(\boldsymbol{y})\rangle \to 0$. Therefore, in the Gaussian case, δ_s and higher powers of δ_s have no large scale correlations, since all the higher order correlators for Gaussian fields can be expressed in terms of lower order cross correlation and auto correlation functions, both of which become zero on large scales as shown above. However, in the non-Gaussian case, the non-Gaussianities can kick in and modulate the correlators – the correlators $\langle \delta_s(\boldsymbol{x})\delta_L(\boldsymbol{y})\rangle$ and $\langle \delta_s(\boldsymbol{x})\delta_s(\boldsymbol{y})\rangle$ still vanish on large scales, but the correlator $\langle \delta_s^2(\boldsymbol{x})\delta_L(\boldsymbol{y})\rangle$ no longer vanishes and therefore needs to be included in the bias expansion [20]. Since the leading order contribution comes from δ_s^2, we define

$$y_*(\boldsymbol{x}) = \frac{1}{2}\left(\frac{\delta_s^2(\boldsymbol{x})}{\sigma_s^2} - 1\right), \tag{3.40}$$

where

$$\sigma_s^2 = \int \frac{\mathrm{d}^3\boldsymbol{k}}{(2\pi)^3}\, |\tilde{W}_s(k)|^2\mathcal{P}(k). \tag{3.41}$$

We now include the dependence of tracer density on y_*:

$$n_h(\boldsymbol{x}) = F_{h,L}(\delta_L(\boldsymbol{x}), y_*(\boldsymbol{x}); \delta_s). \tag{3.42}$$

The tracer density field can then be expressed as

$$n_h(\boldsymbol{x}) = \sum_{n,m=0}^{\infty} \frac{F_{h,L}^{(n,m)}(0;\delta_s)}{n!m!}\, \delta_L^n(\boldsymbol{x}) y_*^m(\boldsymbol{x}). \tag{3.43}$$

We can take the expectation value of the equation (3.43):

$$\langle n_h\rangle = \langle F_{h,L}(0;\delta_s)\rangle \sum_{n,m=0}^{\infty} \frac{c_{nm}}{n!m!}\, \langle \delta_L^n y_*^m\rangle, \tag{3.44}$$

where

$$c_{nm} = \frac{1}{\langle F_{h,L}(0;\delta_s)\rangle}\left\langle F_{h,L}^{(n,m)}(0;\delta_s)\right\rangle \tag{3.45}$$

Now, we want to redefine the renormalised bias parameters such that they absorb disconnected correlators such as the one obtained in equation (3.32). To do so, we use an analogous approach to the one we took in section 3.2 [20]. We consider the following transformations

$$\begin{aligned} \delta_L(\boldsymbol{x}) &\to (1+\varepsilon)\delta_L(\boldsymbol{x}) + D \\ y_*(\boldsymbol{x}) &\to y_*(\boldsymbol{x}) + \left(\varepsilon + \frac{\varepsilon^2}{2}\right)\frac{\delta_s^2(\boldsymbol{x})}{\sigma_s^2}. \end{aligned} \tag{3.46}$$

Under this transformation, the mean tracer density becomes

$$\langle n_h \rangle = \langle F_{h,L}(0;\delta_s)\rangle \sum_{n,m=0}^{\infty} \frac{c_{nm}}{n!m!} \left\langle [(1+\varepsilon)\delta_L + D]^n \left[y_* + \left(\varepsilon + \frac{\varepsilon^2}{2}\right)\frac{\delta_s^2}{\sigma_s^2}\right]^m \right\rangle. \tag{3.47}$$

Then, we can define PBS (renormalised) bias parameters analogous to equation (3.23):

$$b_{NM} = \frac{1}{\langle n_h \rangle|_{D=0,\varepsilon=0}} \left.\frac{\partial^{N+M}\langle n_h\rangle|_{D,\varepsilon}}{\partial D^N \partial \varepsilon^M}\right|_{D=0,\varepsilon=0}. \tag{3.48}$$

Letting $M = 0$ in equation (3.48), then we find $b_{N0} = b_N$. Now, recall the expression for correlation function:

$$\xi_h(r) = \frac{\langle n_h(1) n_h(2)\rangle}{\langle n_h\rangle^2} - 1 = \frac{1}{\mathcal{N}^2} \sum_{n,m,k,l=0}^{\infty} \frac{c_{nm}}{n!m!}\frac{c_{kl}}{k!l!} \left\langle \delta_L^n(1) y_*^m(1) \delta_L^k(2) y_*^l(2) \right\rangle - 1, \tag{3.49}$$

where

$$\mathcal{N} = \sum_{n,m=0}^{\infty} \frac{c_{nm}}{n!m!} \langle \delta_L^n y_*^m \rangle. \tag{3.50}$$

For simplicity, let's only consider terms in equation (3.49) that need to be renormalised to get rid of the disconnected correlator σ_L^2 in the expression for $\langle \delta_L(1)\delta_L^2(2)\rangle$. We consider terms at first order in f_{NL} and up to fourth order in perturbations, since without these restrictions we would have to sum infinitely many terms. Then it turns out that we only need two other terms:$\langle \delta_L(1) y_*(2)\rangle$ and $\langle \delta_L^3(1) y_*(2)\rangle$ [20]. Then, we have

$$\xi_h(r) \supset \frac{2}{\mathcal{N}^2}\left(c_{10}c_{01}\langle \delta_L(1) y_*(2)\rangle + \frac{c_{10}c_{20}}{2}\langle \delta_L(1)\delta_L^2(2)\rangle + \frac{c_{30}c_{01}}{6}\langle \delta_L^3(1) y_*(2)\rangle \right), \tag{3.51}$$

where the factor of 2 at the front is due to symmetry under exchange of positions '1' and '2'. We already know from equation (3.35) that $\langle \delta_L(1)\delta_L^2(2)\rangle = 4 f_{\mathrm{NL}} \sigma_L^2 \xi_{\Phi\delta,L}(r)$. Using the exact same procedure, one can show that

$$\langle \delta_L(1) y_*(2) \rangle = \frac{1}{2} \left\langle \delta_L(1) \frac{\delta_s^2(2)}{\sigma_s^2} \right\rangle = 2 f_{\rm NL} \xi_{\Phi\delta,L}(r). \tag{3.52}$$

We can also find an expression for $\langle \delta_L^3(1) y_*(2) \rangle$:

$$\langle \delta_L^3(1) y_*(2) \rangle = 3 \langle \delta_L^2(1) \rangle \langle \delta_L(1) y_*(2) \rangle = 6 f_{\rm NL} \sigma_L^2 \xi_{\Phi\delta,L}(r). \tag{3.53}$$

The above two expressions also show that at first order in non-Gaussianity, $y_*(\boldsymbol{x})$ can be treated as equivalent to $2 f_{\rm NL} \Phi(\boldsymbol{x})$ [20]. This simplification will be useful later on when we calculate more correlation functions. Focusing back on the issue at hand, the expression in equation (3.51) becomes

$$\begin{aligned} \xi_h(r) \supset & \frac{2}{\mathcal{N}^2} \left(c_{10} c_{01} + c_{10} c_{20} \sigma_L^2 + \frac{c_{30} c_{01}}{2} \sigma_L^2 \right) 2 f_{\rm NL} \xi_{\Phi\delta,L}(r) \\ = & \frac{2}{\mathcal{N}^2} \left(c_{10} c_{01} + c_{10} c_{20} \sigma_L^2 + \frac{c_{30} c_{01}}{2} \sigma_L^2 \right) \langle \delta_L(1) y_*(2) \rangle. \end{aligned} \tag{3.54}$$

Using the expression in equation (3.48), it can be shown that

$$b_{10} = \frac{1}{\mathcal{N}} \left(c_{10} + \frac{c_{30}}{2} \sigma_L^2 + \dots \right) \tag{3.55}$$

$$b_{01} = \frac{1}{\mathcal{N}} \left(c_{10} + c_{20} \sigma_L^2 + \dots \right). \tag{3.56}$$

The expression in equation (3.54) then simplifies to

$$\xi_h(r) \supset 2 b_{10} b_{01} \langle \delta_L(1) y_*(2) \rangle = 2 b_{10} b_{01} 2 f_{\rm NL} \xi_{\Phi\delta,L}(r), \tag{3.57}$$

which does not contain any disconnected correlators. Therefore the disconnected correlator in $\langle \delta_L(1) \delta_L^2(2) \rangle$ has been absorbed by the "new" (renormalised) bias parameters. Other disconnected correlators in the expansion can be taken care of in a similar manner. This completes our introduction to non-Gaussianity in the bias expansion. In the next section, we will add one more variable – the CIPs.

3.4. Compensated Isocurvature perturbations in the bias expansion

One of the predictions of multi-field inflation is that the primordial perturbations are non-adiabatic, meaning that there can be perturbations between different energy components, and we call them isocurvature perturbations. The matter-radiation isocurvature perturbations are observationally constrained to be very small. Regardless, the matter-radiation isocurvature perturbations would have a negligible effect anyway, since the formation of galaxies and clusters only depend on the matter content. The bias coefficient for such a perturbation has been found to be much less than 1 [14]. The isocurvature perturbations that contribute to the bias expansion are the CIPs, which are relative perturbations in number density of baryonic matter and dark matter, first defined in equation (2.26), since such a perturbation would have a direct effect on the formation of tracers such as galaxies and clusters as their formation highly depend on the abundance of baryonic matter and dark matter in their vicinity. It has been shown that the bias parameter for CIPs is of order 1, meaning that it is indeed a significant contributor to the galaxy bias expansion [14]. In this section, we incorporate these CIPs into the galaxy bias expansion. Recall that in section 2.2, we established that we can use $\mathcal{S}$ as a measure of CIPs, and therefore we incorporate $\mathcal{S}$ into our galaxy bias expansion. We do so by generalising the tracer density field that we have encountered in the previous sections to include $\mathcal{S}$, as shown below:

$$n_h(\boldsymbol{x}) = \sum_{n=0}^{\infty} \frac{F_{h,L}^{(n,m,l)}(0;\delta_s)}{n!m!l!}\,\delta_L^n(\boldsymbol{x})y_*^m(\boldsymbol{x})\mathcal{S}_L^l(\boldsymbol{x}). \tag{3.58}$$

Using this tracer density field, we now determine the galaxy statistics in terms of statistics of the initial conditions (y_* and $\mathcal{S}$) and the density field δ. This is done in the following section.

3.4.1. Two point function

Recall that the correlation function is defined as

$$\xi_h(r) = \left\langle \left(\frac{n_h(1) - \langle n_h\rangle}{\langle n_h\rangle}\right)\left(\frac{(n_h(2) - \langle n_h\rangle)}{\langle n_h\rangle}\right)\right\rangle = \frac{\langle n_h(1)n_h(2)\rangle}{\langle n_h\rangle^2} - 1, \tag{3.59}$$

To make our calculations simpler, we define

$$f(\boldsymbol{x}) = \sum_{n=0}^{\infty} \frac{c_{nml}}{n!m!l!}\,\delta_L^n(\boldsymbol{x})y_*^m(\boldsymbol{x})\mathcal{S}_L^l(\boldsymbol{x}) - 1, \tag{3.60}$$

where

$$c_{nml} = \frac{1}{\langle F_{h,L}(0;\delta_s)\rangle}\left\langle F_{h,L}^{(n,m,l)}(0;\delta_s)\right\rangle \tag{3.61}$$

Then one can show that the correlation function $\xi_h(r)$ becomes

$$\xi_h(r) = \left\langle \left(\frac{f(1) - \langle f\rangle}{\mathcal{N}}\right)\left(\frac{f(2) - \langle f\rangle)}{\mathcal{N}}\right)\right\rangle = \frac{1}{\mathcal{N}^2}(\langle f(1)f(2)\rangle - \langle f\rangle^2, \tag{3.62}$$

where

$$\mathcal{N} = \sum_{n=0}^{\infty} \frac{c_{nml}}{n!m!l!} \langle \delta_L^n y_*^m \mathcal{S}_L^l \rangle \tag{3.63}$$

We want to determine the correlation function at second order in perturbations, so we will ignore any higher order terms. First note that

$$\langle f \rangle = \frac{c_{200}}{2}\sigma^2_{\delta,L} + \frac{c_{020}}{2}\langle y_*^2 \rangle + \frac{c_{002}}{2}\sigma^2_{\mathcal{S},L} + c_{110}\langle \delta_L y_* \rangle + c_{011}\langle \mathcal{S}_L y_* \rangle + c_{101}\langle \delta_L \mathcal{S}_L \rangle + \text{higher order terms} \tag{3.64}$$

The above expression implies that $\langle f \rangle^2$ is fourth order in perturbations and can be ignored. Therefore,

$$\begin{aligned}
\xi_h(r) =& \frac{1}{\mathcal{N}^2}\langle f(1)f(2) \rangle \\
=& \frac{1}{\mathcal{N}^2}\langle (c_{100}\delta_L + c_{010}y_* + c_{001}\mathcal{S}_L)(1)\ (c_{100}\delta_L + c_{010}y_* + c_{001}\mathcal{S}_L)(2) \rangle \\
=& \frac{1}{\mathcal{N}^2}\Bigg(c_{100}^2\langle \delta_L(1)\delta_L(2) \rangle + 2c_{100}c_{010}\langle \delta_L(1)y_*(2) \rangle + 2c_{100}c_{001}\langle \delta_L(1)\mathcal{S}_L(2) \rangle \\
&+ c_{010}^2\langle y_*(1)y_*(2) \rangle + 2c_{010}c_{001}\langle y_*(1)\mathcal{S}_L(2) \rangle + c_{001}^2\langle \mathcal{S}_L(1)\mathcal{S}_L(2) \rangle \Bigg).
\end{aligned} \tag{3.65}$$

Renormalisation becomes very straightforward in this case, since there are no zero lag terms, meaning that there are no disconnected correlators that need to be absorbed. So, if we define renormalised bias parameters b_{nml} using the peak background split approach as we have done previously, but incorporating an additional transformation of S_L, then the bias parameters b_{nml} simply equate to

$$b_{nml} = \frac{1}{\mathcal{N}} c_{nml} \tag{3.66}$$

As a result, the expression in equation (3.65) becomes

$$\begin{aligned}
\xi_h(r) =\ & b_{100}^2\langle \delta_L(1)\delta_L(2) \rangle + 2b_{100}b_{010}\langle \delta_L(1)y_*(2) \rangle + 2b_{100}b_{001}\langle \delta_L(1)\mathcal{S}_L(2) \rangle + b_{010}^2\langle y_*(1)y_*(2) \rangle \\
&+ 2b_{010}b_{001}\langle y_*(1)\mathcal{S}_L(2) \rangle + b_{001}^2\langle \mathcal{S}_L(1)\mathcal{S}_L(2) \rangle.
\end{aligned} \tag{3.67}$$

The individual terms of the sum are presented may be expressed as

$$\langle\delta_L(1)\delta_L(2)\rangle = \xi_{\delta\delta,L}(r) = \int \frac{\mathrm{d}^3\boldsymbol{k}}{(2\pi)^3} e^{i\boldsymbol{k}.\boldsymbol{r}} \left|\mathcal{M}_L(k)\right|^2 \mathcal{P}_\Phi(k) = \int \frac{\mathrm{d}^3\boldsymbol{k}}{(2\pi)^3} e^{i\boldsymbol{k}.\boldsymbol{r}} \left|\mathcal{M}(k)\right|^2 \mathcal{P}_\Phi(k) \tag{3.68}$$

$$\langle\delta_L(1)y_*(2)\rangle = 2f_{\mathrm{NL}}\xi_{\phi\delta,L}(r) = 2f_{\mathrm{NL}} \int \frac{\mathrm{d}^3\boldsymbol{k}}{(2\pi)^3} e^{i\boldsymbol{k}.\boldsymbol{r}} \mathcal{M}_L(k)\mathcal{P}_\Phi(k) = 2f_{\mathrm{NL}} \int \frac{\mathrm{d}^3\boldsymbol{k}}{(2\pi)^3} e^{i\boldsymbol{k}.\boldsymbol{r}} \mathcal{M}(k)\mathcal{P}_\Phi(k) \tag{3.69}$$

$$\langle\delta_L(1)\mathcal{S}_L(2)\rangle = \xi_{\delta\mathcal{S},L}(r) = \int \frac{\mathrm{d}^3\boldsymbol{k}}{(2\pi)^3} e^{i\boldsymbol{k}.\boldsymbol{r}} \mathcal{M}_L(k)\tilde{W}_L(k)\mathcal{P}_{\Phi S}(k) = \int \frac{\mathrm{d}^3\boldsymbol{k}}{(2\pi)^3} e^{i\boldsymbol{k}.\boldsymbol{r}} \mathcal{M}(k)\mathcal{P}_{\Phi S}(k) \tag{3.70}$$

$$\langle y_*(1)y_*(2)\rangle = 4f_{\mathrm{NL}}^2\xi_{\Phi\Phi}(r) = 4f_{\mathrm{NL}}^2 \int \frac{\mathrm{d}^3\boldsymbol{k}}{(2\pi)^3} e^{i\boldsymbol{k}.\boldsymbol{r}} \mathcal{P}_\Phi(k) = 4f_{\mathrm{NL}}^2 \int \frac{\mathrm{d}^3\boldsymbol{k}}{(2\pi)^3} e^{i\boldsymbol{k}.\boldsymbol{r}} \mathcal{P}_\Phi(k) \tag{3.71}$$

$$\langle y_*(1)\mathcal{S}_L(2)\rangle = 2f_{\mathrm{NL}}\xi_{\phi\mathcal{S},L}(r) = 2f_{\mathrm{NL}} \int \frac{\mathrm{d}^3\boldsymbol{k}}{(2\pi)^3} e^{i\boldsymbol{k}.\boldsymbol{r}} \tilde{W}_L(k)\mathcal{P}_{\Phi\mathcal{S}}(k) = 2f_{\mathrm{NL}} \int \frac{\mathrm{d}^3\boldsymbol{k}}{(2\pi)^3} e^{i\boldsymbol{k}.\boldsymbol{r}} \mathcal{P}_{\Phi\mathcal{S}}(k) \tag{3.72}$$

$$\langle\mathcal{S}_L(1)\mathcal{S}_L(2)\rangle = \xi_{\mathcal{S}\mathcal{S},L}(r) = \int \frac{\mathrm{d}^3\boldsymbol{k}}{(2\pi)^3} e^{i\boldsymbol{k}.\boldsymbol{r}} |\tilde{W}_L(k)|^2 \mathcal{P}_\mathcal{S}(k) = \int \frac{\mathrm{d}^3\boldsymbol{k}}{(2\pi)^3} e^{i\boldsymbol{k}.\boldsymbol{r}} \mathcal{P}_\mathcal{S}(k), \tag{3.73}$$

where in the last step of each equation, we have assumed $\tilde{W}_L(k) \approx 1$. Since we are working on very large scales $r \gg R_L$, we can equivalently take the limit $R_L \to 0$. In this limit, $W_L(\boldsymbol{x}-\boldsymbol{y})$ approximates to a delta function $\delta^{(3)}(\boldsymbol{x}-\boldsymbol{y})$, and in Fourier space that translates to $\tilde{W}_L(k) \approx 1$. Therefore, from here on, we assume $\tilde{W}_L(k) \approx 1$ and $\mathcal{M}_L(k) \approx \mathcal{M}(k)$.

We now intend to plot the various contributions. Before we do so, we need to make various assumptions about some unknown parameters. The value of f_{NL} has been constrained by the Planck Collaboration to be -0.9 ± 5.1 [11]. For our purposes, we take $f_{\mathrm{NL}} = 1$, with no other justification than that it lies within the range of values. We also need to approximate the power spectrum of $\mathcal{S}$ and the cross spectrum of $\mathcal{S}$ and Φ. To do so, first recall that at first order in perturbations, we have the following result:

$$\begin{pmatrix} \Phi \\ \mathcal{S} \end{pmatrix} = \begin{pmatrix} T_{\Phi\sigma} & T_{\Phi s} \\ 0 & T_{\mathcal{S}s} \end{pmatrix} \begin{pmatrix} \delta\sigma_* \\ \delta s_* \end{pmatrix}, \tag{3.74}$$

where we have defined

$$T_{\Phi\sigma} = -\frac{3}{5}\frac{H}{\dot{\bar{\sigma}}}\Big|_*, T_{\Phi s} = \left(-\int_{t_*}^{t_c} \frac{3}{5}\frac{2H}{\dot{\bar{\sigma}}}\dot{\theta}T_{\delta s}(t,t_*)\,\mathrm{d}t\right), \text{ and } T_{\mathcal{S}s} = \left(\frac{2HV_s}{2V_\sigma\dot{\bar{\sigma}} + 3H\dot{\bar{\sigma}}^2}\right)_c T_{\delta s}(t_c,t_*).$$

Recall that $\delta\sigma_*$ and δs_* have the same power spectra. In addition, we can assume that the transfer functions $T_{\Phi\sigma}$, $T_{\Phi s}$ and $T_{\mathcal{S}s}$ are slowly changing functions of time since they involve slowly varying background quantities such as H and $\dot{\bar{\sigma}}$. This means that the transfer functions barely affect the k-dependence of Φ and $\mathcal{S}$, and therefore we can expect the power spectrum of $\mathcal{S}$ to be the same form as that of Φ [24]. The amplitude of $\mathcal{P}_\mathcal{S}$ is usually taken to be about 1 to 10 times larger than that of $\mathcal{P}_\Phi$, but being conservative, we have taken it to be 1 [14]. In order to find the cross spectrum of Φ and $\mathcal{S}$, recall that we have already established in equation (2.60) that $\delta\sigma_*$ and δs_* have negligible correlation, and therefore $\mathcal{P}_{\Phi\mathcal{S}}$ only depends on relative contributions of $T_{\Phi\sigma}$ and $T_{\Phi s}$. We write $P_{\Phi\mathcal{S}}$ as

$$P_{\Phi\mathcal{S}} = r\sqrt{P_\Phi P_\mathcal{S}}, \tag{3.75}$$

where r is the correlation coefficient and is between -1 and 1. So if $T_{\Phi\sigma} = 0$, then Φ and $\mathcal{S}$ are perfectly correlated and r is either 1 or -1. On the other hand, if $T_{\Phi s} = 0$, then Φ and $\mathcal{S}$ are uncorrelated and r is 0. We have no knowledge of the exact expressions for $T_{\Phi\sigma}$ and $T_{\Phi s}$, so we make an assumption of a weak positive correlation, with $r = 0.5$. With these assumptions, the power spectra for various terms that contribute to the galaxy power spectrum have been plotted in figure 3.2. The power spectrum $\mathcal{P}_\phi$, the transfer function and parameters necessary for the growth factor $\mathcal{M}(k)$ were all evaluated using the **CLASS** code [42], [43]. Note that we had to make various assumptions in order to come up with these plots, and different assumptions will result in different plots.

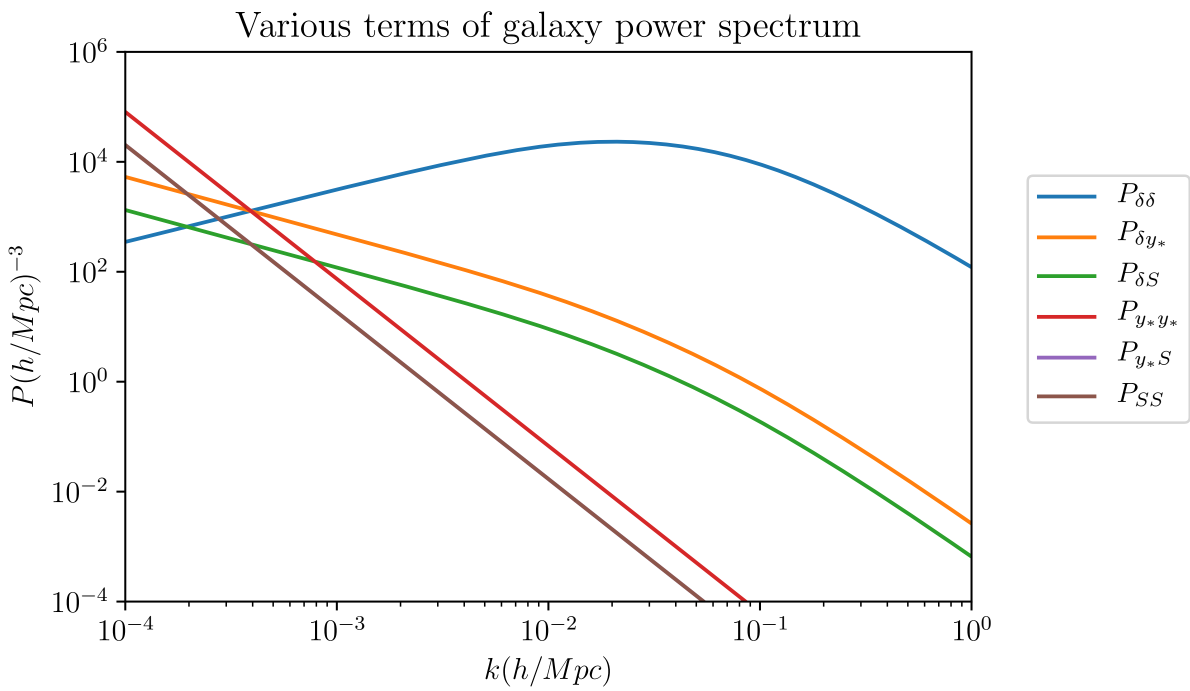

Figure 3.2.: Plotting the contributions of various terms in equation (3.67) to the galaxy power spectrum (First note that we have a slight change of convention as we use $\mathcal{P}_{\delta\delta}$ instead of $\mathcal{P}_\delta$, $\mathcal{P}_{y_* y_*}$ instead of $\mathcal{P}_{y_*}$ and $\mathcal{P}_{\mathcal{S}\mathcal{S}}$ instead of $\mathcal{P}_\mathcal{S}$, as this new convention highlights the fields involved in the power spectrum, making the subsequent explanations easier to follow. Also note that the plots of $\mathcal{P}_{y_*\mathcal{S}}$ and $\mathcal{P}_{\mathcal{S}\mathcal{S}}$ coincide - this is simply a coincidence due to our choice of r.)

In figure 3.2, we have a log-log graph of the various terms that contribute to the galaxy power spectrum. We see that the power spectrum terms involving only y_* and $\mathcal{S}$, i.e. $\mathcal{P}_{y_*y_*}$, $\mathcal{P}_{y_*\mathcal{S}}$ and $\mathcal{P}_{\mathcal{SS}}$ are all linear (log-linear = power law) with gradients of approximately three. This is because $y_*(= 2f_{\rm NL}\Phi)$ and $\mathcal{S}$ are both primordial quantities and therefore their dimensionless power spectra are nearly scale invariant (assuming that Φ and $\mathcal{S}$ have the same power spectrum and that they are positively correlated), meaning the power spectra $\mathcal{P}_{y_*y_*}$, $\mathcal{P}_{y_*\mathcal{S}}$ and $\mathcal{P}_{\mathcal{SS}}$ nearly scale as k^{-3}. In contrast, $P_{\delta\delta}$ has a completely different shape. This is because the density field δ gets an extra contribution of $\mathcal{M}(k,z)$ compared to Φ (and hence $\mathcal{S}$). The factor $\mathcal{M}(k,z)$ gets a contribution of k^2 due to the fact that $\delta \propto \nabla^2\Phi$ [4]. On small scales (large k), there is an extra factor of k^{-2} in $\mathcal{M}(k,z)$ due to the fact that Φ decays as k^{-2} at horizon re-entry during radiation dominated era (which happens for all k greater than $0.02h/Mpc$) [3]. As a result, we see that the power spectrum of $\mathcal{P}_{\delta\delta}$ scales as $k\,(= k^{-3} * (k^2)^2)$ until the turnover point of around $0.02h/Mpc$, after which the power spectrum scales as $k^{-3}\,(= k^{-3} * (k^2)^2 * (k^{-2})^2)$ [8]. In addition, we also have terms such as $\mathcal{P}_{\delta y_*}$ and $\mathcal{P}_{\delta\mathcal{S}}$, which contain both the evolved density field and the primordial perturbations, and their power spectra, as seen in figure 3.2 lie in the "middle".

The analysis above explains the shapes of the various power spectra terms, but it doesn't explain the large discrepancy in the values of the power spectra. The contribution of $\mathcal{P}_{\delta\delta}$ is the largest across all relevant values of $k\,(> 10^{-3}h/Mpc)$. This is because of the fact the density field perturbation δ grows at some locations (and declines at others) over time as matter evolves under gravitational forces, resulting in very large overdensities and underdensities. This growth is also encapsulated in the factor of $M(k,z)$ relating $\delta(k,z)$ to the primordial curvature perturbations $\Phi(k)$. On the other hand, the power spectrum terms involving only y_* and $\mathcal{S}$ don't enjoy the effect of the growth factor $\mathcal{M}(k,z)$. The power spectrum terms involving one primordial perturbation do enjoy the effect of the growth factor $\mathcal{M}(k,z)$, but not as much as the power spectrum term involving only the matter density field. We see that on small scales (large k), only $P_{\delta\delta}$ is significant, and the other power spectra contribute very negligibly on these scales. However, on large scales (small k), as the power spectra terms such as $\mathcal{P}_{y_*y_*}$, $\mathcal{P}_{y_*\mathcal{S}}$ and $\mathcal{P}_{\mathcal{SS}}$ get contributions of k^{-3} and $\mathcal{P}_{\delta y_*}$ and $\mathcal{P}_{\delta\mathcal{S}}$ get contributions of $k^{-3/2}$, they overtake $\mathcal{P}_{\delta\delta}$ when k is of the order $10^{-4}h/Mpc$, as shown in figure 3.2. One way to understand this is that large scales exit the causal horizon much earlier than small scales during inflation and as a result the fluctuations there do not have the chance to "homogenize", and therefore remain large. What this means for us is that if we are to look for signatures of primordial perturbations, we would have to search for them on very large scales, as these are the scales where they can have significant effects on the galaxy power spectrum.

3.4.2. Three point function

The tracer three point function can provide us with more information regarding the primordial perturbations, since we want to determine PNG in curvature perturbations and isocurvature perturbations. The tracer three function function can be defined as

$$\xi_{hhh}(\boldsymbol{x}_1, \boldsymbol{x}_2, \boldsymbol{x}_3) = \left\langle \left(\frac{n_h(1) - \langle n_h \rangle}{\langle n_h \rangle} \right) \left(\frac{(n_h(2) - \langle n_h \rangle)}{\langle n_h \rangle} \right) \left(\frac{n_h(3) - \langle n_h \rangle}{\langle n_h \rangle} \right) \right\rangle, \tag{3.76}$$

which can be re-expressed using the definition of the function $f(\boldsymbol{x})$ in equation (3.60) as

$$\begin{aligned}\xi_{hhh}(\boldsymbol{x}_1, \boldsymbol{x}_2, \boldsymbol{x}_3) &= \left\langle \left(\frac{f(1) - \langle f \rangle}{\mathcal{N}} \right) \left(\frac{f(2) - \langle f \rangle)}{\mathcal{N}} \right) \left(\frac{f(3) - \langle f \rangle)}{\mathcal{N}} \right) \right\rangle \\ &= \frac{1}{\mathcal{N}^3} \Big(\langle f(1)f(2)f(3) \rangle - \langle f(1)f(2) \rangle \langle f \rangle - \langle f(2)f(3) \rangle \langle f \rangle - \langle f(1)f(3) \rangle \langle f \rangle + 2\langle f \rangle^3 \Big)\end{aligned} \tag{3.77}$$

We want to calculate $\xi_{hhh}(r)$ up to fourth order in perturbations (as products of 2 two point functions). Then, the $\langle f \rangle^3$ term in the expression above can be ignored since it is sixth order in perturbations. On the other hand, terms such as $\langle f(1)f(2) \rangle \langle f \rangle$ get rid of all the zero lag terms at the fourth order (it becomes evident after some thought). This means that similar to the calculation of the two point function, there are no disconnected correlators to be absorbed and therefore the renormalised bias parameters b_{nml} may be expressed as

$$b_{nml} = \frac{1}{\mathcal{N}} c_{nml} \tag{3.78}$$

We can now express the tracer three point function in terms of the field perturbations. The result has been presented in the following page (for reasons that will be clear very very shortly).

$$
\begin{aligned}
&\xi_{hhh}(\boldsymbol{x}_1, \boldsymbol{x}_2, \boldsymbol{x}_3)\\
=&\frac{1}{\mathcal{N}^3}\langle f(1)f(2)f(3)\rangle_{\rm nzl}\\
=&\frac{1}{\mathcal{N}^3}\Big\langle\Big(c_{100}\delta_L + c_{010}y_* + c_{001}\mathcal{S}_L + \frac{c_{200}}{2}\delta_L^2 + \frac{c_{020}}{2}y_*^2 + \frac{c_{002}}{2}\mathcal{S}_L^2 + c_{110}\delta_L y_* + c_{101}\delta_L\mathcal{S}_L + c_{011}y_*\mathcal{S}_L\Big)(1)\\
&\Big(c_{100}\delta_L + c_{010}y_* + c_{001}\mathcal{S}_L + \frac{c_{200}}{2}\delta_L^2 + \frac{c_{020}}{2}y_*^2 + \frac{c_{002}}{2}\mathcal{S}_L^2 + c_{110}\delta_L y_* + c_{101}\delta_L\mathcal{S}_L + c_{011}y_*\mathcal{S}_L\Big)(2)\\
&\Big(c_{100}\delta_L + c_{010}y_* + c_{001}\mathcal{S}_L + \frac{c_{200}}{2}\delta_L^2 + \frac{c_{020}}{2}y_*^2 + \frac{c_{002}}{2}\mathcal{S}_L^2 + c_{110}\delta_L y_* + c_{101}\delta_L\mathcal{S}_L + c_{011}y_*\mathcal{S}_L\Big)(3)\Big\rangle_{\rm nzl}\\
=&\, b_{100}^3\langle\delta_L(1)\delta_L(2)\delta_L(3)\rangle_{\rm nzl} + b_{010}^3\langle y_*(1)y_*(2)y_*(3)\rangle_{\rm nzl} + b_{001}^3\langle\mathcal{S}_L(1)\mathcal{S}_L(2)\mathcal{S}_L(3)\rangle_{\rm nzl}\\
&+ b_{100}^2 b_{010}\big(\langle\delta_L(1)\delta_L(2)y_*(3)\rangle_{\rm nzl} + 2\text{ perms}\big) + b_{100}^2 b_{001}\big(\langle\delta_L(1)\delta_L(2)\mathcal{S}_L(3)\rangle_{\rm nzl} + 2\text{ perms}\big)\\
&+ b_{100}b_{001}^2\big(\langle\delta_L(1)\mathcal{S}_L(2)\mathcal{S}_L(3)\rangle_{\rm nzl} + 2\text{ perms}\big) + b_{100}b_{010}^2\big(\langle\delta_L(1)y_*(2)y_*(3)\rangle_{\rm nzl} + 2\text{ perms}\big)\\
&+ b_{010}b_{001}^2\big(\langle y_*(1)\mathcal{S}_L(2)\mathcal{S}_L(3)\rangle_{\rm nzl} + 2\text{ perms}\big) + b_{010}^2 b_{001}\big(\langle y_*(1)y_*(2)\mathcal{S}_L(3)\rangle_{\rm nzl} + 2\text{ perms}\big)\\
&+ b_{100}b_{010}b_{001}\big(\langle\delta_L(1)y_*(2)\mathcal{S}_L(3)\rangle_{\rm nzl} + 5\text{ perms}\big) + \frac{b_{200}b_{100}^2}{2}\big(\langle\delta_L^2(1)\delta_L(2)\delta_L(3)\rangle_{\rm nzl} + 2\text{ perms}\big)\\
&+ \frac{b_{200}b_{010}^2}{2}\big(\langle\delta_L^2(1)y_*(2)y_*(3)\rangle_{\rm nzl} + 2\text{ perms}\big) + \frac{b_{200}b_{001}^2}{2}\big(\langle\delta_L^2(1)\mathcal{S}_L(2)\mathcal{S}_L(3)\rangle_{\rm nzl} + 2\text{ perms}\big)\\
&+ \frac{b_{200}b_{100}b_{010}}{2}\big(\langle\delta_L^2(1)\delta_L(2)y_*(3)\rangle_{\rm nzl} + 5\text{ perms}\big) + \frac{b_{200}b_{100}b_{001}}{2}\big(\langle\delta_L^2(1)\delta_L(2)\mathcal{S}_L(3)\rangle_{\rm nzl} + 5\text{ perms}\big)\\
&+ \frac{b_{200}b_{010}b_{001}}{2}\big(\langle\delta_L^2(1)y_*(2)\mathcal{S}_L(3)\rangle_{\rm nzl} + 5\text{ perms}\big) + \frac{b_{020}b_{100}^2}{2}\big(\langle y_*^2(1)\delta_L(2)\delta_L(3)\rangle_{\rm nzl} + 2\text{ perms}\big)\\
&+ \frac{b_{020}b_{010}^2}{2}\big(\langle y_*^2(1)y_*(2)y_*(3)\rangle_{\rm nzl} + 2\text{ perms}\big) + \frac{b_{020}b_{001}^2}{2}\big(\langle y_*^2(1)\mathcal{S}_L(2)\mathcal{S}_L(3)\rangle_{\rm nzl} + 2\text{ perms}\big)\\
&+ \frac{b_{020}b_{100}b_{010}}{2}\big(\langle y_*^2(1)\delta_L(2)y_*(3)\rangle_{\rm nzl} + 5\text{ perms}\big) + \frac{b_{020}b_{100}b_{001}}{2}\big(\langle y_*^2(1)\delta_L(2)\mathcal{S}_L(3)\rangle_{\rm nzl} + 5\text{ perms}\big)\\
&+ \frac{b_{020}b_{010}b_{001}}{2}\big(\langle y_*^2(1)y_*(2)\mathcal{S}_L(3)\rangle_{\rm nzl} + 5\text{ perms}\big) + \frac{b_{002}b_{100}^2}{2}\big(\langle\mathcal{S}_L^2(1)\delta_L(2)\delta_L(3)\rangle_{\rm nzl} + 2\text{ perms}\big)\\
&+ \frac{b_{002}b_{010}^2}{2}\big(\langle\mathcal{S}_L^2(1)y_*(2)y_*(3)\rangle_{\rm nzl} + 2\text{ perms}\big) + \frac{b_{002}b_{001}^2}{2}\big(\langle\mathcal{S}_L^2(1)\mathcal{S}_L(2)\mathcal{S}_L(3)\rangle_{\rm nzl} + 2\text{ perms}\big)\\
&+ \frac{b_{002}b_{100}b_{010}}{2}\big(\langle\mathcal{S}_L^2(1)\delta_L(2)y_*(3)\rangle_{\rm nzl} + 5\text{ perms}\big) + \frac{b_{002}b_{100}b_{001}}{2}\big(\langle\mathcal{S}_L^2(1)\delta_L(2)\mathcal{S}_L(3)\rangle_{\rm nzl} + 5\text{ perms}\big)\\
&+ \frac{b_{002}b_{010}b_{001}}{2}\big(\langle\mathcal{S}_L^2(1)y_*(2)\mathcal{S}_L(3)\rangle_{\rm nzl} + 5\text{ perms}\big) + b_{110}b_{100}^2\big(\langle(\delta_L y_*)(1)\delta_L(2)\delta_L(3)\rangle_{\rm nzl} + 2\text{ perms}\big)\\
&+ b_{110}b_{010}^2\big(\langle(\delta_L y_*)(1)y_*(2)y_*(3)\rangle_{\rm nzl} + 2\text{ perms}\big) + b_{110}b_{001}^2\big(\langle(\delta_L y_*)(1)\mathcal{S}_L(2)\mathcal{S}_L(3)\rangle_{\rm nzl} + 2\text{ perms}\big)\\
&+ b_{110}b_{100}b_{010}\big(\langle(\delta_L y_*)(1)\delta_L(2)y_*(3)\rangle_{\rm nzl} + 5\text{ perms}\big) + b_{110}b_{100}b_{001}\big(\langle(\delta_L y_*)(1)\delta_L(2)\mathcal{S}_L(3)\rangle_{\rm nzl} + 5\text{ perms}\big)\\
&+ b_{110}b_{010}b_{001}\big(\langle(\delta_L y_*)(1)y_*(2)\mathcal{S}_L(3)\rangle_{\rm nzl} + 5\text{ perms}\big) + b_{101}b_{100}^2\big(\langle(\delta_L\mathcal{S}_L)(1)\delta_L(2)\delta_L(3)\rangle_{\rm nzl} + 2\text{ perms}\big)\\
&+ b_{101}b_{010}^2\big(\langle(\delta_L\mathcal{S}_L)(1)y_*(2)y_*(3)\rangle_{\rm nzl} + 2\text{ perms}\big) + b_{101}b_{001}^2\big(\langle(\delta_L\mathcal{S}_L)(1)\mathcal{S}_L(2)\mathcal{S}_L(3)\rangle_{\rm nzl} + 2\text{ perms}\big)\\
&+ b_{101}b_{100}b_{010}\big(\langle(\delta_L\mathcal{S}_L)(1)\delta_L(2)y_*(3)\rangle_{\rm nzl} + 5\text{ perms}\big) + b_{101}b_{100}b_{001}\big(\langle(\delta_L\mathcal{S}_L)(1)\delta_L(2)\mathcal{S}_L(3)\rangle_{\rm nzl} + 5\text{ perms}\big)\\
&+ b_{101}b_{010}b_{001}\big(\langle(\delta_L\mathcal{S}_L)(1)y_*(2)\mathcal{S}_L(3)\rangle_{\rm nzl} + 5\text{ perms}\big) + b_{011}b_{100}^2\big(\langle(y_*\mathcal{S}_L)(1)\delta_L(2)\delta_L(3)\rangle_{\rm nzl} + 2\text{ perms}\big)\\
&+ b_{011}b_{010}^2\big(\langle(y_*\mathcal{S}_L)(1)y_*(2)y_*(3)\rangle_{\rm nzl} + 2\text{ perms}\big) + b_{011}b_{001}^2\big(\langle(y_*\mathcal{S}_L)(1)\mathcal{S}_L(2)\mathcal{S}_L(3)\rangle_{\rm nzl} + 2\text{ perms}\big)\\
&+ b_{011}b_{100}b_{010}\big(\langle(y_*\mathcal{S}_L)(1)\delta_L(2)y_*(3)\rangle_{\rm nzl} + 5\text{ perms}\big) + b_{011}b_{100}b_{001}\big(\langle(y_*\mathcal{S}_L)(1)\delta_L(2)\mathcal{S}_L(3)\rangle_{\rm nzl} + 5\text{ perms}\big)\\
&+ b_{011}b_{010}b_{001}\big(\langle(y_*\mathcal{S}_L)(1)y_*(2)\mathcal{S}_L(3)\rangle_{\rm nzl} + 5\text{ perms}\big)
\end{aligned}
\tag{3.79}
$$

In the calculation for the three point function, we have allowed $n_h(\boldsymbol{x})$ to depend on second order in perturbations. So, it would make sense to include the dependence of $n_h(\boldsymbol{x})$ on the coarse grained tidal field squared $(K_{ij,L})^2(\boldsymbol{x})$ (defined below), since this is a local observable and is also second order in perturbations [18]. The tidal field is defined as a scaled dimensionless quantity K_{ij} as follows

$$\nabla^2 K_{ij}(\boldsymbol{x}) = \left(\partial_i\partial_j - \frac{1}{3}\delta_{ij}\nabla^2\right)\delta(\boldsymbol{x}) \tag{3.80}$$

In Fourier space, this becomes

$$K_{ij}(\boldsymbol{k}) = \left(\frac{k_i k_j}{k^2} - \frac{1}{3}\delta_{ij}\right)\delta(\boldsymbol{k}) \tag{3.81}$$

So, we include a bias term for tidal field in the tracer density field

$$n_h(\boldsymbol{x}) \supset b_{K^2}\,(K_{ij,L})^2(\boldsymbol{x}), \tag{3.82}$$

which results in additional terms in the three point function $\xi_{hhh}(\boldsymbol{x}_1,\boldsymbol{x}_2,\boldsymbol{x}_3)$ in equation (3.79), as shown below

$$\begin{aligned}
\xi_{hhh}(\boldsymbol{x}_1,\boldsymbol{x}_2,\boldsymbol{x}_3) \supset\ & \frac{b_{K^2}b_{100}^2}{2}\left(\langle(K_{ij,L})^2(1)\delta_L(2)\delta_L(3)\rangle_{\rm nzl} + 2\ \text{perms}\right)\\
&+ \frac{b_{K^2}b_{010}^2}{2}\left(\langle(K_{ij,L})^2(1)y_*(2)y_*(3)\rangle_{\rm nzl} + 2\ \text{perms}\right)\\
&+ \frac{b_{K^2}b_{001}^2}{2}\left(\langle(K_{ij,L})^2(1)\mathcal{S}_L(2)\mathcal{S}_L(3)\rangle_{\rm nzl} + 2\ \text{perms}\right)\\
&+ \frac{b_{K^2}b_{100}b_{010}}{2}\left(\langle(K_{ij,L})^2(1)\delta_L(2)y_*(3)\rangle_{\rm nzl} + 5\ \text{perms}\right)\\
&+ \frac{b_{K^2}b_{100}b_{001}}{2}\left(\langle(K_{ij,L})^2(1)\delta_L(2)\mathcal{S}_L(3)\rangle_{\rm nzl} + 5\ \text{perms}\right)\\
&+ \frac{b_{K^2}b_{010}b_{001}}{2}\left(\langle(K_{ij,L})^2(1)y_*(2)\mathcal{S}_L(3)\rangle_{\rm nzl} + 5\ \text{perms}\right)
\end{aligned} \tag{3.83}$$

It turns out that it is not possible to get a closed form in position space for all the terms in the expansion in equation (3.79) (as will be evident later), so we calculate them in Fourier space, where they do attain a closed form. First note that we have two different kinds of terms in the expansion - the first ten terms have three field perturbations, while the remaining terms have four field perturbations. This means that the first ten terms would only be non-zero if we include the non-Gaussianity in the field perturbations, while the rest of the terms can already be written as products of power spectra. So far we have only considered one form of non-Gaussianity, namely the PNG, where the field perturbations can be expressed as follows

$$\Phi = \Phi_G + f_{\rm NL}\Phi_G^2 \tag{3.84}$$

$$\mathcal{S} = \mathcal{S}_G + h_{\rm NL}\mathcal{S}_G^2 \tag{3.85}$$

However, along with this non-Gaussianity, these fields also attain non-Gaussianity through their coupling to gravity. In the case of the fields y_* ($\approx 2f_{\rm NL}\Phi$) and $\mathcal{S}$, which appear in the galaxy bias expansion as their primordial selves, we do not consider their subsequent evolution under gravity. So, the natural question is how do these fields attain gravitational non-Gaussianity? The answer to this question is through the gravitational evolution of the universe itself. To understand this, recall that we want to determine the contribution of these fields at position $\boldsymbol{x}(\tau)$ as shown in equation 3.61. However, the reality is that in the early universe, the fluid at position $\boldsymbol{x}(\tau)$ today was at some other position in the early universe, say $\boldsymbol{q}$, and has reached position $\boldsymbol{x}(\tau)$ today due to gravitational evolution of the fluid [18]. Therefore, the galaxy density function $n_h(\boldsymbol{x})$ actually depends on the value of the fields y_* and $\mathcal{S}$ at position $\boldsymbol{q}$, and one can show that these values can be expressed as follows:

$$\Phi(\boldsymbol{q}) = \Phi(\boldsymbol{x}) - s^i(\boldsymbol{x},\tau)\partial_i\Phi(\boldsymbol{x}) \tag{3.86}$$

$$\mathcal{S}(\boldsymbol{q}) = \mathcal{S}(\boldsymbol{x}) - s^i(\boldsymbol{x},\tau)\partial_i\mathcal{S}(\boldsymbol{x}), \tag{3.87}$$

where $\boldsymbol{s}(\boldsymbol{x},\tau)$ is called the displacement vector and is given by

$$\nabla^2\boldsymbol{s}(\boldsymbol{x},\tau) = -\boldsymbol{\nabla}\delta^{(1)}(\boldsymbol{x},\tau), \tag{3.88}$$

and $\delta^{(1)}$ is the first order density field [50], [51]. So, we can see from equations (3.86) and (3.87) that we have new contributions to the primordial values of Φ (and hence y_*) and $\mathcal{S}$, and these would have a direct effect on the bispectrum terms involving y_* and $\mathcal{S}$. In addition to y_* and $\mathcal{S}$, the density field δ also receives higher order contributions due to gravity. However, in the case of the density field, the non-Gaussianity comes from the gravitational evolution of the density field over time. We consider the gravitational evolution of the density field, not just its primordial value, since we expect density field to play an active role in the formation of tracers such as galaxies and clusters. The non-Gaussian contribution to density field due to gravitational evolution is given by

$$\delta^{(2)}(\boldsymbol{k}) = \int \frac{\mathrm{d}^3\boldsymbol{q}}{(2\pi)^3}F_2(\boldsymbol{q},\boldsymbol{k}-\boldsymbol{q})\delta^{(1)}(\boldsymbol{q})\delta^{(1)}(\boldsymbol{k}-\boldsymbol{q}), \tag{3.89}$$

where

$$F_2(\boldsymbol{k}_1,\boldsymbol{k}_2) = \frac{5}{7} + \frac{2}{7}\frac{(\boldsymbol{k}_1.\boldsymbol{k}_2)^2}{k_1^2k_2^2} + \frac{1}{2}\frac{\boldsymbol{k}_1.\boldsymbol{k}_2}{k_1k_2}\left(\frac{k_1}{k_2}+\frac{k_2}{k_1}\right) \tag{3.90}$$

and $\delta^{(1)}$ and $\delta^{(2)}$ are first and second order density fields, such that $\delta = \delta^{(1)} + \delta^{(2)}$ [52]. Now, we can start calculating the terms with three fields in the galaxy three point function. We find that

$$\begin{aligned}\langle \delta_L(\boldsymbol{k}_1)\delta_L(\boldsymbol{k}_2)\delta_L(\boldsymbol{k}_3)\rangle_{\rm nzl} =&(2\pi)^3\delta_D^3(\boldsymbol{k}_1+\boldsymbol{k}_2+\boldsymbol{k}_3)\\ &\Big(\underbrace{\mathcal{M}(k_1)\mathcal{M}(k_2)\mathcal{M}(k_3)2f_{\rm NL}\big(\mathcal{P}_\Phi(k_1)\mathcal{P}_\Phi(k_2)+2\text{ perms}\big)}_{\text{primordial non-Gaussianity}}\\ &+\underbrace{\big(2F_2(\boldsymbol{k}_1,\boldsymbol{k}_2)\mathcal{M}^2(k_1)\mathcal{M}^2(k_2)\mathcal{P}_\Phi(k_1)\mathcal{P}_\Phi(k_2)+2\text{ perms}\big)}_{\text{gravitational evolution}}\Big),\end{aligned} \tag{3.91}$$

Next, we have

$$\begin{aligned}\langle \delta_L(\boldsymbol{k}_1)\delta_L(\boldsymbol{k}_2)\mathcal{S}_L(\boldsymbol{k}_3)\rangle_{\rm nzl} =&(2\pi)^3\delta_D^3(\boldsymbol{k}_1+\boldsymbol{k}_2+\boldsymbol{k}_3)\\ &\Big[\mathcal{M}(k_1)\mathcal{M}(k_2)\big(2f_{\rm NL}\big(\mathcal{P}_\Phi(k_1)\mathcal{P}_{\Phi\mathcal{S}}(k_3)+\boldsymbol{k}_1\leftrightarrow\boldsymbol{k}_2\big)+2h_{\rm NL}\mathcal{P}_{\Phi\mathcal{S}}(k_1)\mathcal{P}_{\Phi\mathcal{S}}(k_2)\big)\\ &+\mathcal{M}(k_3)\big(2F_2(\boldsymbol{k}_1,\boldsymbol{k}_3)\mathcal{M}^2(k_1)\mathcal{P}_\Phi(k_1)\mathcal{P}_{\Phi\mathcal{S}}(k_3)+\boldsymbol{k}_1\leftrightarrow\boldsymbol{k}_2\big)\\ &+\left(\frac{\boldsymbol{k}_1.\boldsymbol{k}_2}{k_1^2}\mathcal{M}(k_1)\mathcal{P}_\Phi(k_1)\mathcal{P}_{\Phi\mathcal{S}}(k_2)+\boldsymbol{k}_1\leftrightarrow\boldsymbol{k}_2\right)\Big]\end{aligned} \tag{3.92}$$

$$\begin{aligned}\langle \delta_L(\boldsymbol{k}_1)\mathcal{S}_L(\boldsymbol{k}_2)\mathcal{S}_L(\boldsymbol{k}_3)\rangle_{\rm nzl} =&(2\pi)^3\delta_D^3(\boldsymbol{k}_1+\boldsymbol{k}_2+\boldsymbol{k}_3)\\ &\Big[\mathcal{M}(k_1)\big(2f_{\rm NL}\mathcal{P}_{\Phi\mathcal{S}}(k_2)\mathcal{P}_{\Phi\mathcal{S}}(k_3)+2h_{\rm NL}\big(\mathcal{P}_{\Phi\mathcal{S}}(k_1)\mathcal{P}_{\mathcal{S}}(k_3)+\boldsymbol{k}_2\leftrightarrow\boldsymbol{k}_3\big)\big)\\ &+\mathcal{M}(k_2)\mathcal{M}(k_3)2F_2(\boldsymbol{k}_2,\boldsymbol{k}_3)\mathcal{P}_{\Phi\mathcal{S}}(k_2)\mathcal{P}_{\Phi\mathcal{S}}(k_3)\\ &+\mathcal{M}(k_1)\Big\{\left(\frac{\boldsymbol{k}_1.\boldsymbol{k}_2}{k_1^2}\mathcal{M}(k_1)\mathcal{P}_\Phi(k_1)\mathcal{P}_{\mathcal{S}}(k_2)+\frac{\boldsymbol{k}_1.\boldsymbol{k}_2}{k_2^2}\mathcal{M}(k_2)\mathcal{P}_{\Phi\mathcal{S}}(k_1)\mathcal{P}_{\Phi\mathcal{S}}(k_2)\right)\\ &+\boldsymbol{k}_2\leftrightarrow\boldsymbol{k}_3\Big\}\Big]\end{aligned} \tag{3.93}$$

The remainder of the terms appearing in equation (3.79) have been determined in Appendix A. Eventually, we want to plot the contributions of these terms and determine their relative importance to the galaxy bispectrum, which is simply defined as

$$\xi_{hhh}(\boldsymbol{k}_1,\boldsymbol{k}_2,\boldsymbol{k}_3)=(2\pi)^3\delta_D^3(\boldsymbol{k}_1+\boldsymbol{k}_2+\boldsymbol{k}_3)\mathcal{B}_{hhh}(k_1,k_2,k_3). \tag{3.94}$$

We can express the galaxy bispectrum in terms of the bispectrum corresponding to the correlators appearing in equation (3.79). For instance, the bispectrum corresponding to the term $\langle\delta_L(1)\delta_L(2)\delta_L(3)\rangle_{\rm nzl}$ is defined as

$$\langle\delta_L(1)\delta_L(2)\delta_L(3)\rangle_{\rm nzl}=(2\pi)^3\delta_D^3(\boldsymbol{k}_1+\boldsymbol{k}_2+\boldsymbol{k}_3)\mathcal{B}_{\delta\delta\delta}(k_1,k_2,k_3). \tag{3.95}$$

However, we end up having 52 terms, as shown in equations (3.91), (3.92), (3.93) and Appendix A, and therefore plotting all these terms and their contributions can be very demanding. Fortunately, there is a way to show that most of the terms are well suppressed. To do so, we need to understand how we determine the tracer number density n_h from a survey. Let's take galaxies to be our tracers. Now, we make a naive assumption that the survey is a 3D cube with a comoving side length of L. We cover the entire survey with a cubic grid with K^3_{grid} points, and we can consider the cells of this grid as pixels. We assign every galaxy to a pixel, so each pixel i contains $n_{g,i} = n_g(\boldsymbol{x}_i)$ galaxies. The discrete Fourier transform of the galaxy number density is given by

$$n_g(\boldsymbol{k}) = L^{3/2} \sum_{i}^{K^3_{\text{grid}}} n_g(\boldsymbol{x}_i)\, e^{-i\boldsymbol{k}.\boldsymbol{x}_i}, \quad \text{where} \quad \boldsymbol{k} = (n_x, n_y, n_z)k_F \tag{3.96}$$

and

$$k_F = \frac{2\pi}{L} \tag{3.97}$$

is the wavenumber of the fundamental mode, and (n_x, n_y, n_z) is a set of integers between $-K^3_{\text{grid}}/2$ and $K^3_{\text{grid}}/2$ [52]. Since we want to determine the galaxy power spectrum and bispectrum, we only need to take the magnitudes of the wavevector $\boldsymbol{k}$ into account. For a fixed value of the wavenumber k, there are various combinations of integers n_x, n_y and n_z that can result in this value of k. The higher the value of k, the more combinations of integers n_x, n_y and n_z that we can find. This means there are more contributions to the power spectrum and bispectrum from higher values of k. In the case of bispectrum, we should have at least two values of k, say k_1 and k_2 which should be large (of the order $0.01\, h/Mpc$). Since the Dirac delta $\delta^3_D(\boldsymbol{k}_1 + \boldsymbol{k}_2 + \boldsymbol{k}_3)$ imposes that $\boldsymbol{k}_1$, $\boldsymbol{k}_2$ and $\boldsymbol{k}_3$ form a triangle, we can then take the limit where k_3 can be small, while k_1 and k_2 are large. This is known as the squeezed limit and can be seen at the top left in figure 3.3 [4]. We will now take this limit show that most of the bispectrum contributions are suppressed. The squeezed limit is the limit where we would expect the most significant contributions from the terms, and this can be seen at the top left corner of figures 3.4, 3.5 and 3.6, further justifying our choice to take this limit.

Consider the bispectrum term $B_{\delta^2\delta\delta}$, which can be expressed as

$$B_{\delta^2\delta\delta}(k_1, k_2, k_3) = 2\mathcal{P}_{\delta\delta}(\boldsymbol{k}_2)\mathcal{P}_{\delta\delta}(\boldsymbol{k}_3) = 2\mathcal{M}^2(k_2)\mathcal{M}^2(k_3)\mathcal{P}_\Phi(k_2)\mathcal{P}_\Phi(k_2), \tag{3.98}$$

where we have defined

$$\mathcal{P}_{\delta\delta}(k) = \mathcal{M}^2(k)\mathcal{P}_\Phi(k). \tag{3.99}$$

The result in equation (3.98) is a direct consequence of equation (B.7). We know that the power spectrum $P_{\delta\delta}$ provide significant contributions, as evident in figure 3.2. Therefore, we can use the bispectrum term shown in equation 3.98 as a reference for all the other terms that contribute to the galaxy bispectrum, and any terms that are negligible compared to this term in the squeezed limit discussed above will be discarded. An example of this is provided below. Consider the term in the tracer three point function given by $\langle(\delta_L * \delta_L)(\boldsymbol{k}_1)y_*(\boldsymbol{k}_2)y_*(\boldsymbol{k}_3)\rangle_{\rm nzl}$, as calculated in equation A.10. The bispectrum for this term is given below:

$$\mathcal{B}_{\delta^2 y_* y_*}(k_1,k_2,k_3) = 8f_{\rm NL}^2\mathcal{M}(k_2)\mathcal{M}(k_3)\mathcal{P}_\Phi(k_2)\mathcal{P}_\Phi(k_3) = 8f_{\rm NL}^2\mathcal{M}^{-1}(k_2)\mathcal{M}^{-1}(k_3)\mathcal{P}_{\delta\delta}(k_2)\mathcal{P}_{\delta\delta}(k_3) \tag{3.100}$$

The expression above when compared to equation (3.98) has one major difference: the factors of $\mathcal{M}^{-1}(k_2)$ and $\mathcal{M}^{-1}(k_3)$, noting that $f_{\rm NL}$ is just taken to be 1. Recall that the term in $\langle(\delta_L * \delta_L)(\boldsymbol{k}_1)y_*(\boldsymbol{k}_2)y_*(\boldsymbol{k}_3)\rangle_{\rm nzl}$ appears in the tracer three-point function in equation (3.79) with two other permutations, meaning that the bispectrum also contributes with two other permutations. Therefore, we would have to consider products $\mathcal{M}^{-1}(k_2)\mathcal{M}^{-1}(k_3)$, $\mathcal{M}^{-1}(k_1)\mathcal{M}^{-1}(k_2)$ and $\mathcal{M}^{-1}(k_3)\mathcal{M}^{-1}(k_1)$. In the squeezed limit, without loss of generality, we can assume k_1 and k_2 to be large, meaning that each of the aforementioned products have at least one term with large k. In order to understand the behaviour of $\mathcal{M}(k)$ on large k, consider the figure 3.2. In this figure, we see that $P_{\delta\delta}$ is much larger than $P_{y_*y_*}$ at large k. This is due to the factor of $\mathcal{M}(k)$ in δ compared to y_*, meaning that $\mathcal{M}(k)$ is much larger than unity at large k. In contrast, $P_{\delta\delta}$ and $P_{y_*y_*}$ are comparable at smaller k, meaning that $\mathcal{M}(k)$ is nearly order 1 or 10^{-1} for small k. Therefore, the products such as $\mathcal{M}^{-1}(k_2)\mathcal{M}^{-1}(k_3)$, $\mathcal{M}^{-1}(k_1)\mathcal{M}^{-1}(k_2)$ and $\mathcal{M}^{-1}(k_3)\mathcal{M}^{-1}(k_1)$ would all be negligible in the squeezed limit since they all have at least one $\mathcal{M}(k)$ evaluated at large k. This means that the contribution of the bispectrum term $\mathcal{B}_{\delta^2 y_* y_*}(k_1,k_2,k_3)$ and its permutations can be ignored in the galaxy bispectrum. The same process where we use the values of $\mathcal{M}(k)$ in the squeezed limit is employed to eliminate other negligible terms. We then find that among the 52 possible bispectrum terms and their permutations, only 18 terms (plus permutations) remain.

These terms can be seen in the equation below.

$$
\begin{aligned}
&\mathcal{B}_{hhh}(k_1, k_2, k_3) \\
&= b_{100}^3 \mathcal{B}_{\delta\delta\delta}(k_1, k_2, k_3) + b_{100}^2 b_{010} \big(\mathcal{B}_{\delta\delta y_*}(k_1, k_2, k_3) + 2 \text{ perms}\big) + b_{100}^2 b_{001} \big(\mathcal{B}_{\delta\delta\mathcal{S}}(k_1, k_2, k_3) + 2 \text{ perms}\big) \\
&\quad + b_{100} b_{001}^2 \big(\mathcal{B}_{\delta\mathcal{S}\mathcal{S}}(k_1, k_2, k_3) + 2 \text{ perms}\big) + b_{100} b_{010}^2 \big(\mathcal{B}_{\delta y_* y_*}(k_1, k_2, k_3) + 2 \text{ perms}\big) \\
&\quad + b_{100} b_{010} b_{001} \big(\mathcal{B}_{\delta y_* \mathcal{S}}(k_1, k_2, k_3) + 5 \text{ perms}\big) + \frac{b_{200} b_{100}^2}{2} \big(\mathcal{B}_{\delta^2\delta\delta}(k_1, k_2, k_3) + 2 \text{ perms}\big) \\
&\quad + \frac{b_{200} b_{100} b_{010}}{2} \big(\mathcal{B}_{\delta^2\delta y_*}(k_1, k_2, k_3) + 5 \text{ perms}\big) + \frac{b_{200} b_{100} b_{001}}{2} \big(\mathcal{B}_{\delta^2\delta\mathcal{S}}(k_1, k_2, k_3) + 5 \text{ perms}\big) \\
&\quad + b_{110} b_{100}^2 \big(\mathcal{B}_{(\delta y_*)\,\delta\delta}(k_1, k_2, k_3) + 2 \text{ perms}\big) + b_{110} b_{100} b_{010} \big(\mathcal{B}_{(\delta y_*)\,\delta y_*}(k_1, k_2, k_3) + 5 \text{ perms}\big) \\
&\quad + b_{110} b_{100} b_{001} \big(\mathcal{B}_{(\delta y_*)\,\delta\mathcal{S}}(k_1, k_2, k_3) + 5 \text{ perms}\big) + b_{101} b_{100}^2 \big(\mathcal{B}_{(\delta\mathcal{S})\,\delta\delta}(k_1, k_2, k_3) + 2 \text{ perms}\big) \\
&\quad + b_{101} b_{100} b_{010} \big(\mathcal{B}_{(\delta\mathcal{S})\,\delta y_*}(k_1, k_2, k_3) + 5 \text{ perms}\big) + b_{101} b_{100} b_{001} \big(\mathcal{B}_{(\delta\mathcal{S})\,\delta\mathcal{S}}(k_1, k_2, k_3) + 5 \text{ perms}\big) \\
&\quad + \frac{b_{K^2} b_{100}^2}{2} \big(\mathcal{B}_{K^2\delta\delta}(k_1, k_2, k_3) + 2 \text{ perms}\big) + \frac{b_{K^2} b_{100} b_{010}}{2} \big(\mathcal{B}_{K^2\delta y_*}(k_1, k_2, k_3) + 5 \text{ perms}\big) \\
&\quad + \frac{b_{K^2} b_{100} b_{001}}{2} \big(\mathcal{B}_{K^2\delta\mathcal{S}}(k_1, k_2, k_3) + 5 \text{ perms}\big)
\end{aligned}
\tag{3.101}
$$

The expressions for all these terms are provided in Appendix B. We now plot the contributions of all these terms to the galaxy bispectrum. To do so, we fix $k_1 = 0.01h/Mpc$ and choose k_2 and k_3 such that $k_1 \geq k_2 \geq k_3$ without a loss of generality. The triangle inequality due to $\delta_D^3(\boldsymbol{k_1}+\boldsymbol{k_2}+\boldsymbol{k_3})$ imposes a further constraint $k_1 \leq k_2 + k_3$, resulting in a plot like figure 3.3. The dark blue region is the only region of the figure where the bispectrum is plotted. In the figure we can see that at various vertices of the dark blue triangle, we have various triangles. On the top left, we have a squeezed triangle signifying that in this limit k_1 and k_2 are large while k_3 is small. This is limit we used to discard terms in the galaxy bispectrum, as discussed earlier. On the top right, we have an equilateral triangle with $k_1 = k_2 = k_3$. At the bottom, we have a folded triangle with $k_2 = k_3 = \frac{k_1}{2}$ [4]. The plots of contributions to galaxy bispectrum can then be plotted, as seen in figures 3.4, 3.5 and 3.6. Also note that in each plot, we consider the bispectrum and its permutations. For instance, the plot of $\mathcal{B}_{\delta^2\delta\delta}$ is a plot of the sum $\mathcal{B}_{\delta^2\delta\delta}(k_1, k_2, k_3) + \mathcal{B}_{\delta^2\delta\delta}(k_2, k_3, k_1) + \mathcal{B}_{\delta^2\delta\delta}(k_3, k_1, k_2)$.

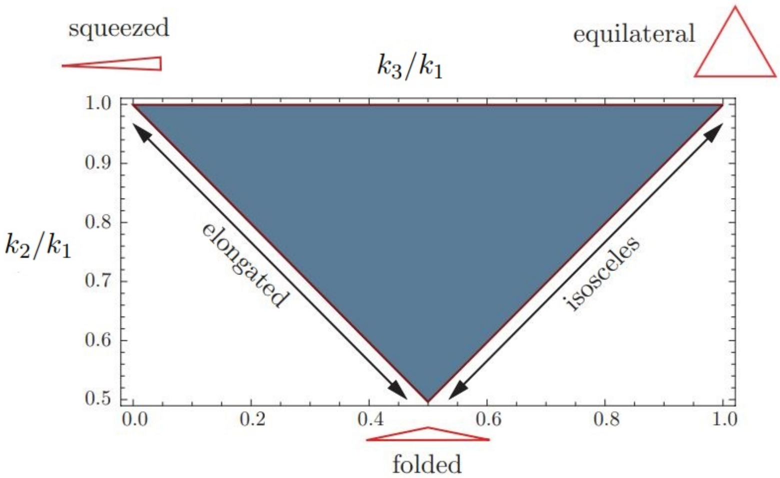

Figure 3.3.: Various shapes of non-Gaussianity [4]

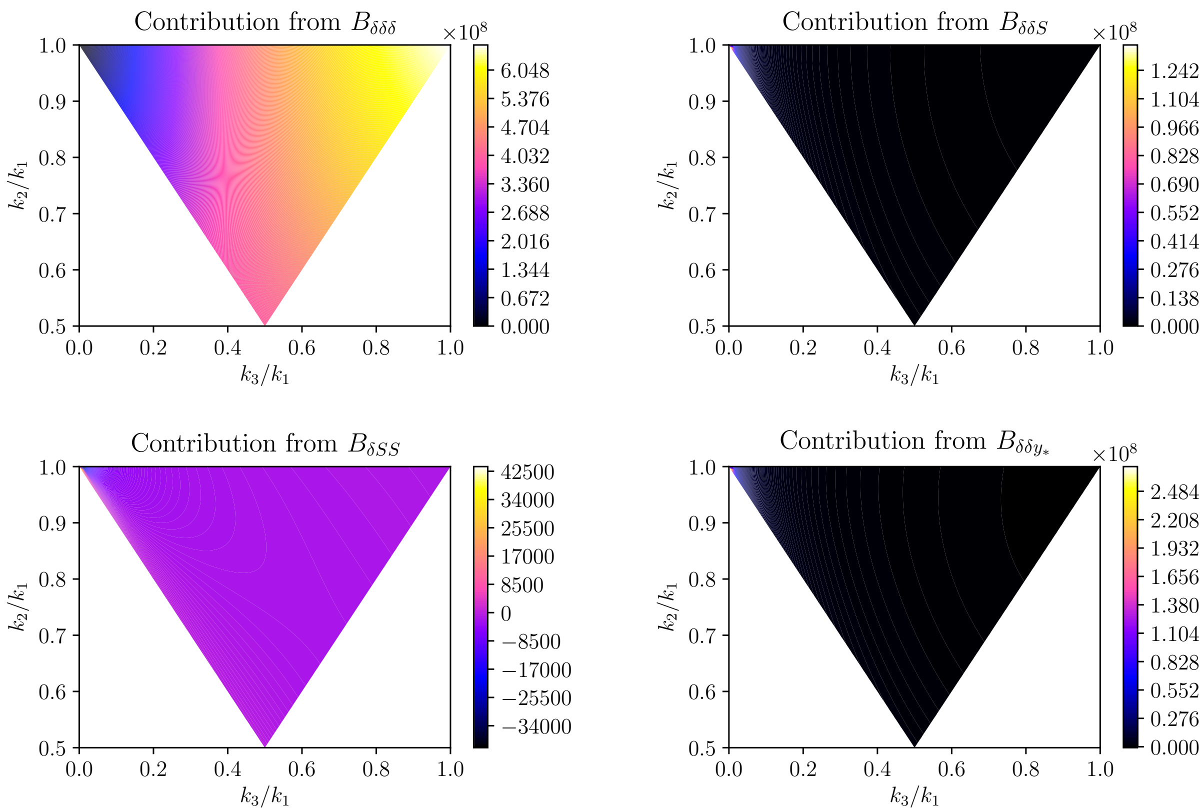

Figure 3.4.: Contributions from various bispectrum terms

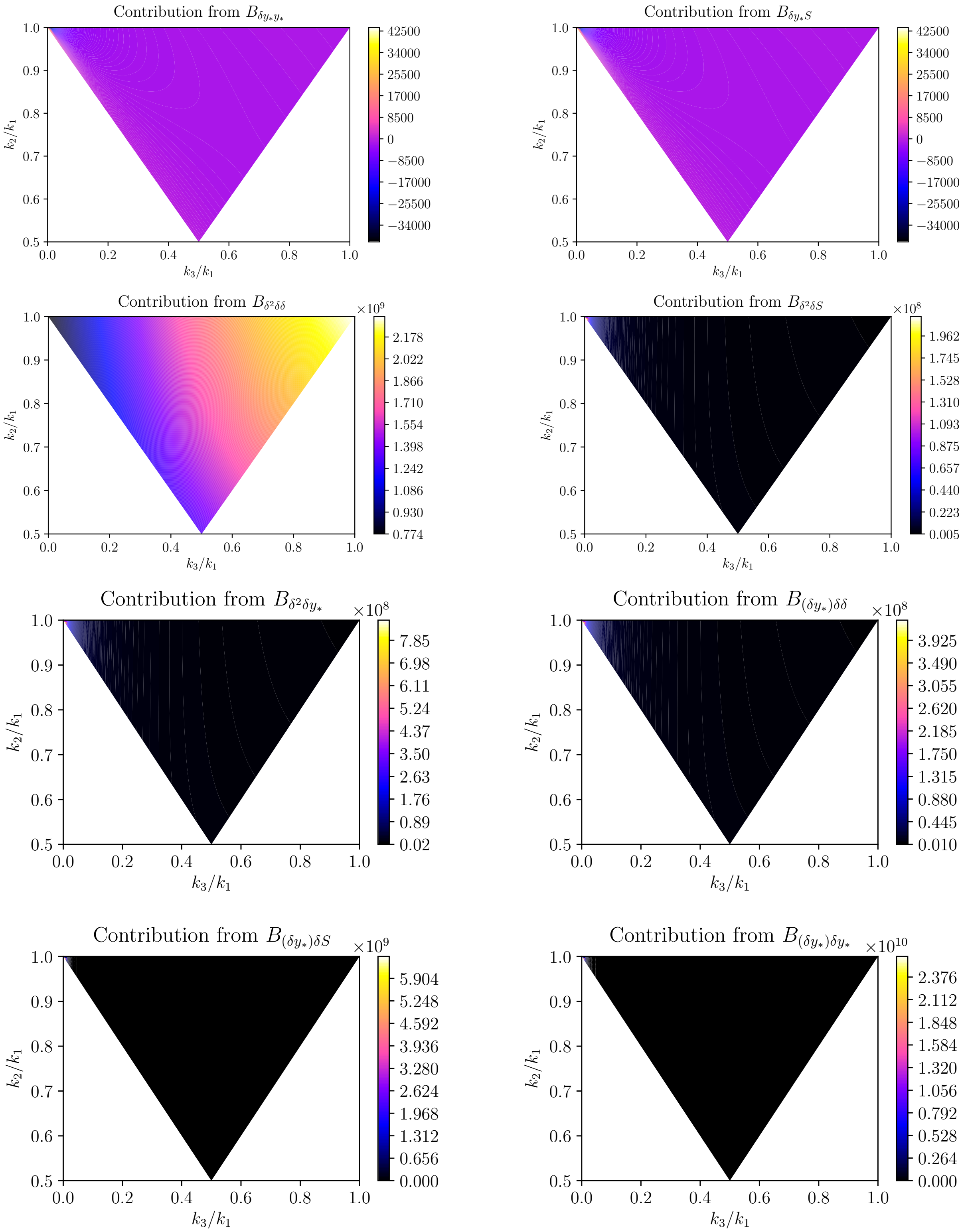

Figure 3.5.: Contributions from various bispectrum terms

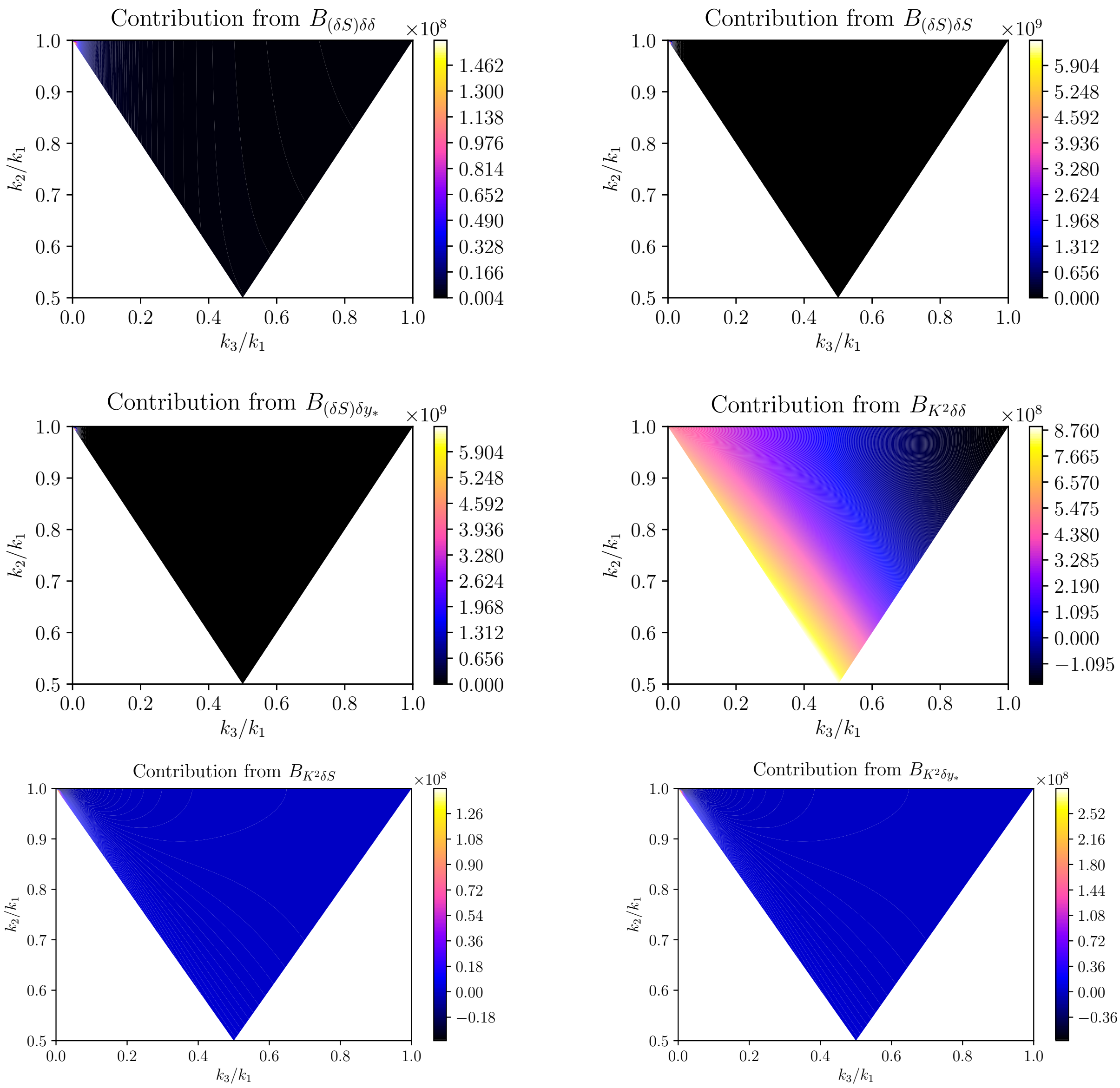

Figure 3.6.: Contributions from various bispectrum terms

First of all, since there is existing literature [18] on bispectrum terms involving only $\delta(\boldsymbol{x})$, $y_*(\boldsymbol{x})$ and $K^2(\boldsymbol{x})$, our plots for these terms were compared to the ones found in the literature, and were found to be identical. This gives us faith in our plots for bispectrum terms involving CIPs. Now, let's try to decode what is happening in the plots above.

In figures 3.4, 3.5 and 3.6, we can see that the bispectrum terms involving only δ, δ^2 and K^2, i.e. $\mathcal{B}_{\delta\delta\delta}$, $\mathcal{B}_{\delta^2\delta\delta}$ and $\mathcal{B}_{K^2\delta\delta}$ are the only ones that have significant contributions on all relevant scales. This can be easily explained by the fact that all of these bispectra can be written as products of matter power spectra, as can be seen in equations B.1, B.7 and B.16, and as we saw in figure 3.2, the matter power spectra enjoy the growth factor associated with gravitational evolution of density field, and hence are large across all scales of interest. The terms $\mathcal{B}_{\delta\delta\delta}$ and $\mathcal{B}_{\delta^2\delta\delta}$ attain the largest values on the vertex where $k_1 = k_2 = k_3 = 0.01h/Mpc$ (the equilateral triangle), and attain their smallest values in the squeezed limit where $k_1 \approx k_2$ and $k_3 \approx 0$. This can again be explained with the help of the matter power spectrum. The matter power spectrum scales as k for all $k < 0.02h/Mpc$ and since the largest k we consider is $k_1 = 0.01h/Mpc$ and $k_2 \geq k_1/2$ and since the bispectrum is a product of the matter power spectra, the k dependence of the power spectra results in a bispectrum that is small for small k_3 and large for large k_3. This is evident in the plots of $\mathcal{B}_{\delta\delta\delta}$ and $\mathcal{B}_{\delta^2\delta\delta}$ in figures 3.4 and 3.5. In the case of $\mathcal{B}_{K^2\delta\delta}$, the pattern is the opposite, i.e. the value is large for small k_3 and small for large k_3. This must be because of the factor $\left(\left[\hat{k}_2.\hat{k}_3\right]^2 - \frac{1}{3}\right)$ that contributes to $\mathcal{B}_{K^2\delta\delta}$, derived in equation (B.16).

On the other hand, all the other plots have barely any structure, bar one - all these bispectrum terms seem to have negligible contributions everywhere apart from at the squeezed limit. Of course there are sub structures within the various groups of terms, but the main feature of all these terms is that they only provide significant contributions at the squeezed limit. This can be seen as a blue hue in the plots of $\mathcal{B}_{\delta\delta\mathcal{S}}$ and $\mathcal{B}_{\delta\delta y_*}$, for instance. The reasoning behind the pattern is simple: these bispectrum terms not only contain the matter density field, but also the primordial perturbations such as y_* and $\mathcal{S}$, and as a result we get products of matter power spectrum, power spectrum of primordial perturbations and mixed power spectrum of matter and primordial perturbations (refer to Appendix B). The primordial (or mixed) power spectra terms only contribute significantly on very large scales (i.e. small k of the order of less than $10^{-3}h/Mpc$), as can be seen from figure 3.2. Since we know that $k_1 = 0.01h/Mpc$ and $k_2 \geq k_1/2$, this means that only k_3 can be small, resulting in a bispectrum that is only significant in the squeezed limit (low values of k_3).

In the explanation above, we only analysed the plots of $\mathcal{B}_{\delta\delta y_*}$ and $\mathcal{B}_{\delta\delta\mathcal{S}}$, but it is evident from the plots that the pattern is essentially the same in all the other contributions involving primordial

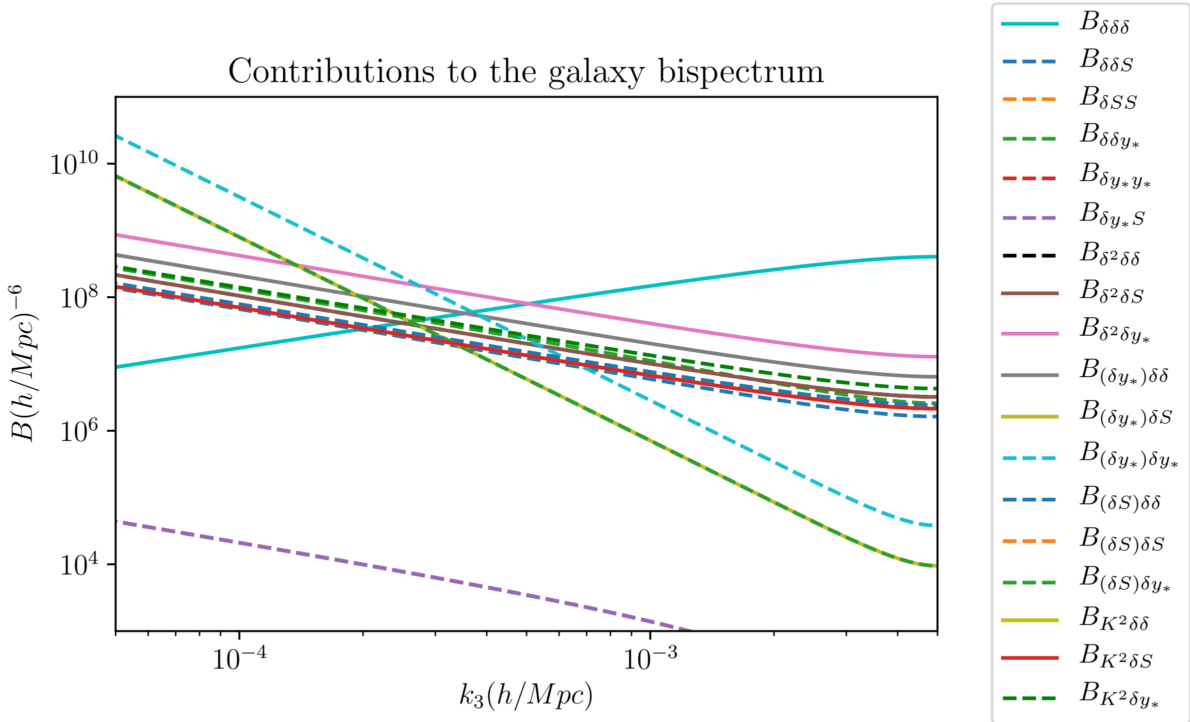

Figure 3.7.: Contributions of various bispectrum terms to the galaxy bispectrum on the elongated branch ($k_2 = k_1 - k_3$). (Please note that the contributions due to $\mathcal{B}_{\delta\mathcal{S}\mathcal{S}}$, $\mathcal{B}_{\delta y_* y_*}$ and $\mathcal{B}_{\delta y_* \mathcal{S}}$ coincide and the contributions due to $\mathcal{B}_{(\delta y_*)\delta\mathcal{S}}$, $\mathcal{B}_{(\delta\mathcal{S})\delta y_*}$ and $\mathcal{B}_{(\delta\mathcal{S})\delta\mathcal{S}}$ also coincide. This comes down to the value we chose for the correlation coefficient r between Φ and $\mathcal{S}$.)

perturbations. Nevertheless, there are still some differences such as the value of the bispectrum in the squeezed limit, like in the case of $\mathcal{B}_{\delta\mathcal{S}\mathcal{S}}$ and $\mathcal{B}_{\delta y_* y_*}$, where the values are of the order $10^4(h/Mpc)^{-6}$, in contrast to $\mathcal{B}_{\delta\delta\mathcal{S}}$ and $\mathcal{B}_{\delta\delta y_*}$ which are of the order $10^8(h/Mpc)^{-6}$ in the squeezed limit. We would like to delve further into these differences, and the bispectrum plots that we currently have just won't suffice. Therefore, we look at the elongated branch of the bispectrum (see figure 3.3), since this branch leads us to the squeezed limit. Along this branch, we have $k_2 = k_1 - k_3$, and fixing $k_1 = 0.01h/Mpc$, we can completely parametrise the bispectrum in terms of k_3, resulting in the plot shown in figure 3.7.

In figure 3.7, we can notice that terms such as $\mathcal{B}_{\delta\mathcal{S}\mathcal{S}}$, $\mathcal{B}_{\delta y_* y_*}$ and $\mathcal{B}_{\delta y_* \mathcal{S}}$ seem to contribute very little to the galaxy bispectrum, even along the elongated branch. They do become larger at the squeezed limit, but they are still insignificant compared to the contributions of other terms. Therefore, the contributions of these terms can be removed from the plot, and we obtain the plot in figure 3.8.

We see that all the bispectrum terms except $\mathcal{B}_{\delta\delta\delta}$ have a negative gradient, meaning that all the terms except $\mathcal{B}_{\delta\delta\delta}$ become significant on large scales (or small k_3). The $\mathcal{B}_{\delta\delta\delta}$ term increases as k_3

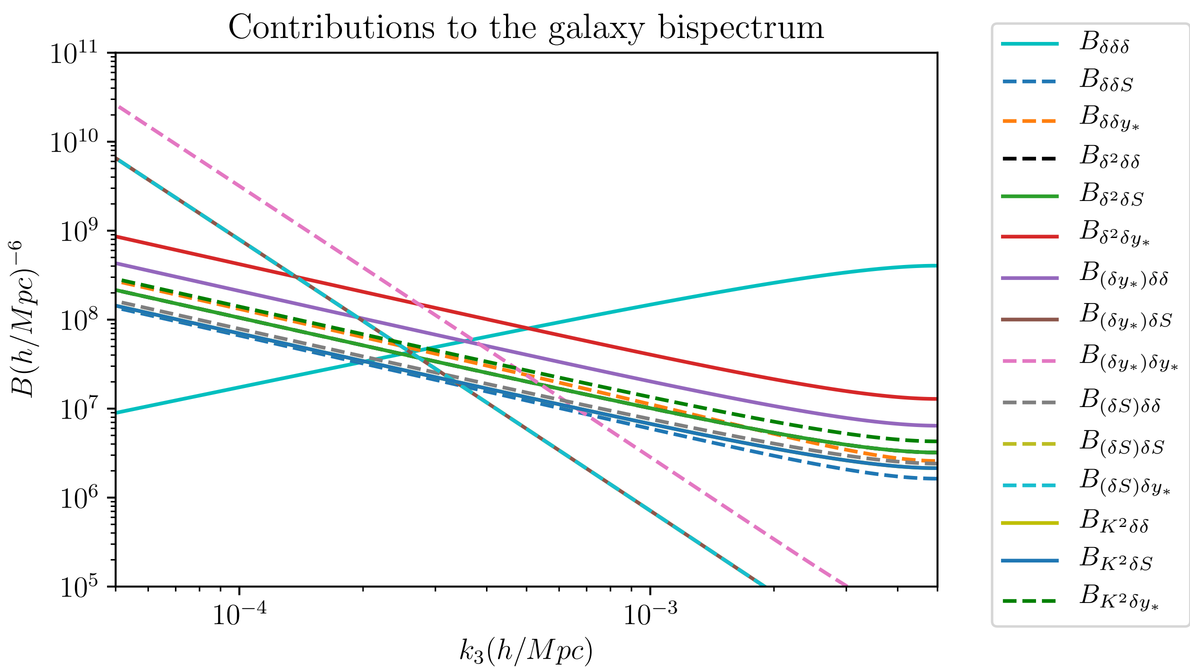

Figure 3.8.: Contributions of significant bispectrum terms to the galaxy bispectrum on the elongated branch ($k_2 = k_1 - k_3$). (Please note that the contributions due to $\mathcal{B}_{(\delta y_*)\delta\mathcal{S}}$, $\mathcal{B}_{(\delta\mathcal{S})\delta y_*}$ and $\mathcal{B}_{(\delta\mathcal{S})\delta\mathcal{S}}$ coincide, and this again comes down to our choice of r.)

increases, a pattern we would expect given that it is a product of matter power spectra and that the matter power spectra scales as k for small values of $k\,(< 0.02h/Mpc)$. The negative gradient of the bispectrum terms involving primordial perturbations strongly aligns with our findings for the power spectra for primordial perturbations as shown in figure 3.2. This makes sense since the bispectrum is roughly a product of the power spectra plotted in figure 3.2. (Note that this is an over simplistic assumption since the bispectrum terms also involve other factors such as $(\boldsymbol{k}_1.\boldsymbol{k}_2)$, $F_2(\boldsymbol{k}_1, \boldsymbol{k}_2)$, etc.) The pattern that we see in figures 3.7 and 3.8, where we see that a lot of the bispectrum terms drastically increase their contributions at the squeezed limit further corroborates our claim that if we are to find any traces of PNG and CIPs, we would have to look for them on large scales. The biggest contributions at the squeezed limit come from the bispectrum of $\mathcal{B}_{(\delta y_*)\delta y_*}, \mathcal{B}_{(\delta y_*)\delta\mathcal{S}}, \mathcal{B}_{(\delta\mathcal{S})\delta y_*}$ and $\mathcal{B}_{(\delta\mathcal{S})\delta\mathcal{S}}$, as can be seen in figure 3.8. (note that $\mathcal{B}_{(\delta y_*)\delta\mathcal{S}}, \mathcal{B}_{(\delta\mathcal{S})\delta y_*}$ and $\mathcal{B}_{(\delta\mathcal{S})\delta\mathcal{S}}$ coincide in the plot.) Therefore, these are the terms that provide us with the strongest chance to find PNG and CIPs.

4. Conclusion

The goal of my project was to develop a model of galaxy bias expansion which incorporates predictions of various theories of inflation, in particular single field inflation and multi-field inflation. This model, along with observational data, could then be used to constrain various models of inflation. In sections 2.3 and 2.4, we showed that while single field inflation predicts the primordial perturbations to be adiabatic, multi-field inflation predicts deviations from adiabaticity. We found that isocurvature perturbations $\mathcal{S}$ (see equation (2.21)), which are perturbations orthogonal to the adiabatic perturbations Φ, vanish in a single field inflationary model, but would contribute non-trivially if there were more fields. Adiabatic perturbations lead to perturbations in the total energy density while non-adiabatic perturbations correspond to perturbations that not only affect the total energy density, but also the distribution of energy density across various energy components. These perturbations were seen to arise in multi-field inflation since the field perturbations can follow directions orthogonal to the classical trajectory, unlike in single field inflation, where the field perturbation can only move along the classical path.

We determined expressions for the non-Gaussianity for both adiabatic and isocurvature perturbations in multi-field inflation, with the aim of incorporating these features into the galaxy bias expansion. The results can be found in equations (2.79) and (2.96), where we see that both perturbations assume a local form of non-Gaussianity. These expressions involve a very long list of unknown parameters, some pertaining to the nature of the slow roll potential while others pertaining to the evolution of field perturbations upon horizon exit. Constraining non-Gaussianity through galaxy clustering would therefore help us a great deal in constraining these unknown inflationary parameters, of which there are plenty.

In chapter 3, we incorporated the non-Gaussian initial conditions and the isocurvature perturbations into the galaxy bias expansion. The form of isocurvature perturbations that we know would have the most significant effect on galaxy clustering are the CIPs. We used the existing literature on multi-field inflationary models such as the curvaton scenario as a motivation for using the isocurvature perturbation $\mathcal{S}$ defined in equation (2.21) as a measure of CIPs. However, this relationship is highly dependent on one's assumptions regarding the reheating era, and hasn't been explored in detail in our model. We then evaluated the contributions of PNG and CIPs to the galaxy statistics, in particular the power spectrum and the bispectrum, as seen in equations 3.67, 3.79 and 3.101.

In figure 3.2, where we have plotted various contributions to the galaxy power spectrum, we find that the matter power spectrum $\mathcal{P}_{\delta\delta}$ contributes much more significantly than the power spectra of primordial perturbations on the most relevant scales $k > 10^{-3}h/Mpc$. This is due to the fact that Φ and $\mathcal{S}$ are included in the bias expansion as their primordial selves, while the density field δ appears in its evolved form since the gravitational evolution of δ is what leads to the formation of tracers. As a result, we find that δ enjoys a large growth in comparison to Φ and $\mathcal{S}$. Nevertheless, the power spectra involving Φ and $\mathcal{S}$ contribute much more significantly for very low k due to the scale invariance of primordial fluctuations causing a k^{-3} growth of their power spectra for low k (or $k^{-3/2}$ growth for cross spectra of matter and primordial perturbations). Therefore, if we were to precisely constrain the initial conditions, we would have to probe very large scales ($k \sim 10^{-4}h/Mpc$).

The bispectrum plots in figures 3.4, 3.5 and 3.6 sing the same tune. We find that while the bispectrum contributions involving only density fields generally contribute for all scales, the bispectrum contributions involving primordial perturbations only become significant in the squeezed limit, where two scales (say k_1^{-1}, k_2^{-1}) are small and satisfy $k_1 \approx k_2$ while one (say k_3^{-1}) is large satisfying $k_3 \approx 0$. This is due to the fact that the bispectrum terms involve products of power spectra terms calculated in section 3.4.1, and the power spectra of primordial perturbations only become significant on large scales ($k \sim 10^{-4}h/Mpc$) as seen from figure 3.2. To better understand the k_3 dependence of the bispectrum plots, we decided to evaluate these on the elongated branch ($k_1 = k_2 + k_3$), which approaches the squeezed limit when $k_3 = 0$. This can be seen in figures 3.7 and 3.8. We find the expected pattern that the terms pertaining to primordial perturbations all become significant only on large scales ($k_3 < 10^{-3}h/Mpc$). This further strengthens our case for probing very large scales to find PNG and CIPs.

In this project, we have developed a theoretical model for the galaxy power spectrum $\mathcal{P}_g(k)$ and bispectrum $\mathcal{B}_{ggg}(k_1, k_2, k_3)$ in terms of cosmological and bias parameters. In practice, we would compare this to observed galaxy power spectrum and bispectrum via a likelihood function, which is defined as the probability for a given theory that an experiment yields the observed data. This would help us determine the parameters of the theory (such as $f_{\mathrm{NL}}, h_{\mathrm{NL}}$, etc.) along with their errors. This is an endeavor for the future. But even before delving into that, one can determine how well the experiment is expected to determine the parameters. This is known as *forecasting* and is done with the help of the *Fisher matrix*, which is the curvature matrix of the likelihood, and quantifies the amount of information that an experiment can provide about a set of parameters. The idea can be summarized as follows: we assume values for the cosmological parameters that we believe describes the real universe and our goal is to forecast the errors in these values. These values give us a theoretical prediction for $\mathcal{P}_g(k)$ and $\mathcal{B}_{ggg}(k_1, k_2, k_3)$. Assuming an expected uncertainty in observational data, we can then predict the errors in the parameters by determining how the observational data would be affected by changes in the parameter values. This information is encoded in the Fisher matrix, and helps us determine whether a new signal predicted by theory could in fact be detected experimentally [52].

Bibliography

[1] M. Colless. (2003). The 2df galaxy redshift survey, [Online]. Available: http://magnum.anu.edu.au/~TDFgg/ (visited on 30/09/2020).

[2] D. Baumann, "Primordial Cosmology", *PoS*, vol. TASI2017, p. 009, 2018. [arxiv:1807.03098].

[3] D. Baumann and L. McAllister, *Inflation and String Theory*, ser. Cambridge Monographs on Mathematical Physics. Cambridge University Press, 2015. [arxiv:1404.2601].

[4] D. Baumann, "Inflation", in *Theoretical Advanced Study Institute in Elementary Particle Physics*, 2009. [arxiv:0907.5424].

[5] V. Mukhanov, *Physical Foundations of Cosmology*. Cambridge, UK: Cambridge University Press, 2005.

[6] G. I. Rigopoulos and E. P. S. Shellard, "The separate universe approach and the evolution of nonlinear superhorizon cosmological perturbations", *Phys. Rev. D*, vol. 68, p. 123 518, 2003. [arxiv:astro-ph/0306620].

[7] B. A. Bassett, S. Tsujikawa and D. Wands, "Inflation dynamics and reheating", *Rev. Mod. Phys.*, vol. 78, pp. 537–589, 2 2006.

[8] J. M. Bardeen, J. R. Bond, N. Kaiser and A. S. Szalay, "The Statistics of Peaks of Gaussian Random Fields", *Astrophys. J.*, vol. 304, pp. 15–61, 1986.

[9] F. Schmidt, "Non-Gaussian Halo Bias Beyond the Squeezed Limit", *Phys. Rev. D*, vol. 87, no. 12, p. 17, 2013. [arxiv:1304.1817].

[10] N. Aghanim *et al.*, "Planck 2018 results. VI. Cosmological parameters", *Astron. Astrophys.*, vol. 641, A6, 2020. [arxiv:1807.06209].

[11] Y. Akrami *et al.*, "Planck 2018 results. IX. Constraints on primordial non-Gaussianity", *Astron. Astrophys.*, vol. 641, A9, 2020. [arxiv:1905.05697].

[12] C. Gordon, "Adiabatic and entropy perturbations in cosmology", PhD thesis, University of Plymouth, 2001.

[13] Y. Akrami *et al.*, "Planck 2018 results. X. Constraints on inflation", *Astron. Astrophys.*, vol. 641, A10, 2020. [arxiv:1807.06211].

[14] A. Barreira, G. Cabass, K. D. Lozanov and F. Schmidt, "Compensated Isocurvature Perturbations in the Galaxy Power Spectrum", *JCAP*, vol. 07, p. 049, 2020. [arxiv:2002.12931].

[15] M. P. Salem, "On the generation of density perturbations at the end of inflation", *Phys. Rev. D*, vol. 72, p. 123 516, 2005. [arxiv:astro-ph/0511146].

[16] D. H. Lyth and D. Wands, "The CDM isocurvature perturbation in the curvaton scenario", *Phys. Rev. D*, vol. 68, p. 103 516, 2003. [arxiv:astro-ph/0306500].

[17] F. Schmidt, D. Jeong and V. Desjacques, "Peak-Background Split, Renormalization, and Galaxy Clustering", *Phys. Rev. D*, vol. 88, no. 2, p. 023 515, 2013. [arxiv:1212.0868].

[18] V. Desjacques, D. Jeong and F. Schmidt, "Large-Scale Galaxy Bias", *Phys. Rept.*, vol. 733, pp. 1–193, 2018. [arxiv:1611.09787].

[19] D. Langlois, F. Vernizzi and D. Wands, "Non-linear isocurvature perturbations and non-Gaussianities", *JCAP*, vol. 12, p. 004, 2008. [arxiv:0809.4646].

[20] F. Schmidt. (2013). Mpa lectures on galaxy clustering, [Online]. Available: https://wwwmpa.mpa-garching.mpg.de/~komatsu/lecturenotes/Fabian_Schmidt_on_clustering.pdf (visited on 21/10/2020).

[21] C. Gordon, D. Wands, B. A. Bassett and R. Maartens, "Adiabatic and entropy perturbations from inflation", *Phys. Rev. D*, vol. 63, p. 11, 2 2000.

[22] D. Langlois, "Correlated adiabatic and isocurvature perturbations from double inflation", *Phys. Rev. D*, vol. 59, p. 24, 1999. [arxiv:astro-ph/9906080].

[23] D. Wands, N. Bartolo, S. Matarrese and A. Riotto, "An Observational test of two-field inflation", *Phys. Rev. D*, vol. 66, p. 043 520, 2002. [arxiv:astro-ph/0205253].

[24] H. Kurki-Suonio. (2020). Cosmological perturbation theory, part 2, [Online]. Available: https://www.mv.helsinki.fi/home/hkurkisu//CosPer2.pdf (visited on 26/09/2020).

[25] C. T. Byrnes and D. Wands, "Curvature and isocurvature perturbations from two-field inflation in a slow-roll expansion", *Phys. Rev. D*, vol. 74, p. 043 529, 2006. [arxiv:astro-ph/0605679].

[26] D. Langlois and F. Vernizzi, "Nonlinear perturbations of cosmological scalar fields", *JCAP*, vol. 02, p. 017, 2007. [arxiv:astro-ph/0610064].

[27] A. A. Starobinsky, "Multicomponent de Sitter (Inflationary) Stages and the Generation of Perturbations", *JETP Lett.*, vol. 42, pp. 152–155, 1985.

[28] P. Catelan, F. Lucchin, S. Matarrese and C. Porciani, "The bias field of dark matter halos", *Mon. Not. Roy. Astron. Soc.*, vol. 297, pp. 692–712, 1998. [arxiv:astro-ph/9708067].

[29] A. Barreira, G. Cabass, F. Schmidt, A. Pillepich and D. Nelson, "Galaxy bias and primordial non-Gaussianity: insights from galaxy formation simulations with IllustrisTNG", *JCAP*, vol. 12, p. 013, 2020. [arxiv:2006.09368].

[30] D. Seery and J. E. Lidsey, "Primordial non-Gaussianities from multiple-field inflation", *JCAP*, vol. 09, p. 011, 2005. [arxiv:astro-ph/0506056].

[31] F. Vernizzi and D. Wands, "Non-gaussianities in two-field inflation", *JCAP*, vol. 05, p. 019, 2006. [arxiv:astro-ph/0603799].

[32] J. Maldacena, “Non-Gaussian features of primordial fluctuations in single field inflationary models”, *JCAP*, vol. 05, p. 013, 2003. [arxiv:astro-ph/0210603].

[33] M. Tegmark *et al.*, “Cosmological parameters from SDSS and WMAP”, *Phys. Rev. D*, vol. 69, p. 28, 2004. [arxiv:astro-ph/0310723].

[34] E. Komatsu, “The Pursuit of Non-Gaussian Fluctuations in the Cosmic Microwave Background”, p. 141, 2002. [arxiv:astro-ph/0206039].

[35] D. Langlois and B. van Tent, “Isocurvature modes in the CMB bispectrum”, *JCAP*, vol. 07, p. 040, 2012. [arxiv:1204.5042].

[36] K. A. Malik and D. Wands, “Evolution of second-order cosmological perturbations”, *Class. Quant. Grav.*, vol. 21, pp. L65–L72, 2004. [arxiv:astro-ph/0307055].

[37] H. J. Mo, Y. P. Jing and S. D. M. White, “High-order correlations of peaks and halos: A Step toward understanding galaxy biasing”, *Mon. Not. Roy. Astron. Soc.*, vol. 284, p. 189, 1997. [arxiv:astro-ph/9603039].

[38] F. Bernardeau and J.-P. Uzan, “NonGaussianity in multifield inflation”, *Phys. Rev. D*, vol. 66, p. 19, 2002. [arxiv:hep-ph/0207295].

[39] D. Wands, K. A. Malik, D. H. Lyth and A. R. Liddle, “A New approach to the evolution of cosmological perturbations on large scales”, *Phys. Rev. D*, vol. 62, p. 043 527, 2000. [arxiv:astro-ph/0003278].

[40] T. Battefeld and R. Easther, “Non-Gaussianities in Multi-field Inflation”, *JCAP*, vol. 03, p. 020, 2007. [arxiv:astro-ph/0610296].

[41] P. McDonald, “Primordial non-gaussianity: Large-scale structure signature in the perturbative bias model”, *Phys. Rev. D*, vol. 78, p. 9, 12 2008.

[42] J. Lesgourgues. (2019). CLASS-the cosmic linear anisotropy solving system, [Online]. Available: https://lesgourg.github.io/class_public/class.html (visited on 10/01/2021).

[43] ——, “The Cosmic Linear Anisotropy Solving System (CLASS) I: Overview”, 2011. [arxiv:1104.2932].

[44] D. Tseliakhovich, C. Hirata and A. Slosar, “Non-gaussianity and large-scale structure in a two-field inflationary model”, *Phys. Rev. D*, vol. 82, p. 9, 4 2010.

[45] A. Lewis, A. Challinor and A. Lasenby, “Efficient computation of CMB anisotropies in closed FRW models”, *Astrophys. J.*, vol. 538, pp. 473–476, 2000. [arxiv:astro-ph/9911177].

[46] R. Barkana and A. Loeb, “Scale-Dependent Bias of Galaxies from Baryonic Acoustic Oscillations”, *Mon. Not. Roy. Astron. Soc.*, vol. 415, p. 3113, 2011. [arxiv:1009.1393].

[47] F. Schmidt, “Effect of relative velocity and density perturbations between baryons and dark matter on the clustering of galaxies”, *Phys. Rev. D*, vol. 94, no. 6, 2016. [arxiv:1602.09059].

[48] R. Scoccimarro, E. Sefusatti and M. Zaldarriaga, “Probing primordial non-Gaussianity with large - scale structure”, *Phys. Rev. D*, vol. 69, p. 103 513, 2004. [arxiv:astro-ph/0312286].

[49] N. Dalal, O. Doré, D. Huterer and A. Shirokov, "Imprints of primordial non-gaussianities on large-scale structure: Scale-dependent bias and abundance of virialized objects", *Phys. Rev. D*, vol. 77, p. 17, 12 2008.

[50] T. Giannantonio and C. Porciani, "Structure formation from non-gaussian initial conditions: Multivariate biasing, statistics, and comparison with n-body simulations", *Phys. Rev. D*, vol. 81, p. 24, 6 2010.

[51] T. Baldauf, U. Seljak and L. Senatore, "Primordial non-Gaussianity in the Bispectrum of the Halo Density Field", *JCAP*, vol. 04, p. 006, 2011. [arxiv:1011.1513].

[52] S. Dodelson and F. Schmidt, *Modern Cosmology.* Cambridge, Massachussetts: Academic Press, 2020.

Appendices

A. Three point correlators: all contributions

In this section, we calculate the remainder of the terms that contribute to the tracer three-point function illustrated in equation (3.79). We have already calculated three terms involving primordial and gravitational non-Gaussianity, as shown in equations (3.91) through to (3.93). We continue with the calculation of more terms involving primordial and gravitational non-Gaussianity, as shown below:

$$\begin{aligned}\langle \mathcal{S}_L(\boldsymbol{k}_1)\mathcal{S}_L(\boldsymbol{k}_2)\mathcal{S}_L(\boldsymbol{k}_3)\rangle_{\text{nzl}} =&(2\pi)^3\delta_D^3(\boldsymbol{k}_1+\boldsymbol{k}_2+\boldsymbol{k}_3)\\ &\Big[2h_{\text{NL}}\big(\mathcal{P}_{\mathcal{S}}(k_1)\mathcal{P}_{\mathcal{S}}(k_2)+2\text{ perms}\big)+\Big\{\Big(\frac{\boldsymbol{k}_1.\boldsymbol{k}_2}{k_1^2}\mathcal{M}(k_1)\mathcal{P}_{\Phi\mathcal{S}}(k_1)\mathcal{P}_{\mathcal{S}}(k_2)\\ &+\frac{\boldsymbol{k}_1.\boldsymbol{k}_2}{k_2^2}\mathcal{M}(k_2)\mathcal{P}_{\mathcal{S}}(k_1)\mathcal{P}_{\Phi\mathcal{S}}(k_2)\Big)+2\text{ perms}\Big\}\Big]\end{aligned} \tag{A.1}$$

$$\begin{aligned}\langle \delta_L(\boldsymbol{k}_1)\delta_L(\boldsymbol{k}_2)y_*(\boldsymbol{k}_3)\rangle_{\text{nzl}} =&(2\pi)^3\delta_D^3(\boldsymbol{k}_1+\boldsymbol{k}_2+\boldsymbol{k}_3)\\ &2f_{\text{NL}}\Big[\mathcal{M}(k_1)\mathcal{M}(k_2)2f_{\text{NL}}(\mathcal{P}_\Phi(k_1)\mathcal{P}_\Phi(k_3)+\boldsymbol{k}_1\leftrightarrow\boldsymbol{k}_2)\\ &+(2F_2(k_1,k_3)\mathcal{M}^2(k_1)\mathcal{M}(k_3)\mathcal{P}_\Phi(k_1)\mathcal{P}_\Phi(k_3)+\boldsymbol{k}_1\leftrightarrow\boldsymbol{k}_2)\\ &+\mathcal{M}(k_1)\mathcal{M}(k_2)\Big(\frac{\boldsymbol{k}_1.\boldsymbol{k}_2}{k_1^2}\mathcal{M}(k_1)\mathcal{P}_\Phi(k_1)\mathcal{P}_\Phi(k_2)+\boldsymbol{k}_1\leftrightarrow\boldsymbol{k}_2\Big)\Big]\end{aligned} \tag{A.2}$$

$$\begin{aligned}\langle \delta_L(\boldsymbol{k}_1)y_*(\boldsymbol{k}_2)y_*(\boldsymbol{k}_3)\rangle_{\text{nzl}} =&(2\pi)^3\delta_D^3(\boldsymbol{k}_1+\boldsymbol{k}_2+\boldsymbol{k}_3)\\ &4f_{\text{NL}}^2\Big[\mathcal{M}(k_1)2f_{\text{NL}}\mathcal{P}_\Phi(k_2)\mathcal{P}_\Phi(k_3)+2F_2(k_2,k_3)\mathcal{M}(k_2)\mathcal{M}(k_3)\mathcal{P}_\Phi(k_2)\mathcal{P}_\Phi(k_3)\\ &+\Big\{\mathcal{M}(k_1)\Big(\frac{\boldsymbol{k}_1.\boldsymbol{k}_2}{k_1^2}\mathcal{M}(k_1)\mathcal{P}_\Phi(k_1)\mathcal{P}_\Phi(k_2)+\boldsymbol{k}_1\leftrightarrow\boldsymbol{k}_2\Big)+\boldsymbol{k}_2\leftrightarrow\boldsymbol{k}_3\Big\}\Big]\end{aligned} \tag{A.3}$$

$$
\begin{aligned}
\langle y_*(\boldsymbol{k}_1)\mathcal{S}_L(\boldsymbol{k}_2)\mathcal{S}_L(\boldsymbol{k}_3)\rangle_{\rm nzl} =&(2\pi)^3\delta_D^3(\boldsymbol{k}_1+\boldsymbol{k}_2+\boldsymbol{k}_3)\\
&2f_{\rm NL}\Bigg[2h_{\rm NL}(\mathcal{P}_{\Phi\mathcal{S}}(k_1)\mathcal{P}_{\mathcal{S}}(k_2)+\boldsymbol{k}_2\leftrightarrow\boldsymbol{k}_3)\\
&+\left(\frac{\boldsymbol{k}_2.\boldsymbol{k}_3}{k_2^2}\mathcal{M}(k_2)\mathcal{P}_{\Phi\mathcal{S}}(k_2)\mathcal{P}_{\Phi\mathcal{S}}(k_3)+\boldsymbol{k}_2\leftrightarrow\boldsymbol{k}_3\right)\\
&+\Bigg\{\left(\frac{\boldsymbol{k}_1.\boldsymbol{k}_2}{k_1^2}\mathcal{M}(k_1)\mathcal{P}_{\Phi}(k_1)\mathcal{P}_{\mathcal{S}}(k_2)+\frac{\boldsymbol{k}_1.\boldsymbol{k}_2}{k_2^2}\mathcal{M}(k_2)\mathcal{P}_{\Phi\mathcal{S}}(k_1)\mathcal{P}_{\Phi\mathcal{S}}(k_2)\right)\\
&+\boldsymbol{k}_2\leftrightarrow\boldsymbol{k}_3\Bigg\}\Bigg]
\end{aligned}\tag{A.4}
$$

$$
\begin{aligned}
\langle y_*(\boldsymbol{k}_1)y_*(\boldsymbol{k}_2)\mathcal{S}_L(\boldsymbol{k}_3)\rangle_{\rm nzl} =&(2\pi)^3\delta_D^3(\boldsymbol{k}_1+\boldsymbol{k}_2+\boldsymbol{k}_3)\\
&4f_{\rm NL}^2\Bigg[2h_{\rm NL}(\mathcal{P}_{\Phi\mathcal{S}}(k_1)\mathcal{P}_{\Phi\mathcal{S}}(k_2)\\
&+\Bigg\{\left(\frac{\boldsymbol{k}_1.\boldsymbol{k}_3}{k_1^2}\mathcal{M}(k_1)\mathcal{P}_{\Phi}(k_1)\mathcal{P}_{\Phi\mathcal{S}}(k_3)+\boldsymbol{k}_1\leftrightarrow\boldsymbol{k}_3\right)+\boldsymbol{k}_1\leftrightarrow\boldsymbol{k}_2\Bigg\}\\
&\left(\frac{\boldsymbol{k}_1.\boldsymbol{k}_2}{k_1^2}\mathcal{M}(k_1)\mathcal{P}_{\Phi}(k_1)\mathcal{P}_{\Phi\mathcal{S}}(k_2)+\boldsymbol{k}_1\leftrightarrow\boldsymbol{k}_2\right)\Bigg]
\end{aligned}\tag{A.5}
$$

$$
\begin{aligned}
\langle y_*(\boldsymbol{k}_1)y_*(\boldsymbol{k}_2)y_*(\boldsymbol{k}_3)\rangle_{\rm nzl} =&(2\pi)^3\delta_D^3(\boldsymbol{k}_1+\boldsymbol{k}_2+\boldsymbol{k}_3)\\
&8f_{\rm NL}^3\left[\left(\frac{\boldsymbol{k}_1.\boldsymbol{k}_2}{k_1^2}\mathcal{M}(k_1)\mathcal{P}_{\Phi}(k_1)\mathcal{P}_{\Phi}(k_2)+\boldsymbol{k}_1\leftrightarrow\boldsymbol{k}_2\right)+2\text{ perms}\right]
\end{aligned}\tag{A.6}
$$

$$
\begin{aligned}
\langle \delta_L(\boldsymbol{k}_1)y_*(\boldsymbol{k}_2)\mathcal{S}_L(\boldsymbol{k}_3)\rangle_{\rm nzl} =&(2\pi)^3\delta_D^3(\boldsymbol{k}_1+\boldsymbol{k}_2+\boldsymbol{k}_3)\\
&2f_{\rm NL}\Bigg[\mathcal{M}(k_1)(2f_{\rm NL}\mathcal{P}_{\Phi}(k_2)\mathcal{P}_{\Phi\mathcal{S}}(k_3)+2h_{\rm NL}\mathcal{P}_{\Phi\mathcal{S}}(k_1)\mathcal{P}_{\Phi\mathcal{S}}(k_2))\\
&+2F_2(k_2,k_3)\mathcal{M}(k_2)\mathcal{M}(k_3)\mathcal{P}_{\Phi}(k_2)\mathcal{P}_{\Phi\mathcal{S}}(k_3)\\
&+\mathcal{M}(k_1)\left(\frac{\boldsymbol{k}_1.\boldsymbol{k}_3}{k_1^2}\mathcal{M}(k_1)\mathcal{P}_{\Phi}(k_1)\mathcal{P}_{\Phi\mathcal{S}}(k_3)+\boldsymbol{k}_1\leftrightarrow\boldsymbol{k}_3\right)\\
&+\mathcal{M}(k_1)\left(\frac{\boldsymbol{k}_1.\boldsymbol{k}_2}{k_1^2}\mathcal{M}(k_1)\mathcal{P}_{\Phi}(k_1)\mathcal{P}_{\Phi\mathcal{S}}(k_2)+\boldsymbol{k}_1\leftrightarrow\boldsymbol{k}_2\right)\Bigg]
\end{aligned}\tag{A.7}
$$

Now, we consider terms in equation (3.79) with four fields. In this case, we do not need to consider the non-Gaussianity from gravitational evolution, since it only contributes at non-leading (higher) order and is considered to be negligible. We also ignore zero lag terms in the expansion since they are taken care of, as we discussed earlier. Then these correlation functions become

$$\langle(\delta_L * \delta_L)(\boldsymbol{k}_1)\delta_L(\boldsymbol{k}_2)\delta_L(\boldsymbol{k}_3)\rangle_{\rm nzl} = (2\pi)^3\delta^3_D(\boldsymbol{k}_1+\boldsymbol{k}_2+\boldsymbol{k}_3)2\mathcal{M}^2(k_2)\mathcal{M}^2(k_3)\mathcal{P}_\Phi(k_2)\mathcal{P}_\Phi(k_3) \tag{A.8}$$

$$\langle(\delta_L * \delta_L)(\boldsymbol{k}_1)\mathcal{S}_L(\boldsymbol{k}_2)\mathcal{S}_L(\boldsymbol{k}_3)\rangle_{\rm nzl} = (2\pi)^3\delta^3_D(\boldsymbol{k}_1+\boldsymbol{k}_2+\boldsymbol{k}_3)2\mathcal{M}(k_2)\mathcal{M}(k_3)\mathcal{P}_{\Phi\mathcal{S}}(k_2)\mathcal{P}_{\Phi\mathcal{S}}(k_3) \tag{A.9}$$

$$\langle(\delta_L * \delta_L)(\boldsymbol{k}_1)y_*(\boldsymbol{k}_2)y_*(\boldsymbol{k}_3)\rangle_{\rm nzl} = (2\pi)^3\delta^3_D(\boldsymbol{k}_1+\boldsymbol{k}_2+\boldsymbol{k}_3)8f_{\rm NL}^2\mathcal{M}(k_2)\mathcal{M}(k_3)\mathcal{P}_\Phi(k_2)\mathcal{P}_\Phi(k_3) \tag{A.10}$$

$$\langle(\delta_L * \delta_L)(\boldsymbol{k}_1)\delta_L(\boldsymbol{k}_2)\mathcal{S}_L(\boldsymbol{k}_3)\rangle_{\rm nzl} = (2\pi)^3\delta^3_D(\boldsymbol{k}_1+\boldsymbol{k}_2+\boldsymbol{k}_3)2\mathcal{M}^2(k_2)\mathcal{M}(k_3)\mathcal{P}_\Phi(k_2)\mathcal{P}_{\Phi\mathcal{S}}(k_3) \tag{A.11}$$

$$\langle(\delta_L * \delta_L)(\boldsymbol{k}_1)\delta_L(\boldsymbol{k}_2)y_*(\boldsymbol{k}_3)\rangle_{\rm nzl} = (2\pi)^3\delta^3_D(\boldsymbol{k}_1+\boldsymbol{k}_2+\boldsymbol{k}_3)4f_{\rm NL}\mathcal{M}^2(k_2)\mathcal{M}(k_3)\mathcal{P}_\Phi(k_2)\mathcal{P}_\Phi(k_3) \tag{A.12}$$

$$\langle(\delta_L * \delta_L)(\boldsymbol{k}_1)y_*(\boldsymbol{k}_2)\mathcal{S}_L(\boldsymbol{k}_3)\rangle_{\rm nzl} = (2\pi)^3\delta^3_D(\boldsymbol{k}_1+\boldsymbol{k}_2+\boldsymbol{k}_3)4f_{\rm NL}\mathcal{M}(k_2)\mathcal{M}(k_3)\mathcal{P}_\Phi(k_2)\mathcal{P}_{\Phi\mathcal{S}}(k_3) \tag{A.13}$$

$$\langle(y_* * y_*)(\boldsymbol{k}_1)\delta_L(\boldsymbol{k}_2)\delta_L(\boldsymbol{k}_3)\rangle_{\rm nzl} = (2\pi)^3\delta^3_D(\boldsymbol{k}_1+\boldsymbol{k}_2+\boldsymbol{k}_3)8f_{\rm NL}^2\mathcal{M}(k_2)\mathcal{M}(k_3)\mathcal{P}_\Phi(k_2)\mathcal{P}_\Phi(k_3) \tag{A.14}$$

$$\langle(y_* * y_*)(\boldsymbol{k}_1)\mathcal{S}_L(\boldsymbol{k}_2)\mathcal{S}_L(\boldsymbol{k}_3)\rangle_{\rm nzl} = (2\pi)^3\delta^3_D(\boldsymbol{k}_1+\boldsymbol{k}_2+\boldsymbol{k}_3)8f_{\rm NL}^2\mathcal{P}_{\Phi\mathcal{S}}(k_2)\mathcal{P}_{\Phi\mathcal{S}}(k_3) \tag{A.15}$$

$$\langle(y_* * y_*)(\boldsymbol{k}_1)y_*(\boldsymbol{k}_2)y_*(\boldsymbol{k}_3)\rangle_{\rm nzl} = (2\pi)^3\delta^3_D(\boldsymbol{k}_1+\boldsymbol{k}_2+\boldsymbol{k}_3)32f_{\rm NL}^4\mathcal{P}_\Phi(k_2)\mathcal{P}_\Phi(k_3) \tag{A.16}$$

$$\langle(y_* * y_*)(\boldsymbol{k}_1)\delta_L(\boldsymbol{k}_2)\mathcal{S}_L(\boldsymbol{k}_3)\rangle_{\rm nzl} = (2\pi)^3\delta^3_D(\boldsymbol{k}_1+\boldsymbol{k}_2+\boldsymbol{k}_3)8f_{\rm NL}^2\mathcal{M}(k_2)\mathcal{P}_\Phi(k_2)\mathcal{P}_{\Phi\mathcal{S}}(k_3) \tag{A.17}$$

$$\langle(y_* * y_*)(\boldsymbol{k}_1)\delta_L(\boldsymbol{k}_2)y_*(\boldsymbol{k}_3)\rangle_{\rm nzl} = (2\pi)^3\delta^3_D(\boldsymbol{k}_1+\boldsymbol{k}_2+\boldsymbol{k}_3)16f_{\rm NL}^3\mathcal{M}(k_2)\mathcal{P}_\Phi(k_2)\mathcal{P}_\Phi(k_3) \tag{A.18}$$

$$\langle(y_* * y_*)(\boldsymbol{k}_1)y_*(\boldsymbol{k}_2)\mathcal{S}_L(\boldsymbol{k}_3)\rangle_{\rm nzl} = (2\pi)^3\delta^3_D(\boldsymbol{k}_1+\boldsymbol{k}_2+\boldsymbol{k}_3)16f_{\rm NL}^3\mathcal{P}_\Phi(k_2)\mathcal{P}_{\Phi\mathcal{S}}(k_3) \tag{A.19}$$

$$\langle(\mathcal{S}_L * \mathcal{S}_L)(\boldsymbol{k}_1)\delta_L(\boldsymbol{k}_2)\delta_L(\boldsymbol{k}_3)\rangle_{\rm nzl} = (2\pi)^3\delta^3_D(\boldsymbol{k}_1+\boldsymbol{k}_2+\boldsymbol{k}_3)2\mathcal{M}(k_2)\mathcal{M}(k_3)\mathcal{P}_{\Phi\mathcal{S}}(k_2)\mathcal{P}_{\Phi\mathcal{S}}(k_3) \tag{A.20}$$

$$\langle(\mathcal{S}_L * \mathcal{S}_L)(\boldsymbol{k}_1)\mathcal{S}_L(\boldsymbol{k}_2)\mathcal{S}_L(\boldsymbol{k}_3)\rangle_{\rm nzl} = (2\pi)^3\delta^3_D(\boldsymbol{k}_1+\boldsymbol{k}_2+\boldsymbol{k}_3)2\mathcal{P}_{\mathcal{S}}(k_2)\mathcal{P}_{\mathcal{S}}(k_3) \tag{A.21}$$

$$\langle(\mathcal{S}_L * \mathcal{S}_L)(\boldsymbol{k}_1)y_*(\boldsymbol{k}_2)y_*(\boldsymbol{k}_3)\rangle_{\rm nzl} = (2\pi)^3\delta^3_D(\boldsymbol{k}_1+\boldsymbol{k}_2+\boldsymbol{k}_3)8f_{\rm NL}^2\mathcal{P}_{\Phi\mathcal{S}}(k_2)\mathcal{P}_{\Phi\mathcal{S}}(k_3) \tag{A.22}$$

$$\langle(\mathcal{S}_L * \mathcal{S}_L)(\boldsymbol{k}_1)\delta_L(\boldsymbol{k}_2)\mathcal{S}_L(\boldsymbol{k}_3)\rangle_{\rm nzl} = (2\pi)^3\delta^3_D(\boldsymbol{k}_1+\boldsymbol{k}_2+\boldsymbol{k}_3)2\mathcal{M}(k_2)\mathcal{P}_{\Phi\mathcal{S}}(k_2)\mathcal{P}_{\mathcal{S}}(k_3) \tag{A.23}$$

$$\langle(\mathcal{S}_L * \mathcal{S}_L)(\boldsymbol{k}_1)\delta_L(\boldsymbol{k}_2)y_*(\boldsymbol{k}_3)\rangle_{\rm nzl} = (2\pi)^3\delta^3_D(\boldsymbol{k}_1+\boldsymbol{k}_2+\boldsymbol{k}_3)4f_{\rm NL}\mathcal{M}(k_2)\mathcal{P}_{\Phi\mathcal{S}}(k_2)\mathcal{P}_{\Phi\mathcal{S}}(k_3) \tag{A.24}$$

$$\langle(\mathcal{S}_L * \mathcal{S}_L)(\boldsymbol{k}_1)y_*(\boldsymbol{k}_2)\mathcal{S}_L(\boldsymbol{k}_3)\rangle_{\rm nzl} = (2\pi)^3\delta^3_D(\boldsymbol{k}_1+\boldsymbol{k}_2+\boldsymbol{k}_3)4f_{\rm NL}\mathcal{P}_{\Phi\mathcal{S}}(k_2)\mathcal{P}_{\mathcal{S}}(k_3) \tag{A.25}$$

$$\langle(\delta_L * y_*)(\boldsymbol{k}_1)\delta_L(\boldsymbol{k}_2)\delta_L(\boldsymbol{k}_3)\rangle_{\rm nzl} = (2\pi)^3\delta_D^3(\boldsymbol{k}_1+\boldsymbol{k}_2+\boldsymbol{k}_3) \\ 2f_{\rm NL}(\mathcal{M}^2(k_2)\mathcal{M}(k_3)+\boldsymbol{k}_2\leftrightarrow\boldsymbol{k}_3)\mathcal{P}_\Phi(k_2)\mathcal{P}_\Phi(k_3) \tag{A.26}$$

$$\langle(\delta_L * y_*)(\boldsymbol{k}_1)\mathcal{S}_L(\boldsymbol{k}_2)\mathcal{S}_L(\boldsymbol{k}_3)\rangle_{\rm nzl} = (2\pi)^3\delta_D^3(\boldsymbol{k}_1+\boldsymbol{k}_2+\boldsymbol{k}_3)2f_{\rm NL}(\mathcal{M}(k_2)+\boldsymbol{k}_2\leftrightarrow\boldsymbol{k}_3)\mathcal{P}_{\Phi\mathcal{S}}(k_2)\mathcal{P}_{\Phi\mathcal{S}}(k_3) \tag{A.27}$$

$$\langle(\delta_L * y_*)(\boldsymbol{k}_1)y_*(\boldsymbol{k}_2)y_*(\boldsymbol{k}_3)\rangle_{\rm nzl} = (2\pi)^3\delta_D^3(\boldsymbol{k}_1+\boldsymbol{k}_2+\boldsymbol{k}_3)8f_{\rm NL}^3(\mathcal{M}(k_2)+\boldsymbol{k}_2\leftrightarrow\boldsymbol{k}_3)\mathcal{P}_\Phi(k_2)\mathcal{P}_\Phi(k_3) \tag{A.28}$$

$$\langle(\delta_L * y_*)(\boldsymbol{k}_1)\delta_L(\boldsymbol{k}_2)\mathcal{S}_L(\boldsymbol{k}_3)\rangle_{\rm nzl} = (2\pi)^3\delta_D^3(\boldsymbol{k}_1+\boldsymbol{k}_2+\boldsymbol{k}_3) \\ 2f_{\rm NL}\mathcal{M}(k_2)(\mathcal{M}(k_2)+\boldsymbol{k}_2\leftrightarrow\boldsymbol{k}_3)\mathcal{P}_\Phi(k_2)\mathcal{P}_{\Phi\mathcal{S}}(k_3) \tag{A.29}$$

$$\langle(\delta_L * y_*)(\boldsymbol{k}_1)\delta_L(\boldsymbol{k}_2)y_*(\boldsymbol{k}_3)\rangle_{\rm nzl} = (2\pi)^3\delta_D^3(\boldsymbol{k}_1+\boldsymbol{k}_2+\boldsymbol{k}_3) \\ 4f_{\rm NL}^2\mathcal{M}(k_2)(\mathcal{M}(k_2)+\boldsymbol{k}_2\leftrightarrow\boldsymbol{k}_3)\mathcal{P}_\Phi(k_2)\mathcal{P}_\Phi(k_3) \tag{A.30}$$

$$\langle(\delta_L * y_*)(\boldsymbol{k}_1)y_*(\boldsymbol{k}_2)\mathcal{S}_L(\boldsymbol{k}_3)\rangle_{\rm nzl} = (2\pi)^3\delta_D^3(\boldsymbol{k}_1+\boldsymbol{k}_2+\boldsymbol{k}_3)4f_{\rm NL}^2(\mathcal{M}(k_2)+\boldsymbol{k}_2\leftrightarrow\boldsymbol{k}_3)\mathcal{P}_\Phi(k_2)\mathcal{P}_{\Phi\mathcal{S}}(k_3) \tag{A.31}$$

$$\langle(\delta_L * \mathcal{S}_L)(\boldsymbol{k}_1)\delta_L(\boldsymbol{k}_2)\delta_L(\boldsymbol{k}_3)\rangle_{\rm nzl} = (2\pi)^3\delta_D^3(\boldsymbol{k}_1+\boldsymbol{k}_2+\boldsymbol{k}_3) \\ \mathcal{M}(k_2)\mathcal{M}(k_3)(\mathcal{M}(k_2)\mathcal{P}_\Phi(k_2)\mathcal{P}_{\Phi\mathcal{S}}(k_3)+\boldsymbol{k}_2\leftrightarrow\boldsymbol{k}_3) \tag{A.32}$$

$$\langle(\delta_L * \mathcal{S}_L)(\boldsymbol{k}_1)\mathcal{S}_L(\boldsymbol{k}_2)\mathcal{S}_L(\boldsymbol{k}_3)\rangle_{\rm nzl} = (2\pi)^3\delta_D^3(\boldsymbol{k}_1+\boldsymbol{k}_2+\boldsymbol{k}_3)(\mathcal{M}(k_2)\mathcal{P}_{\Phi\mathcal{S}}(k_2)\mathcal{P}_{\mathcal{S}}(k_3)+\boldsymbol{k}_2\leftrightarrow\boldsymbol{k}_3) \tag{A.33}$$

$$\langle(\delta_L * \mathcal{S}_L)(\boldsymbol{k}_1)y_*(\boldsymbol{k}_2)y_*(\boldsymbol{k}_3)\rangle_{\rm nzl} = (2\pi)^3\delta_D^3(\boldsymbol{k}_1+\boldsymbol{k}_2+\boldsymbol{k}_3)4f_{\rm NL}^2(\mathcal{M}(k_2)\mathcal{P}_\Phi(k_2)\mathcal{P}_{\Phi\mathcal{S}}(k_3)+\boldsymbol{k}_2\leftrightarrow\boldsymbol{k}_3) \tag{A.34}$$

$$\langle(\delta_L * \mathcal{S}_L)(\boldsymbol{k}_1)\delta_L(\boldsymbol{k}_2)\mathcal{S}_L(\boldsymbol{k}_3)\rangle_{\rm nzl} = (2\pi)^3\delta_D^3(\boldsymbol{k}_1+\boldsymbol{k}_2+\boldsymbol{k}_3) \\ \mathcal{M}(k_2)(\mathcal{M}(k_2)\mathcal{P}_\Phi(k_2)\mathcal{P}_{\mathcal{S}}(k_3)+\mathcal{M}(k_3)\mathcal{P}_{\Phi\mathcal{S}}(k_2)\mathcal{P}_{\Phi\mathcal{S}}(k_3)) \tag{A.35}$$

$$\langle(\delta_L * \mathcal{S}_L)(\boldsymbol{k}_1)\delta_L(\boldsymbol{k}_2)y_*(\boldsymbol{k}_3)\rangle_{\rm nzl} = (2\pi)^3\delta_D^3(\boldsymbol{k}_1+\boldsymbol{k}_2+\boldsymbol{k}_3) \\ 2f_{\rm NL}\mathcal{M}(k_2)(\mathcal{M}(k_2)\mathcal{P}_\Phi(k_2)\mathcal{P}_{\Phi\mathcal{S}}(k_3)+\boldsymbol{k}_2\leftrightarrow\boldsymbol{k}_3) \tag{A.36}$$

$$\langle(\delta_L * \mathcal{S}_L)(\boldsymbol{k}_1)y_*(\boldsymbol{k}_2)\mathcal{S}_L(\boldsymbol{k}_3)\rangle_{\rm nzl} = (2\pi)^3\delta_D^3(\boldsymbol{k}_1+\boldsymbol{k}_2+\boldsymbol{k}_3) \\ 2f_{\rm NL}(\mathcal{M}(k_2)\mathcal{P}_\Phi(k_2)\mathcal{P}_{\mathcal{S}}(k_3)+\mathcal{M}(k_3)\mathcal{P}_{\Phi\mathcal{S}}(k_2)\mathcal{P}_{\Phi\mathcal{S}}(k_3)) \tag{A.37}$$

$$\begin{aligned}\langle (y_* * \mathcal{S}_L)(\boldsymbol{k}_1)\delta_L(\boldsymbol{k}_2)\delta_L(\boldsymbol{k}_3)\rangle_{\rm nzl} =& (2\pi)^3\delta_D^3(\boldsymbol{k}_1+\boldsymbol{k}_2+\boldsymbol{k}_3)\\ & 2f_{\rm NL}\mathcal{M}(k_2)\mathcal{M}(k_3)(\mathcal{P}_{\Phi\mathcal{S}}(k_2)\mathcal{P}_{\Phi}(k_3)+\boldsymbol{k}_2\leftrightarrow\boldsymbol{k}_3)\end{aligned} \tag{A.38}$$

$$\langle (y_* * \mathcal{S}_L)(\boldsymbol{k}_1)\mathcal{S}_L(\boldsymbol{k}_2)\mathcal{S}_L(\boldsymbol{k}_3)\rangle_{\rm nzl} = (2\pi)^3\delta_D^3(\boldsymbol{k}_1+\boldsymbol{k}_2+\boldsymbol{k}_3)2f_{\rm NL}(\mathcal{P}_{\Phi\mathcal{S}}(k_2)\mathcal{P}_{\mathcal{S}}(k_3)+\boldsymbol{k}_2\leftrightarrow\boldsymbol{k}_3) \tag{A.39}$$

$$\langle (y_* * \mathcal{S}_L)(\boldsymbol{k}_1)y_*(\boldsymbol{k}_2)y_*(\boldsymbol{k}_3)\rangle_{\rm nzl} = (2\pi)^3\delta_D^3(\boldsymbol{k}_1+\boldsymbol{k}_2+\boldsymbol{k}_3)8f_{\rm NL}^3(\mathcal{P}_{\Phi\mathcal{S}}(k_2)\mathcal{P}_{\Phi}(k_3)+\boldsymbol{k}_2\leftrightarrow\boldsymbol{k}_3) \tag{A.40}$$

$$\begin{aligned}\langle (y_* * \mathcal{S}_L)(\boldsymbol{k}_1)\delta_L(\boldsymbol{k}_2)\mathcal{S}_L(\boldsymbol{k}_3)\rangle_{\rm nzl} =& (2\pi)^3\delta_D^3(\boldsymbol{k}_1+\boldsymbol{k}_2+\boldsymbol{k}_3)\\ & 2f_{\rm NL}\mathcal{M}(k_2)(\mathcal{P}_{\Phi}(k_2)\mathcal{P}_{\mathcal{S}}(k_3)+\mathcal{P}_{\Phi\mathcal{S}}(k_2)\mathcal{P}_{\Phi\mathcal{S}}(k_3))\end{aligned} \tag{A.41}$$

$$\langle (y_* * \mathcal{S}_L)(\boldsymbol{k}_1)\delta_L(\boldsymbol{k}_2)y_*(\boldsymbol{k}_3)\rangle_{\rm nzl} = (2\pi)^3\delta_D^3(\boldsymbol{k}_1+\boldsymbol{k}_2+\boldsymbol{k}_3)4f_{\rm NL}^2\mathcal{M}(k_2)(\mathcal{P}_{\Phi\mathcal{S}}(k_2)\mathcal{P}_{\Phi}(k_3)+\boldsymbol{k}_2\leftrightarrow\boldsymbol{k}_3) \tag{A.42}$$

$$\langle (y_* * \mathcal{S}_L)(\boldsymbol{k}_1)y_*(\boldsymbol{k}_2)\mathcal{S}_L(\boldsymbol{k}_3)\rangle_{\rm nzl} = (2\pi)^3\delta_D^3(\boldsymbol{k}_1+\boldsymbol{k}_2+\boldsymbol{k}_3)4f_{\rm NL}^2(\mathcal{P}_{\Phi}(k_2)\mathcal{P}_{\mathcal{S}}(k_3)+\mathcal{P}_{\Phi\mathcal{S}}(k_2)\mathcal{P}_{\Phi\mathcal{S}}(k_3)) \tag{A.43}$$

$$\begin{aligned}\langle (K_{ij,L} * K_L^{ij})(\boldsymbol{k}_1)\delta_L(\boldsymbol{k}_2)\delta_L(\boldsymbol{k}_3)\rangle_{\rm nzl} =& (2\pi)^3\delta_D^3(\boldsymbol{k}_1+\boldsymbol{k}_2+\boldsymbol{k}_3)2\mathcal{M}^2(k_2)\mathcal{M}^2(k_3)\\ & \left(\left[\hat{k}_2.\hat{k}_3\right]^2-\frac{1}{3}\right)\mathcal{P}_{\Phi}(k_2)\mathcal{P}_{\Phi}(k_3)\end{aligned} \tag{A.44}$$

$$\begin{aligned}\langle (K_{ij,L} * K_L^{ij})(\boldsymbol{k}_1)\mathcal{S}_L(\boldsymbol{k}_2)\mathcal{S}_L(\boldsymbol{k}_3)\rangle_{\rm nzl} =& (2\pi)^3\delta_D^3(\boldsymbol{k}_1+\boldsymbol{k}_2+\boldsymbol{k}_3)2\mathcal{M}(k_2)\mathcal{M}(k_3)\\ & \left(\left[\hat{k}_2.\hat{k}_3\right]^2-\frac{1}{3}\right)\mathcal{P}_{\Phi\mathcal{S}}(k_2)\mathcal{P}_{\Phi\mathcal{S}}(k_3)\end{aligned} \tag{A.45}$$

$$\begin{aligned}\langle (K_{ij,L} * K_L^{ij})(\boldsymbol{k}_1)y_*(\boldsymbol{k}_2)y_*(\boldsymbol{k}_3)\rangle_{\rm nzl} =& (2\pi)^3\delta_D^3(\boldsymbol{k}_1+\boldsymbol{k}_2+\boldsymbol{k}_3)8f_{\rm NL}^2\mathcal{M}(k_2)\mathcal{M}(k_3)\\ & \left(\left[\hat{k}_2.\hat{k}_3\right]^2-\frac{1}{3}\right)\mathcal{P}_{\Phi}(k_2)\mathcal{P}_{\Phi}(k_3)\end{aligned} \tag{A.46}$$

$$\begin{aligned}\langle (K_{ij,L} * K_L^{ij})(\boldsymbol{k}_1)\delta_L(\boldsymbol{k}_2)\mathcal{S}_L(\boldsymbol{k}_3)\rangle_{\rm nzl} =& (2\pi)^3\delta_D^3(\boldsymbol{k}_1+\boldsymbol{k}_2+\boldsymbol{k}_3)2\mathcal{M}^2(k_2)\mathcal{M}(k_3)\\ & \left(\left[\hat{k}_2.\hat{k}_3\right]^2-\frac{1}{3}\right)\mathcal{P}_{\Phi}(k_2)\mathcal{P}_{\Phi\mathcal{S}}(k_3)\end{aligned} \tag{A.47}$$

$$\begin{aligned}\langle (K_{ij,L} * K_L^{ij})(\boldsymbol{k}_1)\delta_L(\boldsymbol{k}_2)y_*(\boldsymbol{k}_3)\rangle_{\rm nzl} =& (2\pi)^3\delta_D^3(\boldsymbol{k}_1+\boldsymbol{k}_2+\boldsymbol{k}_3)4f_{\rm NL}\mathcal{M}^2(k_2)\mathcal{M}(k_3)\\ & \left(\left[\hat{k}_2.\hat{k}_3\right]^2-\frac{1}{3}\right)\mathcal{P}_{\Phi}(k_2)\mathcal{P}_{\Phi}(k_3)\end{aligned} \tag{A.48}$$

$$\begin{aligned}\langle (K_{ij,L} * K_L^{ij})(\boldsymbol{k}_1)y_*(\boldsymbol{k}_2)\mathcal{S}_L(\boldsymbol{k}_3)\rangle_{\rm nzl} =& (2\pi)^3\delta_D^3(\boldsymbol{k}_1+\boldsymbol{k}_2+\boldsymbol{k}_3)4f_{\rm NL}\mathcal{M}(k_2)\mathcal{M}(k_3)\\ & \left(\left[\hat{k}_2.\hat{k}_3\right]^2-\frac{1}{3}\right)\mathcal{P}_{\Phi}(k_2)\mathcal{P}_{\Phi\mathcal{S}}(k_3)\end{aligned} \tag{A.49}$$

B. Bispectrum: relevant contributions

Only the following terms contribute to the galaxy bispectrum in the squeezed limit.

$$\mathcal{B}_{\delta\delta\delta}(k_1,k_2,k_3) = \big(2F_2(\boldsymbol{k}_1,\boldsymbol{k}_2)\mathcal{M}^2(k_1)\mathcal{M}^2(k_2)\mathcal{P}_\Phi(k_1)\mathcal{P}_\Phi(k_2) + 2 \text{ perms}\big) \tag{B.1}$$

$$\mathcal{B}_{\delta\delta\mathcal{S}}(k_1,k_2,k_3) = \mathcal{M}(k_3)\big(2F_2(\boldsymbol{k}_1,\boldsymbol{k}_3)\mathcal{M}^2(k_1)\mathcal{P}_\Phi(k_1)\mathcal{P}_{\Phi\mathcal{S}}(k_3) + \boldsymbol{k}_1 \leftrightarrow \boldsymbol{k}_2\big) \tag{B.2}$$

$$\mathcal{B}_{\delta\mathcal{S}\mathcal{S}}(k_1,k_2,k_3) = \mathcal{M}(k_1)\left(\frac{\boldsymbol{k}_1.\boldsymbol{k}_2}{k_1^2}\mathcal{M}(k_1)\mathcal{P}_\Phi(k_1)\mathcal{P}_\mathcal{S}(k_2) + \boldsymbol{k}_2 \leftrightarrow \boldsymbol{k}_3\right) \tag{B.3}$$

$$\begin{aligned}\mathcal{B}_{\delta\delta y_*}(k_1,k_2,k_3) = \Bigg[&(2F_2(k_1,k_3)\mathcal{M}^2(k_1)\mathcal{M}(k_3)\mathcal{P}_\Phi(k_1)\mathcal{P}_\Phi(k_3) + \boldsymbol{k}_1 \leftrightarrow \boldsymbol{k}_2) \\ &+ \mathcal{M}(k_1)\mathcal{M}(k_2)\left(\frac{\boldsymbol{k}_1.\boldsymbol{k}_2}{k_1^2}\mathcal{M}(k_1)\mathcal{P}_\Phi(k_1)\mathcal{P}_\Phi(k_2) + \boldsymbol{k}_1 \leftrightarrow \boldsymbol{k}_2\right)\Bigg]\end{aligned} \tag{B.4}$$

$$\mathcal{B}_{\delta y_* y_*}(k_1,k_2,k_3) = 4f_{\mathrm{NL}}^2\mathcal{M}(k_1)\left(\frac{\boldsymbol{k}_1.\boldsymbol{k}_2}{k_1^2}\mathcal{M}(k_1)\mathcal{P}_\Phi(k_1)\mathcal{P}_\Phi(k_2) + \boldsymbol{k}_2 \leftrightarrow \boldsymbol{k}_3\right) \tag{B.5}$$

$$\mathcal{B}_{\delta y_*\mathcal{S}}(k_1,k_2,k_3) = 2f_{\mathrm{NL}}\mathcal{M}(k_1)\left(\frac{\boldsymbol{k}_1.\boldsymbol{k}_3}{k_1^2}\mathcal{M}(k_1)\mathcal{P}_\Phi(k_1)\mathcal{P}_{\Phi\mathcal{S}}(k_3) + \boldsymbol{k}_2 \leftrightarrow \boldsymbol{k}_3\right) \tag{B.6}$$

$$\mathcal{B}_{\delta^2\delta\delta}(k_1,k_2,k_3) = 2\mathcal{M}^2(k_2)\mathcal{M}^2(k_3)\mathcal{P}_\Phi(k_2)\mathcal{P}_\Phi(k_3) \tag{B.7}$$

$$\mathcal{B}_{\delta^2\delta\mathcal{S}}(k_1,k_2,k_3) = 2\mathcal{M}^2(k_2)\mathcal{M}(k_3)\mathcal{P}_\Phi(k_2)\mathcal{P}_{\Phi\mathcal{S}}(k_3) \tag{B.8}$$

$$\mathcal{B}_{\delta^2\delta y_*}(k_1,k_2,k_3) = 4f_{\mathrm{NL}}\mathcal{M}^2(k_2)\mathcal{M}(k_3)\mathcal{P}_\Phi(k_2)\mathcal{P}_\Phi(k_3) \tag{B.9}$$

$$\mathcal{B}_{(\delta y_*)\,\delta\delta}(k_1,k_2,k_3) = 2f_{\rm NL}(\mathcal{M}^2(k_2)\mathcal{M}(k_3) + \boldsymbol{k}_2 \leftrightarrow \boldsymbol{k}_3)\mathcal{P}_\Phi(k_2)\mathcal{P}_\Phi(k_3) \tag{B.10}$$

$$\mathcal{B}_{(\delta y_*)\,\delta\mathcal{S}}(k_1,k_2,k_3) = 2f_{\rm NL}\mathcal{M}(k_2)(\mathcal{M}(k_2) + \boldsymbol{k}_2 \leftrightarrow \boldsymbol{k}_3)\mathcal{P}_\Phi(k_2)\mathcal{P}_{\Phi\mathcal{S}}(k_3) \tag{B.11}$$

$$\mathcal{B}_{(\delta y_*)\,\delta y_*}(k_1,k_2,k_3) = 4f_{\rm NL}^2\mathcal{M}(k_2)(\mathcal{M}(k_2) + \boldsymbol{k}_2 \leftrightarrow \boldsymbol{k}_3)\mathcal{P}_\Phi(k_2)\mathcal{P}_\Phi(k_3) \tag{B.12}$$

$$\mathcal{B}_{(\delta\mathcal{S})\,\delta\delta}(k_1,k_2,k_3) = \mathcal{M}(k_2)\mathcal{M}(k_3)(\mathcal{M}(k_2)\mathcal{P}_\Phi(k_2)\mathcal{P}_{\Phi\mathcal{S}}(k_3) + \boldsymbol{k}_2 \leftrightarrow \boldsymbol{k}_3) \tag{B.13}$$

$$\mathcal{B}_{(\delta\mathcal{S})\,\delta\mathcal{S}}(k_1,k_2,k_3) = \mathcal{M}(k_2)(\mathcal{M}(k_2)\mathcal{P}_\Phi(k_2)\mathcal{P}_{\mathcal{S}}(k_3) + \mathcal{M}(k_3)\mathcal{P}_{\Phi\mathcal{S}}(k_2)\mathcal{P}_{\Phi\mathcal{S}}(k_3)) \tag{B.14}$$

$$\mathcal{B}_{(\delta\mathcal{S})\,\delta y_*}(k_1,k_2,k_3) = 2f_{\rm NL}\mathcal{M}(k_2)(\mathcal{M}(k_2)\mathcal{P}_\Phi(k_2)\mathcal{P}_{\Phi\mathcal{S}}(k_3) + \boldsymbol{k}_2 \leftrightarrow \boldsymbol{k}_3) \tag{B.15}$$

$$\mathcal{B}_{(K^2)\,\delta\delta}(k_1,k_2,k_3) = 2\mathcal{M}^2(k_2)\mathcal{M}^2(k_3)\left(\left[\hat{k}_2.\hat{k}_3\right]^2 - \frac{1}{3}\right)\mathcal{P}_\Phi(k_2)\mathcal{P}_\Phi(k_3) \tag{B.16}$$

$$\mathcal{B}_{(K^2)\,\delta\mathcal{S}}(k_1,k_2,k_3) = 2\mathcal{M}^2(k_2)\mathcal{M}(k_3)\left(\left[\hat{k}_2.\hat{k}_3\right]^2 - \frac{1}{3}\right)\mathcal{P}_\Phi(k_2)\mathcal{P}_{\Phi\mathcal{S}}(k_3) \tag{B.17}$$

$$\mathcal{B}_{(K^2)\,\delta y_*}(k_1,k_2,k_3) = 4f_{\rm NL}\mathcal{M}^2(k_2)\mathcal{M}(k_3)\left(\left[\hat{k}_2.\hat{k}_3\right]^2 - \frac{1}{3}\right)\mathcal{P}_\Phi(k_2)\mathcal{P}_\Phi(k_3) \tag{B.18}$$